THE CRUCIAL ROLES OF JMJD3 IN T CELL TRAFFICKING AND PERSISTENCE

A Dissertation

by

CHUNTANG FU

Submitted to the Office of Graduate and Professional Studies of
Texas A&M University
in partial fulfillment of the requirements for the degree of

DOCTOR OF PHILOSOPHY

Chair of Committee,	Jiang Chang
Co-Chair of Committee,	Rongfu Wang
Committee Members,	Yun Huang
	David Reiner
Head of Department,	Warren E. Zimmer

May 2019

Major Subject: Medical Sciences

ABSTRACT

Jmjd3, a histone H3K27 demethylase, regulates macrophage and T-cell differentiation, but its role in T-cell trafficking and persistence remains largely unknown. In this dissertation, I show that *Jmjd3* deficiency in $CD4^+$ T cells limits $CD4^+$ T-cell egress out of the thymus, leading to thymic T-cell accumulation, and *Jmjd3* deletion limits peripheral $CD4^+$ T-cell migration, leading to a reduced number of T cells in secondary lymphoid organs. Further investigation identified *Pdlim4* as a novel Jmjd3 target gene that affects T-cell trafficking by cooperating with S1P1. *Jmjd3* deficiency also enables T-cell persistence due to an increase in proliferation and a decrease in apoptosis, suggesting that the H3K27 demethylase Jmjd3 may be a good therapeutic target for adoptive immunotherapy for the generation of superior T cell grafts.

ACKNOWLEDGEMENTS

I would never have been able to finish my thesis without the guidance of my committee members, help from friends, and support from my family.

First and foremost, I would like to express my deepest appreciation to my advisor, Dr. Rongfu Wang, for his help in supporting me in my dissertation work. I would like to thank Dr. Jiang Chang for serving as the committee chair. I am grateful for his kindness, patience, and support for me during my graduate study period. I would also like to acknowledge and express special appreciation to my other committee members: Dr. Yun Huang and Dr. David Reiner for their advice and encouragement, without which this dissertation would not be possible.

Thanks to Helen Y. Wang for her help not only with lab stuff but also my life. Thanks to all my current and former lab members for the time we spent together in doing experiments and having lunch. It was a pleasure to meet and work with all of them.

I also thank my friends David Blazek and Lindsey Blazek for all those enjoyable Saturday discussions and delicious brunches.

Last but not the least, I would like to express my thanks to my wife and my little daughter for their endless support and love.

CONTRIBUTORS AND FUNDING SOURCES

Contributors

This work was supervised by a dissertation committee consisting of Professor Rongfu Wang of the Department of Epigenetic and Inflammation, Houston Methodist Research Institute and Professor Jiang Chang, Yun Huang and David Reiner of the Institute of Biosciences and Technology, Texas A&M University. Jia Zou and Qingtian Li have also contributed to the projects and designed the experiment.

Funding Sources

This work in Chapter II was supported, in part, by grants from NCI, NIH, (R01CA101795, R01CA121191) and funds from Houston Methodist Research Institute. This work in Chapter III was supported, in part, by grants from DoD, CPRIT (BC151081, RP150611, RP170537) and funds from Houston Methodist Research Institute.

NOMENCLATURE

CFA	Complete Freund'S Adjuvant
CFSE	Carboxyfluorescein Succinimidyl Ester
CNS	Central Nervous System
DLNs	Draining Lns
DP	Double-Positive
EAE	Experimental Autoimmune Encephalomyelitis
EZH2	Enhancer of Zeste Homolog 2
GEO	Gene Expression Omnibus
H3K27	Trimethylation of Histone 3 at Lysine 27
H3K27me2/3	Di- and Trimethylation Of H3K27
H3K4	Trimethylation of Histone 3 at Lysine 4
JmjC	Jumonji C
JMJD3	Jumonji Domain Containing-3
KDM2	Members of The Lysine Demethylase 2
KDM5	Members of The Lysine Demethylase 5
Klf2	Kruppel-Like Factor 2
LNs	Lymph Nodes
MOG	Myelin Oligodendrocyte Glycoprotein
OCR	O2 Consumption Rate
PDLIM4	PDZ and LIM Domain Protein 4

PRC2	Polycomb Repressive Complex 2
PTx	Pertussis Toxin
S1P	Sphingosine 1-Phosphate
S1P1	Sphingosine-1 Phosphate Receptor 1
SP	Single-Positive
Tcm	Central Memory T Cells
TCR	T-Cell Receptor
TCRs	T Cell Receptors
Tem	Effector Memory T Cells
TPCs	Thymic Progenitor Cells
Tscm	T Memory Stem Cells
UTX	Ubiquitously Transcribed X-Chromosome Tetratricopeptide Repeat Protein
WCLs	Whole Cell Lysates

TABLE OF CONTENTS

Page

LIST OF FIGURES

Page

CHAPTER I

INTRODUCTION

1.1 The epigenetic regulation of gene expression

All the cells in an organism have the same DNA. However, cells in different tissues differ because the gene expression differs both qualitatively and quantitatively between cells. Such difference in gene expression could be regulated at the transcription level by modifications of DNA and chromatin proteins, which is known as epigenetic modifications. Epigenetic factors regulate gene expression through DNA methylation and covalent chromatin modifications of histone proteins including their methylation, acetylation, sumoylation, ubiquitination, and phosphorylation (Cloos et al., 2008). Due to their direct involvement in gene transcription activities, histone methylation and acetylation have garnered the greatest attention. These states are dynamically modified by different histone methyltransferases / demethylases and histone acetyltransferases / deacetylases (Klose and Zhang, 2007).

1.1.1 DNA methylation and regulation of gene expression

The cytosine residues in DNA can be reversibly methylated (Newell-price 2000). Once established, DNA methylation patterns can be stably transmitted over cell divisions by DNMT1 maintenance (Allis and Jenuwein, 2016; Bestor and Ingram, 1983). The methylation status in gene promoter and gene body have been reported to influence gene expression (Auclair and Weber, 2012). The methylation marks are written by DNA methyltransferase family proteins (DNMTs) and erased by ten-eleven translocation (TET) family proteins (Tahiliani et al., 2009). Gene expression can be affected by DNA

methylation in direct and indirect ways. DNA methylation can directly block the binding of certain transcription factors (TFs) and restrict regulatory elemenst from positive transcription signals (Schubeler, 2015). On the other hand, the indirect mechanisms including some TFs can actively recognize methylated DNA and bind to these regions to recruit other proteins to remodel chromatin configuration (Jones et al., 1998; Yin et al., 2017).

1.1.2 Histone modification and regulation of gene expression

Although the detailed mechanisms and effects of histone modifications on transcription require more studies, there are three general principles involving the transcription regulation (Bannister and Kouzarides, 2011). (1) Histone modifications directly change the structure of chromatin, such as a more or less compact chromatin structure which impacts DNA access by proteins, such as transcription factors. (2) Histone post transcriptional modifications can disrupt the binding of chromatin associated proteins. (3) These histone modification markers will recruit certain effector proteins to the chromatin.

Previous publications indicated that histone acetylation correlates with transcription. High level of histone acetylation in promoter is positively associated with gene transcription activity. Activators of transcription recruit histone acetyl transferases to acetylate nucleosomal histone, whereas DNA-bound repressors recruit histone deacetylases (HDACs) to deacetylate histone (Bannister and Kouzarides, 2011). Actually, many coactivator and corepressors hold histone acetyltransferases (HAT) or HDAC activity respectively, or associate with these enzymes. The acetylation and deacetylation activities are necessary for their effects on transcription. HAT and HDAC are often part of larger complexes that have

additional functions to histone modification, for example, recruit proteins which can bind TATA box (Sewack et al., 2001).

Histone modifications also change the structure of chromatin, either over short or long distances, such as histone acetylation will reduce the positive charge of histones. The electrostatic interactions between DNA and histones are disrupted by positive charge level decrease in histones, thus chromatin shows less compact structure that facilitates transcription activator to access DNA (**Figure 1.1** upper panel). On the other hand, some histone modifications, such as H3S10 phosphorylation, are associated with chromatin becoming more condensed (**Figure 1.1** lower panel). The compact configuration of chromatin can be reversibly regulated by epigenetic factors.

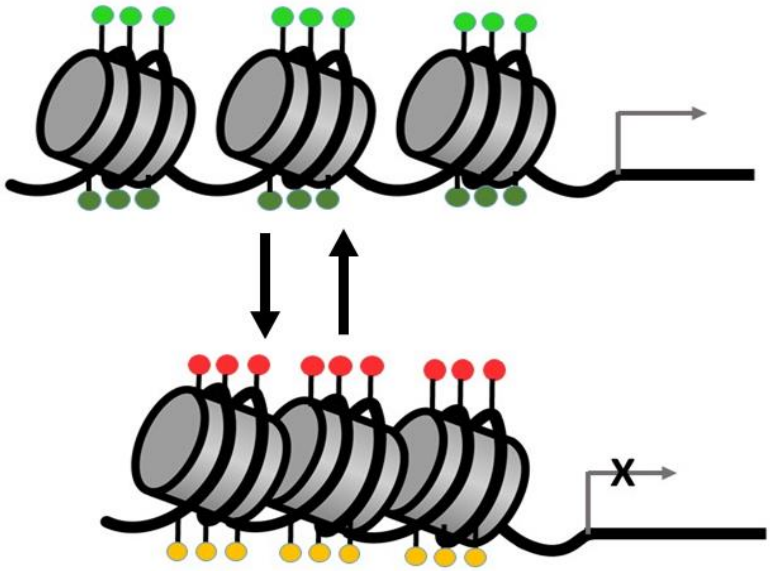

Figure 1.1 Dynamic histone modifications regulate the reversible open and closed chromatin configurations. In the upper panel, histones possess multiple activating modifications (light green and dark green circles). DNA is wrapped in open chromatin configurations. Open chromatin is more accessible for RNA polymerase. In the lower panel, histones possess multiple repressing modifications (red and orange circles). DNA is wrapped in closed chromatin configurations.

1.2 Introduction of JMJD3

Enzymes with a Jumonji C (JmjC) domain are able to remove methyl groups (Klose and Zhang, 2007; Tsukada and Zhang, 2006) from histone. JMJD3 belongs to the JmjC histone demethylases family but specifically demethylates H3K27 (Swigut and Wysocka, 2007). H3K27 tri-methylation in promoter regions is typically associated with gene inactivation, whereas H3K27 monomethylation is associated with gene activation (Barski et al., 2007). As such, the H3K27 demethylation enzyme activity of JMJD3 enables the activation of gene expression. JMJD3 has been reported to play roles in cancer, nervous system disease, cell plasticity, the immune system and development. In this chapter, I will summarize the roles of JMJD3 in different diseases and its functions in immune system.

1.3 JMJD3 in nervous system diseases

JMJD3 can affect both the peripheral nervous system and the central nervous system (CNS) (Gomez-Sanchez et al., 2013; Tang et al., 2013). In acute CNS injury, inflammation and reactive oxygen species (ROS) mediated damages are the two major problems. It has been reported that the involvement of JMJD3 in the inflammatory response contributes to the pathophysiology after CNS injury. For example, Lee et al., 2012 showed that JMJD3 was acutely increased in endothelial cells after spinal cord injury and bound to the promoter of IL-6 to increase IL-6 expression (Lee et al., 2012). The in vitro experiment showed that JMJD3 knockdown inhibits the expression of IL-6 in response to oxygen/glucose deprivation (Lee et al., 2012). IL-6 may play a crucial role in the early processes after a CNS lesion, as acute IL-6 expression will influence the blood brain barrier integrity (Brett et al., 1995; Tinsley et al., 2009). Thus, JMJD3 contributes to inflammation process in some CNS lesion. Another evidence supporting the critical role of JMJD3 in inflammation is that LPS stimulation significantly increases the expression of JMJD3. JMJD3 was also found to activate the expression of inflammation-associated genes in microglial and macrophage by cooperating with Stat1 and Stat3 (Lee et al., 2014; Przanowski et al., 2014).

Not only does JMJD3 play a role in inflammation, it also regulates the expression of brain-derived neurotrophic factor (BDNF) in neural cells after nerve lesions. It has been shown that BDNF contributes to neuropathic pain (Uchida et al., 2013). The in vitro experiment showed that JMJD3 was recruited to the promoter of BDNF and leads to histone H3K27 demethylation and increase the expression of BDNF. Additionally, the BDNF gene contains multiple promoters that are specifically regulated by polycomb repressive complexes and

JMJD3 under different neural differentiation stage. JMJD3 also involved in the synaptic activity by regulating BDNF expression in long-term depression and long-term potentiation (Palomer et al., 2016). Thus, histone modification of the BDNF promoter by JMJD3 not only contributes to the increased BDNF expression observed after neuronal injury but also plays a crucial role in neuronal development and activation. These results suggest that JMJD3 can be a therapeutic target to reduce neurotrophic pain and inflammation after neural traumatic lesion. Besides acute injuries, chronic and mild stress can also induce an increase in JMJD3 expression with a corresponding decrease in H3K27me3 levels in the prefrontal cortex and hippocampus of both adolescent and adult rats (Wang et al., 2018).

Furthermore, JMJD3 also plays an important role in neurodegenerative diseases. The causes of neurodegenerative disease include genetic predisposition, abnormal neuronal apoptosis, and inflammation-mediated damage. JMJD3 expresses and functions in all brain cell types including neurons. JMJD3-/- neurons exhibit inhibited cell apoptosis and tolerance in oxygen-glucose deprivation model by regulating expression of Bac and Caspase-3. JMJD3 deficiency prevents neuronal apoptosis from stroke through the regulate p53 and its downstream Bac and Caspase-3 (Zhang et al., 2018). In Parkinson's disease, JMJD3 has been reported to be involved in microglia polarization and may alter immune pathogenesis (Tang et al., 2013). Moreover, JMJD3 was also found to play a role in Alzheimer's disease and normal neural development by associating with amyloid-beta aggregates and activation of p63 in neuronal cells. During neural differentiation, JMJD3 interacts with P63, which results in the alteration of P63 methylation status and cellular localization. P63 as a member of the P53 tumor suppressor family was demethylated by JMJD3 and distribute in nuclear to

drive neurogenesis (Fonseca et al., 2012a; Fonseca et al., 2012b). In these two publications, JMJD3 could lead to the demethylation of p63, thereby promoting its nuclear localization and antagonizes neural apoptosis which suggesting a protective role of JMJD3 in Alzheimer's disease. JMJD3 was reported as binding the promoters and the enhancers of several genes which were reported involving in neurogenesis and neuronal differentiation and upregulated their expression (Park et al., 2014). All these studies have shown that JMJD3 affects the apoptosis and differentiation of cells in nervous system, but whether we can stimulate or antagonize JMJD3 to treat neurodegenerative disease is, as yet, unknown.

1.4 JMJD3 in immune system diseases

JMJD3 has been shown to promote both anti-inflammatory and pro-inflammatory responses in the process of infection and wound healing (as reviewed in (Salminen et al., 2014)). As to pro-inflammatory responses, it has been shown that JMJD3 promotes its own expression during inflammation response to drive autoimmune disease. Inhibition of JMJD3 suppresses IL-6 and IL-12 upregulation in human periodontal ligament cells in inflammation response (Wang et al., 2018). Rheumatoid arthritis (RA) is an autoimmune disease with the characteristics of progressive joint destruction. JMJD3 promoted the proliferation and migration of fibroblast-like synoviocytes, which play a critical role in RA joint destruction and pathologic process. JMJD3 inhibitor treatment significantly attenuated the severity of arthritis in collagen-induced arthritis mice by decreasing inflammatory response in synovial fibroblasts (SF)(Jia et al., 2018). One recent paper reported that increased mPR3, which was activated by JMJD3 in neutrophils, promotes the production of proinflammatory IL-1β in early sepsis (Chen et al., 2018). JMJD3 also was found down-regulated in systemic sclerosis

fibroblast. JMJD3 modulated fibroblast activation by regulating the levels of H3K27me3 at the promoter of *FRA2*. JMJD3 inhibition limits the aberrant activation of systemic sclerosis fibroblasts and shows antifibrotic effects (Bergmann et al., 2018).

Pro-fibrotic pathways were strongly suppressed in JMJD3 deficient foam cells. JMJD3 plays a crucial role in foam cell formation and induced a pro-fibrotic gene signature (Neele et al., 2017). In innate immunity, JMJD3 has been proven as an import participant in the bacterial, parasitical, and viral induced immune responses. The bacterial toxin lipopolysaccharide (LPS) recruited Jmjd3 and NF-κB to the promoter region of target genes in vascular endothelial cells, suggesting that Jmjd3 may serve as a partner to NF-κB to activate the expression of target genes (Liu et al., 2018). JMJD3 can also cooperate with polycomb proteins to enhance antiviral innate immunity. For example, Cbx recruits JMJD3 to the Ifnb locus to upregulate IFN-B production in macrophages during viral infection (Sun et al., 2018). The JMJD3 inhibitor GSK-J4 has a selective inhibition effect on LPS-induced gene expression in microglia, which demonstrates that JMJD3 inhibitor could have therapeutic application for neuroinflammatory disease (Das et al., 2017). A recent publication reported a novel pathway involving GM-CSF, JMJD3 demethylase, Interferon regulatory factor 4 (IRF4), and CCL17 is active in monocytes/macrophages in vitro and is important for inflammatory pain (Lee et al., 2018). Furthermore, JMJD3 involves inflammation and cell migration in keratinocyte wound healing by regulating Notch1 signaling pathway (Na et al., 2017).

1.5 JMJD3 in Cancer

One of most important tumor suppressor proteins, P53, physically interacts with JMJD3, which suggests that JMJD3 may play an important role in cancer development (Williams et al., 2014). In cancer, the roles of JMJD3 are complex and may function in both cancer promotion and cancer repression. Publications show that JMJD3 promotes apoptosis and induction of cell death. Decreased expression of JMJD3 is associated with poor outcomes in clear cell renal cell carcinoma (Wang et al., 2017). Upregulation of JMJD3 increases p16INK4A expression and cell senescence (Shen et al., 2017). In glioblastoma, dysfunction of JMJD3 contributes to glioblastoma formation by preventing cellular terminal differentiation (Ene et al., 2012). Overexpression of JMJD3 slows glioblastoma stem cell growth and sphere formation. This is because JMJD3 is a downstream target of the STAT3 response which allows expression of neural differentiation genes such as *Myt1*, *FGF21*, and *GDF15*. These genes are important for the maintenance of self-renewal in normal neural and glioblastoma stem cells (Sherry-Lynes et al., 2017). All of these result support JMJD3 as a tumor suppressor.

On the other hand, JMJD3 has been reported to promote tumor genesis and metastasis, which suggests that JMJD3 may be important in promoting cancer development. In neuroblastoma, JMJD3 inhibitor GSK-J4 induced neuroblastoma differentiation and endoplasmic reticulum stress by upregulating P53 and p53 upregulated modulator of apoptosis (PUMA) (Lochmann et al., 2018). In epithelial ovarian cancer cells, JMJD3 promotes migration, invasion and enhanced metastatic capacities by modulating the expression of transforming growth factor-beta1 (Liang et al., 2019). JMJD3 was up-regulated in AML patients and was correlated with

poor survival. GSK-J4 treatment significantly inhibits cell proliferation and colony-forming ability in AML cells. In Hepatocellular carcinoma, JMJD3 expression upregulates SLUG and promotes tumor cell migration, invasion, and stem cell-like behaviors (Tang et al., 2016).

In breast cancer, two recent publications showed conflicting result. One group reported JMJD3 suppresses stem-like characteristics in breast cancer cells by downregulation of Oct4 (Xun et al., 2017). However, another group showed that JMJD3 inhibitor suppresses breast cancer stem cells expansion and self-renewal. (Pan et al., 2018).

In summary, dysregulation of JMJD3 is heavily linked to oncogenesis by involving many different processes in various cancer types. It's difficult to claim JMJD3 is a tumor suppressor or oncoprotein as JMJD3 shows various functions in different cancer types and stages. It's not clear whether stimulating or antagonizing JMJD3 will benefit cancer patient's outcomes. Any therapeutic effects on cancer models may be context-dependent.

1.6 JMJD3 and development related diseases and other diseases

During differentiation, dynamic modification of H3K27 methylation in a tissue- and cell-specific manner is crucial to regulating target gene expression. This suggests a crucial role for JMJD3 in development. Indeed, Recently, one of our reviews has summarized the roles of JMJD3 in development (Burchfield et al., 2015). In this section, I will focus on the diseases that are caused by abnormal JMJD3 expression during tissue and cell differentiation.

Recent results have shown that JMJD3 partners with SIRT1 and the nuclear receptor PPARalpha to form a positive autoregulatory loop upon fasting-activated PKA signaling and epigenetically activated beta-oxidation-promoting genes. Inhibition of JMJD3 resulted in intrinsic defects in beta-oxidation, which contributed, to hepatosteatosis as well as glucose and insulin intolerance (Seok et al., 2018). Thus, histone demethylase JMJD3 may serve as an epigenetic drug target for obesity, hepatosteatosis, and type2 diabetes that would allow selective lowering of lipid levels without increasing glucose levels. In vascular disease, JMJD3 deficiency reduces neointima formation after vascular injury by inhibiting Nox4-autophagy signaling pathways, which suggests that JMJD3 may be a prospective target for vascular disease (Luo et al., 2018). Additional sex comb-like 1 (ASXL1) mutations are commonly associated with myeloid malignancies, bone loss, and increased abundance of osteoclasts. A recent publication showed that ASXL1 deficiency will cause a 40-fold increase in expression of JMJD3, which contributes to a global reduction of H3K27 trimethylation during osteoclast differentiation (Rohatgi et al., 2018). In addition, JMJD3 is an estrogen target gene in the hypothalamus (Song et al., 2017). This report provides evidence that JMJD3 is a key mediator for the kisspeptin-extrogen feedback loop, which is an important neuroendocrine control loop for the hypothalamic-pituitary-gonadal axis (Song et al., 2017). In a mouse sepsis model, inhibition of JMJD3 protected mice against early sepsis via upregulation of the anti-inflammatory microRNA-146a and reduction of the pro-inflammatory cytokines interleukin-1b, IL-6, tumor necrosis factor-a, and monocyte chemotactic protein-1 (Pan et al., 2018).

1.7 Epigenetics in cell aging and memory

Aging and memory are complex multifactorial biological processes shared by all living cells. In the past decade, a growing number of studies have revealed that progressive changes to epigenetic information accompany aging and memory in both dividing and nondividing cells. Epigenetic regulation involves the physical marking (chemical modification) of DNA or histones to cause or allow long-lasting changes in gene activity. This mechanism plays critical roles in cellular memory maintenance once cell fates are determined (Bonasio et al., 2010).

In mammals, drastic epigenomic reprogramming happens during early embryonic development (Burton and Torres-Padilla, 2014). The data from mouse zygotes showed the plasticity of H3K27 methylation and H3K4 methylation landscape and pervasive remodeling of the epigenome during early development (Borensztein et al., 2017; Zheng et al., 2016). Dynamic H3K27 landscape was regulate by Ploycomb group proteins and histone lysine demethylases JMJD3 and UTX (Schwartz and Pirrotta, 2007). On the other hand, aging induced cellular changes leading to a decline in the organism's function. The results from model animals demonstrated that the alteration in H3K27 methylation was associated with aging-related gene expression, aging phenotypes, and animal lifespan (Lopez-Otin et al., 2013; Zhan et al., 2007). A widely accepted marker for aged cells is high expression of p16INK4a, which was reported as a target of JMJD3 (Agger et al., 2009; Molofsky et al., 2006). Whether JMJD3 plays similar roles in regulating immune cell senescence is an important and interesting question for me. In this dissertation I will explore the role of JMJD3 in immune system senescence.

1.8 JMJD3 and epigenomic alteration

The establishment of stable patterns of gene expression is accomplished by the imposition of a layer of lineage specific epigenetic information onto the genome. This epigenetic information thus distinguishes one cell type from another. Histone methylation shows much more flexible and dynamic alterations compared to DNA methylation. The knockout of JMJD3, a histone H3K27 demethylase, leads to increased methylation of H3K27. However, JMJD3 has been shown to control locus-specifically in differentiated adult stem cells and somatic cells rather than global H3K27 methylation based on published data (Burgold et al., 2012). In our study, only 25 genes showed significant up or down regulation (2-fold change in mRNA level) in *Jmjd3* cKO thymic CD4 single positive (SP) T cells. There are several potential principles that are thought to explain JMJD3's impact on specific loci rather than global epigenomic alterations.

1) Many histone-modifying enzymes need transcription factor to recruitment for lacking DNA binding domain. Transcription factors in vivo are highly variable across different cell types. The recruitment of JMJD3 to specific gene promoters is mediated by transcription and epigenetic factors. Each cell type is limited in its expression to a specific subset of transcription factors, only some of which may interact with JMJD3. Therefore the impact of Jmjd3 on gene regulation is cell type dependent. As we see from our study in T cell trafficking, Klf2 recruits Jmjd3 to regulate trafficking genes *Pdlim4, S1p1, CCR7, CD62L* in naive CD4 T cells, whereas in activated effector T cells without Klf2 protein, Jmjd3 can't target these T cell trafficking genes.

2) Genetic redundancy provides backup when an individual gene is disrupted by mutation or targeted knockout. Jmjd3 is not the only histone H3K27 demethylase. UTX is another reported H3K27 demethylase, which has redundant functions in T cell differentiation and NK cell mature and early embryonic development (Manna et al., 2015; Northrup et al., 2017; Shpargel et al., 2014).

3) Gene expression is regulated by multiple epigenetic regulations. H3K27 methylation is one of these epigenetic modifications. Decreased H3K27me3 levels in gene promoters and gene bodies are not sufficient to fully activate target gene expressions (Bannister and Kouzarides, 2011). Taking the result of our thymic CD4 SP T cells microarray and ChIP-seq as an example, 2705 genes had increased H3K27me3 levels at approximately 2kb around the transcription start site in *Jmjd3* knockout CD4 SP T cells compared with WT controls. However, only 7 of the 2705 genes had decreased H3K4me3 level (**Figure 1.2**). Jmjd3 deficiency may dramatically impact those target genes in which the promoter shows bivalent modification (poised and paused), such as H3K4me3 and H3K27me3 modification at the same location (Bernhart et al., 2016). These bivalent epigenetic marks at promoter or enhancer regions keep genes expressed at low levels but poised for rapid activation. Removing the methylation of H3K27 by Jmjd3 will cause dominant activated modifications in these target genes' promoters.

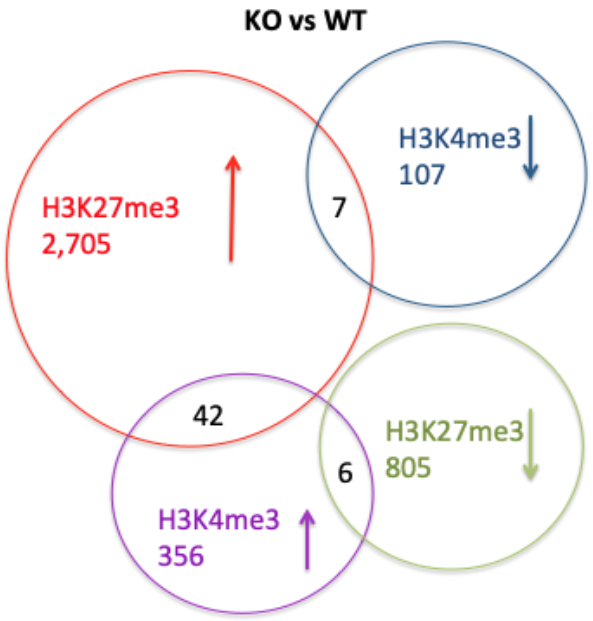

Figure 1.2 The H3K4me3 and H3K27me3 level in WT and *Jmjd3* cKO CD4 SP T cells were analyzed by genome-wide ChIP-Seq.

4) Many published studies have confirmed JMJD3 as a stress or stimulation induced gene. The expression level of JMJD3 is low in most of tissues in adult mammals, whereas the level of JMJD3 will dramatically alter upon stress challenge. For example, in macrophages, the expression of JMJD3 was profoundly induced in response to microbial stimuli. Jmjd3 RNA and protein levels show a ten-fold increase after LPS stimulation (De Santa et al., 2009). Similarly, the expression level of JMJD3 is rapidly increased under hypoxic conditions or Clioquinol treatment (Lee et al., 2014). In our study, after 2-hour stimulation by anti-CD3 and anti-CD28 antibodies in mouse CD4 T cells, *Jmjd3* RNA level shows a dramatic increase (**Figure 1.3**). Without challenges, JMJD3 expression will remain low, which may limit the number of target genes.

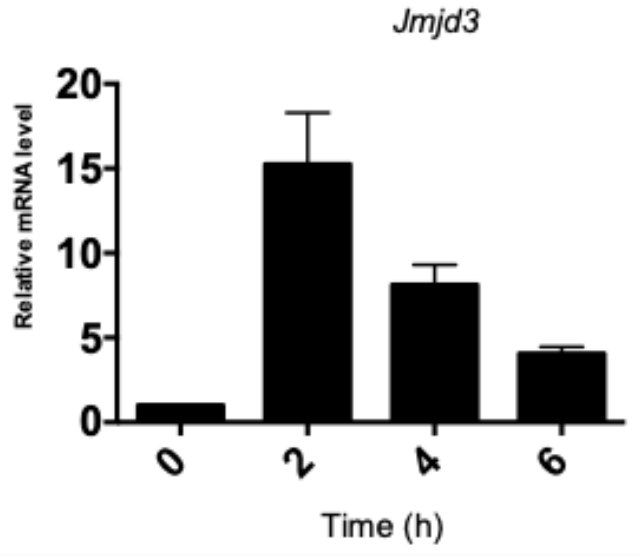

Figure 1.3 *Jmjd3* mRNA level after TCR stimulation.

In summary, the pre-existent epigenetic landscape and gene expression pattern can't be ignored when we discuss the affection of certain genes. Certain proteins in certain time and space only regulate limited targets, and this is important for the steady state of organism. Similarly, JMJD3 in special cell types and cell status only impact limited targets; though thousands of Jmjd3 related publications (7650 publications google scholar) showed broad impactions in development, cell plasticity and memory, immune system and different diseases.

1.9 JMJD3 in T cells

Before I joined my current lab, previous lab members had already explored the role of JMJD3 in development (Li et al., 2014a), T cell differentiation (Li et al., 2014b) and cellular reprogramming (Zhao et al., 2013). They found that JMJD3 knockout prevents endodermal differentiation into lung tissue. JMJD3 global knockout mice die within 30 minutes after

birth due to respiratory failure (Li et al., 2014a; Satoh et al., 2010). In terms of cellular reprogramming, Dr. Wei Zhao and his colleagues found that JMJD3 is a potential negative regulator of cellular reprogramming. JMJD3 deficiency increases iPSC formation, whereas JMJD3 overexpression inhibits cellular reprogramming through histone demethylase-dependent and –independent mechanisms. A recent publication showed that JMJD3 plays a dominant role in global H3K27me3 alterations during CD4 T cell activation. This reveals that JMJD3-driven H3K27 demethylation is critical for CD4 T cell function (LaMere et al., 2017). However, the role of JMJD3 in immune cell function is not fully clear. How immune cells save extra-cellular stimulation as memory is a "cloud" over immunology. Published results prove that epigenetic modification is an important mechanism to cell memory (Day and Sweatt, 2010; Lubin et al., 2011; Sims et al., 2003). The role of JMJD3, an important epigenetic regulator, in T cell memory function and T cell therapy is the question I want to explore in my Ph.D. training. In this dissertation, I will discuss the role of JMJD3 in T cell function including trafficking, memory, activation, and engineered T cell survival and lifespan.

1.10 References

Agger, K., P.A. Cloos, L. Rudkjaer, K. Williams, G. Andersen, J. Christensen, and K. Helin. 2009. *The H3K27me3 demethylase JMJD3 contributes to the activation of the INK4A-ARF locus in response to oncogene- and stress-induced senescence.* Genes Dev. 23:1171-1176.

Allis, C.D., and T. Jenuwein. 2016. *The molecular hallmarks of epigenetic control.* Nat Rev Genet. 17:487-500.

Auclair, G., and M. Weber. 2012. *Mechanisms of DNA methylation and demethylation in mammals.* Biochimie. 94:2202-2211.

Bannister, A.J., and T. Kouzarides. 2011. *Regulation of chromatin by histone modifications.* Cell Res. 21:381-395.

Barski, A., S. Cuddapah, K. Cui, T.Y. Roh, D.E. Schones, Z. Wang, G. Wei, I. Chepelev, and K. Zhao. 2007. *High-resolution profiling of histone methylations in the human genome.* Cell. 129:823-837.

Bergmann, C., A. Brandt, B. Merlevede, L. Hallenberger, C. Dees, T. Wohlfahrt, S. Potter, Y. Zhang, C.W. Chen, T. Mallano, R. Liang, R. Kagwiria, A. Kreuter, I. Pantelaki, A. Bozec, D. Abraham, R. Rieker, A. Ramming, O. Distler, G. Schett, and J.H.W. Distler. 2018. *The histone demethylase Jumonji domain-containing protein 3 (JMJD3) regulates fibroblast activation in systemic sclerosis.* Ann Rheum Dis. 77:150-158.

Bernhart, S.H., H. Kretzmer, L.M. Holdt, F. Juhling, O. Ammerpohl, A.K. Bergmann, B.H. Northoff, G. Doose, R. Siebert, P.F. Stadler, and S. Hoffmann. 2016. *Changes of bivalent chromatin coincide with increased expression of developmental genes in cancer.* Sci Rep. 6:37393.

Bestor, T.H., and V.M. Ingram. 1983. *Two DNA methyltransferases from murine erythroleukemia cells: purification, sequence specificity, and mode of interaction with DNA.* Proc Natl Acad Sci U S A. 80:5559-5563.

Bonasio, R., S. Tu, and D. Reinberg. 2010. *Molecular signals of epigenetic states.* Science. 330:612-616.

Borensztein, M., I. Okamoto, L. Syx, G. Guilbaud, C. Picard, K. Ancelin, R. Galupa, P. Diabangouaya, N. Servant, E. Barillot, A. Surani, M. Saitou, C.J. Chen, K. Anastassiadis, and E. Heard. 2017. *Contribution of epigenetic landscapes and transcription factors to X-chromosome reactivation in the inner cell mass.* Nat Commun. 8:1297.

Brett, F.M., A.P. Mizisin, H.C. Powell, and I.L. Campbell. 1995. *Evolution of neuropathologic abnormalities associated with blood-brain barrier breakdown in transgenic mice expressing interleukin-6 in astrocytes.* J Neuropathol Exp Neurol. 54:766-775.

Burchfield, J.S., Q. Li, H.Y. Wang, and R.F. Wang. 2015. *JMJD3 as an epigenetic regulator in development and disease.* Int J Biochem Cell Biol. 67: 148-157.

Burgold, T., N. Voituron, M. Caganova, P.P. Tripathi, C. Menuet, B.K. Tusi, F. Spreafico, M. Bevengut, C. Gestreau, S. Buontempo, A. Simeone, L. Kruidenier, G. Natoli, S. Casola, G. Hilaire, and G. Testa. 2012. *The H3K27 demethylase JMJD3 is required for maintenance of the embryonic respiratory neuronal network, neonatal breathing, and survival.* Cell Rep. 2:1244-1258.

Burton, A., and M.E. Torres-Padilla. 2014. *Chromatin dynamics in the regulation of cell fate allocation during early embryogenesis.* Nat Rev Mol Cell Biol. 15:723-734.

Chen, Y., Z. Liu, T. Pan, E. Chen, E. Mao, Y. Chen, R. Tan, X. Wang, R. Tian, J. Liu, and H. Qu. 2018. *JMJD3 is involved in neutrophil membrane proteinase 3 overexpression during the hyperinflammatory response in early sepsis.* Int Immunopharmacol. 59:40-46.

Cloos, P.A., J. Christensen, K. Agger, and K. Helin. 2008. *Erasing the methyl mark: histone demethylases at the center of cellular differentiation and disease.* Genes Dev. 22:1115-1140.

Das, A., S. Arifuzzaman, T. Yoon, S.H. Kim, J.C. Chai, Y.S. Lee, K.H. Jung, and Y.G. Chai. 2017. *RNA sequencing reveals resistance of TLR4 ligand-activated microglial cells to inflammation mediated by the selective jumonji H3K27 demethylase inhibitor.* Sci Rep. 7:6554.

Day, J.J., and J.D. Sweatt. 2010. *DNA methylation and memory formation.* Nat Neurosci. 13:1319-1323.

De Santa, F., V. Narang, Z.H. Yap, B.K. Tusi, T. Burgold, L. Austenaa, G. Bucci, M. Caganova, S. Notarbartolo, S. Casola, G. Testa, W.K. Sung, C.L. Wei, and G. Natoli. 2009. *Jmjd3 contributes to the control of gene expression in LPS-activated macrophages.* EMBO J. 28:3341-3352.

Ene, C.I., L. Edwards, G. Riddick, M. Baysan, K. Woolard, S. Kotliarova, C. Lai, G. Belova, M. Cam, J. Walling, M. Zhou, H. Stevenson, H.S. Kim, K. Killian, T. Veenstra, R. Bailey, H. Song, W. Zhang, and H.A. Fine. 2012. *Histone demethylase Jumonji D3 (JMJD3) as a tumor suppressor by regulating p53 protein nuclear stabilization.* PLoS One. 7:e51407.

Etienne-Manneville, S. 2013. *Microtubules in cell migration.* Annu Rev Cell Dev Biol. 29:471-499.

Fonseca, M.B., A.F. Nunes, A.L. Morgado, S. Sola, and C.M. Rodrigues. 2012a. *TAp63gamma demethylation regulates protein stability and cellular distribution during neural stem cell differentiation.* PLoS One. 7:e52417.

Fonseca, M.B., A.F. Nunes, and C.M. Rodrigues. 2012b. *c-Jun regulates the stability of anti-apoptotic DeltaNp63 in amyloid-beta-induced apoptosis.* J Alzheimers Dis. 28:685-694.

Gomez-Sanchez, J.A., C. Gomis-Coloma, C. Morenilla-Palao, G. Peiro, E. Serra, M. Serrano, and H. Cabedo. 2013. *Epigenetic induction of the Ink4a/Arf locus prevents Schwann cell overproliferation during nerve regeneration and after tumorigenic challenge.* Brain. 136:2262-2278.

Hong, S., Y.W. Cho, L.R. Yu, H. Yu, T.D. Veenstra, and K. Ge. 2007. *Identification of JmjC domain-containing UTX and JMJD3 as histone H3 lysine 27 demethylases.* Proc Natl Acad Sci U S A. 104:18439-18444.

Jia, W., W. Wu, D. Yang, C. Xiao, Z. Su, Z. Huang, Z. Li, M. Qin, M. Huang, S. Liu, F. Long, J. Mao, X. Liu, and Y.Z. Zhu. 2018. *Histone demethylase JMJD3 regulates fibroblast-like synoviocyte-mediated proliferation and joint destruction in rheumatoid arthritis.* FASEB J. 32:4031-4042.

Jones, P.L., G.J. Veenstra, P.A. Wade, D. Vermaak, S.U. Kass, N. Landsberger, J. Strouboulis, and A.P. Wolffe. 1998. *Methylated DNA and MeCP2 recruit histone deacetylase to repress transcription.* Nat Genet. 19:187-191.

Klose, R.J., and Y. Zhang. 2007. *Regulation of histone methylation by demethylimination and demethylation.* Nat Rev Mol Cell Biol. 8:307-318.

LaMere, S.A., R.C. Thompson, X. Meng, H.K. Komori, A. Mark, and D.R. Salomon. 2017. *H3K27 Methylation Dynamics during CD4 T Cell Activation: Regulation of JAK/STAT and IL12RB2 Expression by JMJD3.* J Immunol. 199:3158-3175.

Lee, H.T., S.K. Kim, S.H. Kim, K. Kim, C.H. Lim, J. Park, T.Y. Roh, N. Kim, and Y.G. Chai. 2014a. *Transcription-related element gene expression pattern differs between microglia and macrophages during inflammation.* Inflamm Res. 63:389-397.

Lee, H.Y., K. Choi, H. Oh, Y.K. Park, and H. Park. 2014b. *HIF-1-dependent induction of Jumonji domain-containing protein (JMJD) 3 under hypoxic conditions.* Mol Cells. 37:43-50.

Lee, K., W. Na, J.Y. Lee, J. Na, H. Cho, H. Wu, T.Y. Yune, W.S. Kim, and B.G. Ju. 2012. *Molecular mechanism of Jmjd3-mediated interleukin-6 gene regulation in endothelial cells underlying spinal cord injury.* J Neurochem. 122:272-282.

Lee, M.C., R. Saleh, A. Achuthan, A.J. Fleetwood, I. Forster, J.A. Hamilton, and A.D. Cook. 2018. *CCL17 blockade as a therapy for osteoarthritis pain and disease.* Arthritis Res Ther. 20:62.

Li, Q., H.Y. Wang, I. Chepelev, Q. Zhu, G. Wei, K. Zhao, and R.F. Wang. 2014a. *Stage-dependent and locus-specific role of histone demethylase Jumonji D3 (JMJD3) in the embryonic stages of lung development.* PLoS Genet. 10:e1004524.

Li, Q., J. Zou, M. Wang, X. Ding, I. Chepelev, X. Zhou, W. Zhao, G. Wei, J. Cui, K. Zhao, H.Y. Wang, and R.F. Wang. 2014b. *Critical role of histone demethylase Jmjd3 in the regulation of CD4+ T-cell differentiation.* Nat Commun. 5:5780.

Liang, S., Q. Yao, D. Wei, M. Liu, F. Geng, Q. Wang, and Y.S. Wang. 2019. *KDM6B promotes ovarian cancer cell migration and invasion by induced transforming growth factor-beta1 expression.* J Cell Biochem. 120:493-506.

Liu, S., X. Wang, L. Pan, W. Wu, D. Yang, M. Qin, W. Jia, C. Xiao, F. Long, J. Ge, X. Liu, and Y. Zhu. 2018. *Endogenous hydrogen sulfide regulates histone demethylase JMJD3-mediated inflammatory response in LPS-stimulated macrophages and in a mouse model of LPS-induced septic shock.* Biochem Pharmacol. 149:153-162.

Lochmann, T.L., K.M. Powell, J. Ham, K.V. Floros, D.A.R. Heisey, R.I.J. Kurupi, M.L. Calbert, M.S. Ghotra, P. Greninger, M. Dozmorov, M. Gowda, A.J. Souers, C.P. Reynolds, C.H. Benes, and A.C. Faber. 2018. *Targeted inhibition of histone H3K27 demethylation is effective in high-risk neuroblastoma.* Sci Transl Med. 10(441):1-13.

Lopez-Otin, C., M.A. Blasco, L. Partridge, M. Serrano, and G. Kroemer. 2013. *The hallmarks of aging.* Cell. 153:1194-1217.

Lubin, F.D., S. Gupta, R.R. Parrish, N.M. Grissom, and R.L. Davis. 2011. *Epigenetic mechanisms: critical contributors to long-term memory formation.* Neuroscientist. 17:616-632.

Luo, X., D. Yang, W. Wu, F. Long, C. Xiao, M. Qin, B.Y. Law, R. Suguro, X. Xu, L. Qu, X. Liu, and Y.Z. Zhu. 2018. *Critical role of histone demethylase Jumonji domain-containing protein 3 in the regulation of neointima formation following vascular injury.* Cardiovasc Res. 114:1894-1906.

Manna, S., J.K. Kim, C. Bauge, M. Cam, Y. Zhao, J. Shetty, M.S. Vacchio, E. Castro, B. Tran, L. Tessarollo, and R. Bosselut. 2015. *Histone H3 Lysine 27 demethylases Jmjd3 and Utx are required for T-cell differentiation.* Nat Commun. 6:8152.

Molofsky, A.V., S.G. Slutsky, N.M. Joseph, S. He, R. Pardal, J. Krishnamurthy, N.E. Sharpless, and S.J. Morrison. 2006. *Increasing p16INK4a expression decreases forebrain progenitors and neurogenesis during ageing.* Nature. 443:448-452.

Na, J., J.Y. Shin, H. Jeong, J.Y. Lee, B.J. Kim, W.S. Kim, T.Y. Yune, and B.G. Ju. 2017. *JMJD3 and NF-kappaB-dependent activation of Notch1 gene is required for keratinocyte migration during skin wound healing.* Sci Rep. 7:6494.

Neele, A.E., K.H. Prange, M.A. Hoeksema, S. van der Velden, T. Lucas, S. Dimmeler, E. Lutgens, J. Van den Bossche, and M.P. de Winther. 2017. *Macrophage Kdm6b controls the pro-fibrotic transcriptome signature of foam cells.* Epigenomics. 9:383-391.

Northrup, D., R. Yagi, K. Cui, W.R. Proctor, C. Wang, K. Placek, L.R. Pohl, R. Wang, K. Ge, J. Zhu, and K. Zhao. 2017. *Histone demethylases UTX and JMJD3 are required for NKT cell development in mice.* Cell Biosci. 7:25.

Ouderkirk, J.L., and M. Krendel. 2014. *Non-muscle myosins in tumor progression, cancer cell invasion, and metastasis.* Cytoskeleton (Hoboken). 71:447-463.

Palomer, E., J. Carretero, S. Benvegnu, C.G. Dotti, and M.G. Martin. 2016. *Neuronal activity controls Bdnf expression via Polycomb de-repression and CREB/CBP/JMJD3 activation in mature neurons.* Nat Commun. 7:11081.

Pan, Y., J. Wang, Y. Xue, J. Zhao, D. Li, S. Zhang, K. Li, Y. Hou, and H. Fan. 2018. GSKJ4 Protects *Mice Against Early Sepsis via Reducing Proinflammatory Factors and Up-Regulating MiR-146a.* Front Immunol. 9:2272.

Park, D.H., S.J. Hong, R.D. Salinas, S.J. Liu, S.W. Sun, J. Sgualdino, G. Testa, M.M. Matzuk, N. Iwamori, and D.A. Lim. 2014. *Activation of neuronal gene expression by the JMJD3 demethylase is required for postnatal and adult brain neurogenesis.* Cell Rep. 8:1290-1299.

Przanowski, P., M. Dabrowski, A. Ellert-Miklaszewska, M. Kloss, J. Mieczkowski, B. Kaza, A. Ronowicz, F. Hu, A. Piotrowski, H. Kettenmann, J. Komorowski, and B. Kaminska. 2014. *The signal transducers Stat1 and Stat3 and their novel target Jmjd3 drive the expression of inflammatory genes in microglia.* J Mol Med (Berl). 92:239-254.

Rohatgi, N., W. Zou, P.L. Collins, J.R. Brestoff, T.H. Chen, Y. Abu-Amer, and S.L. Teitelbaum. 2018. *ASXL1 impairs osteoclast formation by epigenetic regulation of NFATc1*. Blood Adv. 2:2467-2477.

Rottner, K., and T.E. Stradal. 2011. *Actin dynamics and turnover in cell motility.* Curr Opin Cell Biol. 23:569-578.

Salminen, A., K. Kaarniranta, M. Hiltunen, and A. Kauppinen. 2014. *Histone demethylase Jumonji D3 (JMJD3/KDM6B) at the nexus of epigenetic regulation of inflammation and the aging process.* J Mol Med (Berl). 92:1035-1043.

Satoh, T., O. Takeuchi, A. Vandenbon, K. Yasuda, Y. Tanaka, Y. Kumagai, T. Miyake, K. Matsushita, T. Okazaki, T. Saitoh, K. Honma, T. Matsuyama, K. Yui, T. Tsujimura, D.M. Standley, K. Nakanishi, K. Nakai, and S. Akira. 2010. *The Jmjd3-Irf4 axis regulates M2 macrophage polarization and host responses against helminth infection.* Nat Immunol. 11:936-944.

Schubeler, D. 2015. *Function and information content of DNA methylation.* Nature. 517:321-326.

Schwartz, Y.B., and V. Pirrotta. 2007. *Polycomb silencing mechanisms and the management of genomic programmes.* Nat Rev Genet. 8:9-22.

Seok, S., Y.C. Kim, S. Byun, S. Choi, Z. Xiao, N. Iwamori, Y. Zhang, C. Wang, J. Ma, K.Ge, B. Kemper, and J.K. Kemper. 2018. *Fasting-induced JMJD3 histone demethylase epigenetically activates mitochondrial fatty acid beta-oxidation.* J Clin Invest. 128:3144-3159.

Sewack, G.F., T.W. Ellis, and U. Hansen. 2001. *Binding of TATA binding protein to a naturally positioned nucleosome is facilitated by histone acetylation.* Mol Cell Biol. 21:1404-1415.

Shen, Y., D. Yu, P. Qi, X. Wang, X. Guo, and A. Zhang. 2017. *Calcitriol induces cell senescence of kidney cancer through JMJD3 mediated histone demethylation.* Oncotarget. 8:100187-100195.

Sherry-Lynes, M.M., S. Sengupta, S. Kulkarni, and B.H. Cochran. 2017. *Regulation of the JMJD3 (KDM6B) histone demethylase in glioblastoma stem cells by STAT3.* PLoS One. 12:e0174775.

Shpargel, K.B., J. Starmer, D. Yee, M. Pohlers, and T. Magnuson. 2014. *KDM6 demethylase independent loss of histone H3 lysine 27 trimethylation during early embryonic development.* PLoS Genet. 10:e1004507.

Sims, R.J., 3rd, K. Nishioka, and D. Reinberg. 2003. *Histone lysine methylation: a signature for chromatin function.* Trends Genet. 19:629-639.

Song, A., S. Jiang, Q. Wang, J. Zou, Z. Lin, and X. Gao. 2017. *JMJD3 Is Crucial for the Female AVPV RIP-Cre Neuron-Controlled Kisspeptin-Estrogen Feedback Loop and Reproductive Function.* Endocrinology. 158:1798-1811.

Sun, D., X. Cao, and C. Wang. 2018. *Polycomb chromobox Cbx2 enhances antiviral innate immunity by promoting Jmjd3-mediated demethylation of H3K27 at the Ifnb promoter.* Protein Cell. 10: 285-294.

Swigut, T., and J. Wysocka. 2007. *H3K27 demethylases, at long last.* Cell. 131:29-32.

Tahiliani, M., K.P. Koh, Y. Shen, W.A. Pastor, H. Bandukwala, Y. Brudno, S. Agarwal, L.M. Iyer, D.R. Liu, L. Aravind, and A. Rao. 2009. *Conversion of 5-methylcytosine to 5-hydroxymethylcytosine in mammalian DNA by MLL partner TET1.* Science. 324:930-935.

Tang, Y., T. Li, J. Li, J. Yang, H. Liu, X.J. Zhang, and W. Le. 2013. *Jmjd3 is essential for the epigenetic modulation of microglia phenotypes in the immune pathogenesis of Parkinson's disease.* Cell Death Differ. 21:369-380.

Tinsley, J.H., F.A. Hunter, and E.W. Childs. 2009. *PKC and MLCK-dependent, cytokine-induced rat coronary endothelial dysfunction.* J Surg Res. 152:76-83.

Tsukada, Y., and Y. Zhang. 2006. *Purification of histone demethylases from HeLa cells.* Methods. 40:318-326.

Uchida, H., Y. Matsushita, and H. Ueda. 2013. *Epigenetic regulation of BDNF expression in the primary sensory neurons after peripheral nerve injury: implications in the development of neuropathic pain.* Neuroscience. 240:147-154.

Wang, J., L. Liu, Q. Long, Q. Bai, Y. Xia, W. Xi, J. Xu, and J. Guo. 2017. *Decreased expression of JMJD3 predicts poor prognosis of patients with clear cell renal cell carcinoma.* Oncol Lett. 14:1550-1560.

Wang, P., J. Yue, W. Xu, X. Chen, X. Yi, L. Ye, L. Zhang, and D. Huang. 2018a. *Jumonji domain-containing protein 3 regulates the early inflammatory response epigenetically in human periodontal ligament cells.* Arch Oral Biol. 93:87-94.

Wang, R., W. Wang, J. Xu, D. Liu, H. Jiang, and F. Pan. 2018b. *Dynamic Effects of Early Adolescent Stress on Depressive-Like Behaviors and Expression of Cytokines and JMJD3 in the Prefrontal Cortex and Hippocampus of Rats.* Front Psychiatry. 9:471.

Williams, K., J. Christensen, J. Rappsilber, A.L. Nielsen, J.V. Johansen, and K. Helin. 2014. *The histone lysine demethylase JMJD3/KDM6B is recruited to p53 bound promoters and enhancer elements in a p53 dependent manner.* PLoS One. 9:e96545.

Xun, J., D. Wang, L. Shen, J. Gong, R. Gao, L. Du, A. Chang, X. Song, R. Xiang, and X. Tan. 2017. *JMJD3 suppresses stem cell-like characteristics in breast cancer cells by downregulation of Oct4 independently of its demethylase activity.* Oncotarget. 8:21918-21929.

Yin, Y., E. Morgunova, A. Jolma, E. Kaasinen, B. Sahu, S. Khund-Sayeed, P.K. Das, T. Kivioja, K. Dave, F. Zhong, K.R. Nitta, M. Taipale, A. Popov, P.A. Ginno, S. Domcke, J. Yan, D. Schubeler, C. Vinson, and J. Taipale. 2017. *Impact of cytosine methylation on DNA binding specificities of human transcription factors.* Science. 356:489-503.

Zhan, M., H. Yamaza, Y. Sun, J. Sinclair, H. Li, and S. Zou. 2007. *Temporal and spatial transcriptional profiles of aging in Drosophila melanogaster.* Genome Res. 17:1236-1243.

Zhang, H., J. Wang, J. Huang, T. Shi, X. Ma, X. Luo, X. Li, and M. Li. 2018. *Inhibiting Jumoji domain containing protein 3 (JMJD3) prevent neuronal apoptosis from stroke.* Exp Neurol. 308:132-142.

Zhao, W., Q. Li, S. Ayers, Y. Gu, Z. Shi, Q. Zhu, Y. Chen, H.Y. Wang, and R.F. Wang. 2013. *Jmjd3 inhibits reprogramming by upregulating expression of INK4a/Arf and targeting PHF20 for ubiquitination.* Cell. 152:1037-1050.

Zheng, H., B. Huang, B. Zhang, Y. Xiang, Z. Du, Q. Xu, Y. Li, Q. Wang, J. Ma, X. Peng, F. Xu, and W. Xie. 2016. *Resetting Epigenetic Memory by Reprogramming of Histone Modifications in Mammals.* Mol Cell. 63:1066-1079.

CHAPTER II

PDLIM4: A KEY TARGET OF JMJD3 REGULATES CD4 T CELL TRAFFICKING BY CONNECTING S1P1 AND ACTIN CYTOSKELETON

Histone H3K27 demethylase, Jmjd3 plays a critical role in gene expression and T-cell differentiation. However, the role and mechanisms of Jmjd3 in T cell trafficking remain poorly understood. Here we show that Jmjd3 deficiency in $CD4^+$ T cells resulted in an accumulation of T cells in the thymus, and reduction of T cell number in the secondary lymphoid organs. We identified PDLIM4 as a significantly down-regulated target gene in Jmjd3-deficient $CD4^+$ T cells by gene profiling and ChIP-seq analyses. We further showed that PDLIM4 functioned as an adaptor protein to interact with S1P1 and filamentous actin (F-actin), thus serving as a key regulator of T cell trafficking. Mechanistically, Jmjd3 bound to the promoter and gene body regions of *Pdlim4* gene and regulated its expression by interacting with zinc finger transcription factor Klf2. Our findings have identified *Pdlim4* as a novel Jmjd3 target gene that affects T-cell trafficking by cooperating with S1P1, and provided insights into the molecular mechanisms by which Jmjd3 regulates genes involved in T cell trafficking.

2.1 Introduction

T-cell development in the thymus is a multistep process. Inside the thymus, early thymic progenitor cells (TPCs) differentiate into T-cell receptor (TCR)-expressing $CD4^+CD8^+$ double-positive (DP) thymocytes in the cortex, and then mature into single-positive (SP) $CD4^+$ and $CD8^+$ T cells in the medulla (Love and Bhandoola, 2011; Petrie, 2003; Spiegel and Milstien, 2011). It is known that T-cell trafficking from the thymus to the periphery and

then migration into the secondary lymphoid and peripheral organs are regulated by the dynamic cytoskeleton. The dynamic remodeling of the actin cytoskeleton is a key component of cell locomotion and membrane trafficking (Lee and Dominguez, 2010). Of note, cellular mobility and transmigration through the endothelium requires F-actin binding genes for complex cytoskeletal rearrangements (Samstag et al., 2003). After negative and positive selection, the immature T cells express transcription factor Kruppel-like factor 2 (Klf2) and its target gene sphingosine-1 phosphate receptor 1 (S1P1 encoded by *S1pr1*), which are required for T-cell egress from the thymus and subsequent migration to secondary lymphoid organs (Carlson et al., 2006; Lee et al., 2012; Love and Bhandoola, 2011; Matloubian et al., 2004; Sebzda et al., 2008; Spiegel and Milstien, 2011; Weinreich et al., 2009; Yamada et al., 2009). After thymic emigration, the trafficking of mature CD4 or CD8 single-positive T cells is a major process to allow and regulate their immunosurveillance commitment. The motility capabilities of T cells are coupled to their ability to detect and eliminate pathogens and cancer cells. Tumor can be divided into 'hot' (inflamed) or 'cold' (noninflamed) according to the presence of T cells. The presence of tumor-infiltrating lymphocytes in tumor microenvironment has been reported to correlate well with positive clinical outcomes (Trujillo et al., 2018; van der Woude et al., 2017). Thus, the promotion of tumor specific T-cell infiltration into tumor microenvironment would benefit T cell tumor immunotherapy. On the other hand, the abnormal motility capabilities of T cells are coupled to the development of undesirable responses against self-antigens, which is a key step in autoimmune disease and organ transplantation. Recent results show that S1P1 agonist FTY-720 (Glienya) arrests T cell trafficking and prevents multiple sclerosis relapses (Garris et al., 2013). Therefore, T lymphocyte trafficking may be an important target for immunotherapy

and autoimmune response. However, the molecular mechanisms responsible for T lymphocyte trafficking are still poorly understood.

The methylation state of histones is dynamically regulated by histone methyltransferases and demethylases (Chi et al., 2010; Cloos et al., 2008; Klose and Zhang, 2007; Margueron and Reinberg, 2011; Mosammaparast and Shi, 2010). Of note, while trimethylation of the lysine 4 residue of histone 3 (H3K4me3) is usually associated with activation of gene expression, trimethylation of lysine 27 residue of histone 3 (H3K27me3) is conversely associated with repression of gene expression (Chi et al., 2010; Cloos et al., 2008; Klose and Zhang, 2007; Margueron and Reinberg, 2011; Mosammaparast and Shi, 2010). Methylation of H3K4 can be mediated by several histone methyltransferases (Black et al., 2012), while demethylation of H3K4me3 is mediated by members of the lysine demethylase (KDM) 2 and KDM5 families of lysine demethylases. Di- and trimethylation of H3K27 (H3K27me2/3) are mediated by the polycomb repressive complex 2 (PRC2), which contains the H3K27 methyltransferase enhancer of zeste homolog 2 (EZH2) protein (Cao et al., 2002; Margueron and Reinberg, 2011). On the other hand, demethylation of H3K27me2/3 is mediated by two H3K27 demethylases, Ubiquitously transcribed tetratricopeptide repeat, X chromosome (Utx, KDM6A) and Jumonji Domain Containing 3 (Jmjd3, KDM6B) (Agger et al., 2007; Hong et al., 2007; Jepsen et al., 2007; Kouzarides, 2007; Lan et al., 2007). Genetically modified *Utx*-deficient mice develop severe heart defects during development, leading to embryonic lethality (Jin et al., 2011). Similarly, *Jmjd3* whole-body-knockout mice die shortly after birth (Li et al., 2014; Satoh et al., 2010). Although Jmjd3 has been implicated

in the thymic egress (Manna et al., 2015), its target genes and the regulatory mechanisms in T cell trafficking have not been reported.

Here, we show that T-cell trafficking from the thymus to the spleen and to the lymph nodes (LNs) was markedly altered in *Jmjd3*-deficient T cells. Furthermore, we have identified a novel role for PDLIM4, a cytoskeletal protein (Boumber et al., 2007; Guryanova et al., 2011) in mediating T-cell migration by affecting the F-actin remodeling, and also delineated mechanisms by which Jmjd3 stabilizes transcription factor binding to the *Pdlim4* promoter. Specifically, our results indicate that Jmjd3 regulates the expression of cytoskeletal PDLIM4 by stabilizing the Klf2-Ash2L complex, and thus controls T-cell trafficking.

2.2 Results

2.2.1 Critical role of Jmjd3 in T-cell trafficking from the thymus to spleen and lymph nodes

We previously generated T-cell-specific deletion of *Jmjd3* (*Jmjd3* cKO) mice by crossing *Jmjd3*$^{f/f}$ mice with CD4-Cre mice and found that Jmjd3 plays a critical role in T-cell differentiation (Li et al., 2014). To further define the role of Jmjd3 in the homeostasis of T-cell populations and trafficking, we performed flow cytometric analysis of T cells isolated from the thymus, spleen, and LNs. While thymic CD4 SP T cells and CD8 SP T cells were dramatically increased, the percentages of $CD4^+$ T cells were markedly decreased (approximately 50%) in both spleens and LNs of *Jmjd3* cKO mice as compared to WT mice **(Figure 2.1, A** and **B)**. Similarly, CD8 SP T cells were also reduced in *Jmjd3* cKO spleens but not in the LNs **(Figure 2.1, A** and **B)**. Furthermore, the extent of $CD4^+$ T cells, but not

$CD8^+$ T cells, was reduced in the peripheral blood of *Jmjd3* cKO mice **(Figure 2.1 C)**. Taken together, these results suggest that CD4-driven deletion of *Jmjd3* results in marked accumulation of thymic CD4 and CD8 SP T cells, thus reducing their ability to migrate from the thymus to secondary lymphoid organs.

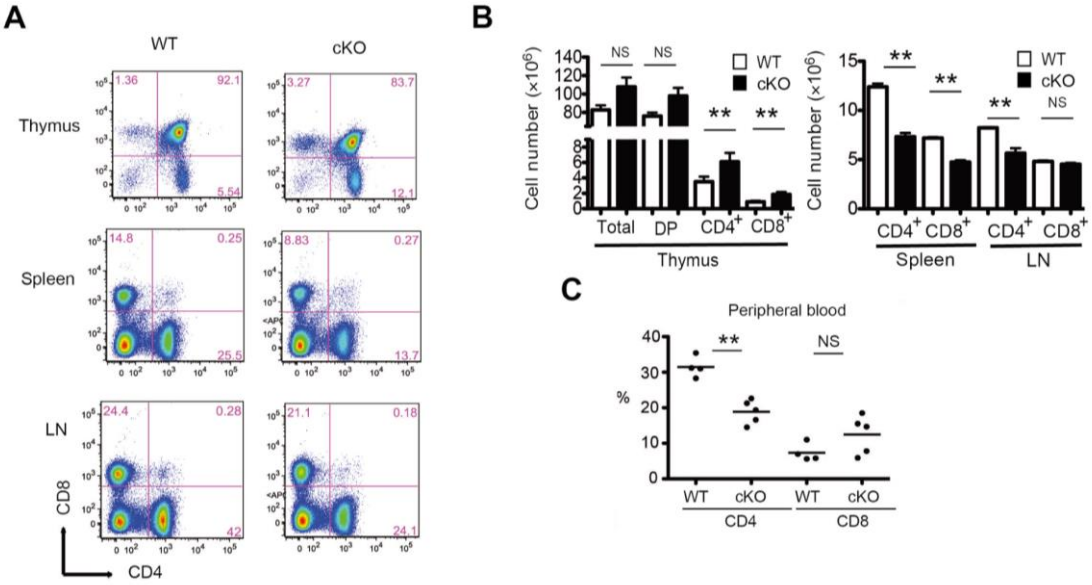

Figure 2.1 Analysis of T-cell populations in different organs between WT and *Jmjd3* cKO mice. (A) Analysis of CD4 and CD8 SP T cells in the thymus, spleen, and LN from WT and *Jmjd3* cKO mice by flow cytometry. (B) Absolute cell numbers for different cell populations, including total, double positive (DP), CD4 SP, CD8 SP, $CD4^+$ and $CD8^+$ cells, in the thymus, spleens and LNs from WT and *Jmjd3* cKO mice. The data are reported as means ± SD from three independent experiments. Asterisks indicate significant differences between groups (**$P < 0.01$ determined by Student's t test). (C) Percentage of $CD4^+$ and $CD8^+$ cells in the peripheral blood from WT and *Jmjd3* cKO mice. Dots represent the individual mouse, and lines represent the mean. Asterisks indicate significant differences determined by Student's t test (**$P < 0.01$) (NS represents no significant differences).

2.2.2 Trafficking of WT and *Jmjd3*-deficient T cells in adoptive transfer models

Next, we sought to determine the intrinsic trafficking properties of WT and *Jmjd3*-deficient T-cells in *Rag2*$^{-/-}\gamma c^{-/-}$ recipient mice, which lack endogenous T cells. Adoptive T-cell transfer of equal numbers of thymic WT and *Jmjd3*-deficient CD4 SP T cells demonstrated reduced number of splenic *Jmjd3*-deficient CD4$^+$ T cells than splenic WT cells **(Figure 2.2 A)**, suggesting defective *Jmjd3*-deficient CD4$^+$ T-cell migration. To further substantiate these findings, we performed adoptive transfer of TCR-specific CD4$^+$ T cells. For this purpose, we crossed TCR 2D2 transgenic mice, harboring myelin oligodendrocyte glycoprotein (MOG) peptide-specific TCRs, with *Jmjd3*$^{f/f}$ mice, with or without CD4-Cre to generate 2D2:*Jmjd3*$^{f/f}$ and 2D2:*Jmjd3*$^{f/f}$:cKO mice. Next, CD4 SP thymocytes were isolated by FACS using antibodies against 2D2 TCR (TCRVα3.2 and TCRVβ11) (**Figure 2.2 B** left up panel). Adoptive transfer of equal numbers of these 2D2 TCR-specific T cells from 2D2:*Jmjd3*$^{f/f}$ (WT) and 2D2:*Jmjd3*-cKO mice into sublethally irradiated C57BL/6 mice demonstrated a lower percentage and a lower absolute number of 2D2:*Jmjd3* cKO CD4$^+$ T cells than 2D2 WT CD4$^+$ T cells in the spleens and LNs **(Figure 2.2 B,** right and left down panels**)**, as assessed by flow cytometry of TCRVα3.2 and CD4 cell surface expression. Taken together, these results suggest that *Jmjd3*-deficient CD4$^+$ T cells reduce ability to migrate to the peripheral lymphoid organs, compared with WT control cells.

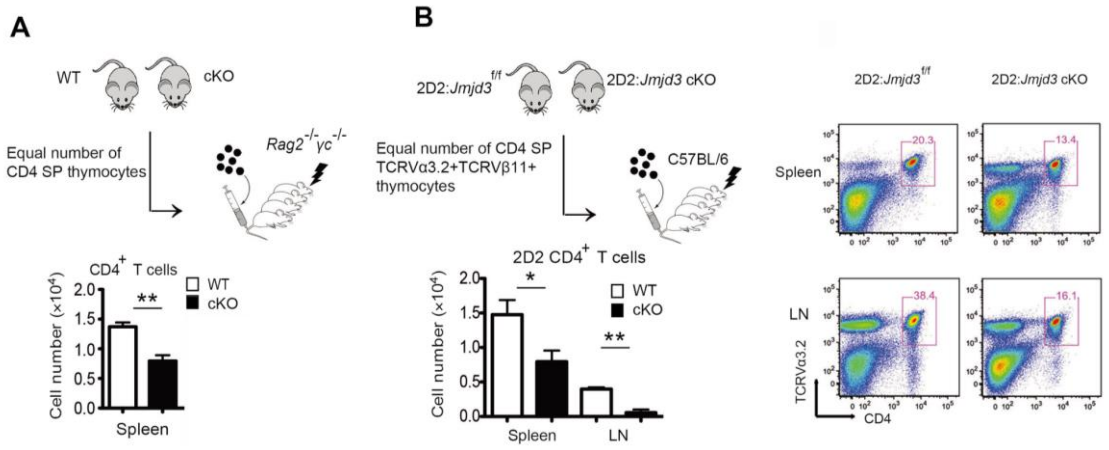

Figure 2.2 *Jmjd3* deficiency causes defects in T-cell migration. (A) Thymic CD4 SP cells from either WT or *Jmjd3* cKO mice were purified by FACS, and equal numbers of cells were intravenously injected into sublethally irradiated *Rag2*$^{-/-}\gamma c^{-/-}$ mice (n=5) (upper panel). Absolute numbers of CD4$^+$ cells in the spleens of recipient *Rag2*$^{-/-}\gamma c^{-/-}$ mice were determined 24 h after adoptive transfer (lower panel). (B) Thymic CD4 SP (TCRVα3.2$^+$/Vβ11$^+$) T cells from either 2D2:*Jmjd3*$^{f/f}$ or 2D2:*Jmjd3* cKO mice were purified by FACS, and equal numbers of cells were intravenously injected into sublethally irradiated C57BL/6 mice (n=5). Absolute numbers of CD4$^+$ TCRVα3.2$^+$ TCRVβ11$^+$ cells in the spleens and LNs of recipient C57BL/6 mice were determined 24 h after adoptive transfer (left segment) and positive cells ratio (right segment) by FACS. The data are plotted as means ± SD from three independent experiments. Asterisks indicate significant differences between groups (*P < 0.05, **P < 0.01 determined by Student's t test).

2.2.3 Identification of PDLIM4 as a key regulator of T-cell migration

We next sought to identify Jmjd3 target genes that might regulate T-cell migration by performing microarray analysis of thymic CD4 SP T cells isolated from WT and *Jmjd3* cKO mice. Gene expression profiling revealed that 16 genes were markedly downregulated, while 5 were upregulated in thymic *Jmjd3* cKO CD4 SP T cells compared to WT cells **(Figure 2.3 A** and **APPENDIX Table A-1)**. Changes in genes involved in cell motility, cell death, and cell proliferation were confirmed by quantitative real-time PCR analysis **(Figure 2.3 B)**. Genes, such as *Amigo2*, *Igfbp4*, and *Lgals1*, were downregulated, while *Slc15a2* and *Gbp1* were upregulated in thymic *Jmjd3* cKO CD4 SP T cells when compared with WT CD4 SP T cells **(Figure 2.3 B)**. We also observed that the expression of *Ccr7* and *Cd62l* were

remarkably downregulated in *Jmjd3*-deficient CD4 SP T cells **(Figure 2.3 B)**. However, there was no significant difference in the expression levels of several other genes, such as *Erdr1*, *Samhd1*, *Akr1c18*, and *Adam11*, between WT and *Jmjd3* cKO CD4 SP T cells **(Figure 2.4)**. *S1p1* and *Pdlim4* (encoding the PDZ and LIM domain protein 4), but not *Klf2*, were significantly downregulated in thymic *Jmjd3* cKO CD4 SP T cells, compared to WT CD4 SP T cells **(Figure 2.3 B)**.

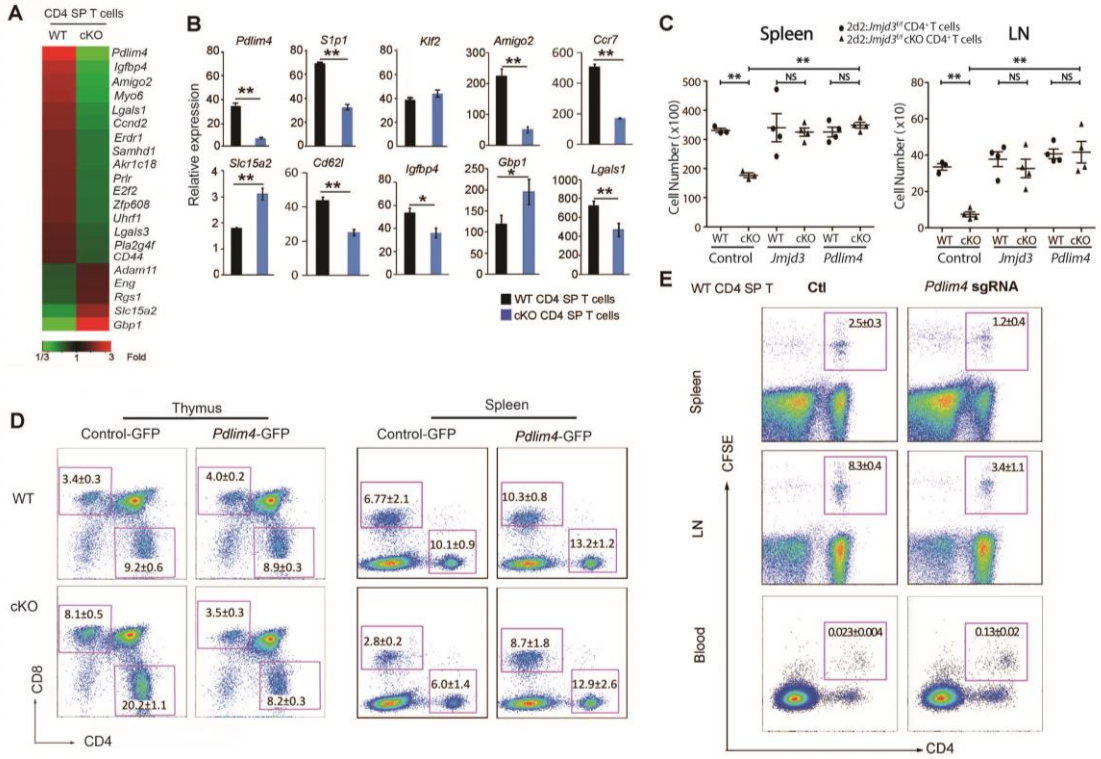

Figure 2.3 Identification of the Jmjd3-target genes in $CD4^+$ T-cells and functional rescue of T cell defects by ectopic expression of Pdlim4. (A) Heat map from microarray analysis of upregulated and downregulated genes in WT and *Jmjd3* cKO thymic CD4 SP T cells. (B) Real-time PCR analysis of a panel of genes between WT and *Jmjd3* cKO thymic CD4 SP T cells. (n=4, $*P < 0.05$, $**P < 0.01$ determined by Student's t test) (C) $CD4^+$ T cells from 2D2:*Jmjd3*$^{f/f}$ (WT) mice or 2D2:*Jmjd3* cKO mice were activated with MOG_{35-55} peptide *in vitro* before transduction with GFP-expressing retroviral vectors containing *Jmjd3* or *Pdlim4*. Equal numbers of GFP^+ $CD4^+$ T cells were intravenously injected into sublethally irradiated C57BL/6 mice (n=4). Absolute numbers of $TCRV\alpha3.2^+/V\beta11^+$ GFP^+ $CD4^+$ T cells in spleens and LNs were determined by flow cytometry 48h after adoptive transfer. The data are presented as means $\pm$ SD from three independent experiments. Asterisks indicate significant differences between groups ($*P < 0.05$, $**P < 0.01$ determined by Student's t test). (D) WT and *Jmjd3*-cKO bone marrow cells overexpressing control-GFP or *Pdlim4*-GFP were transplanted into lethally irradiated C57BL/6 (WT) mice to generate chimeric mice. Flow cytometric analysis of $CD4^+$ and $CD8^+$ T cells from the thymus and the spleens of chimeric mice. (E) Thymic CD4 SP T cells were isolated from WT mice. *Pdlim4* knockout was generated using the CRISPR-Cas9 system. Cells were labeled with carboxyfluorescein succinimidyl ester (CFSE), and then intravenously injected into sublethally irradiated C57BL/6 mice. After 48 hours, spleens, LNs, and peripheral blood were analyzed by flow cytometry for $CD4^+$ and CFSE-stained cells. The experiments were repeated three independent times.

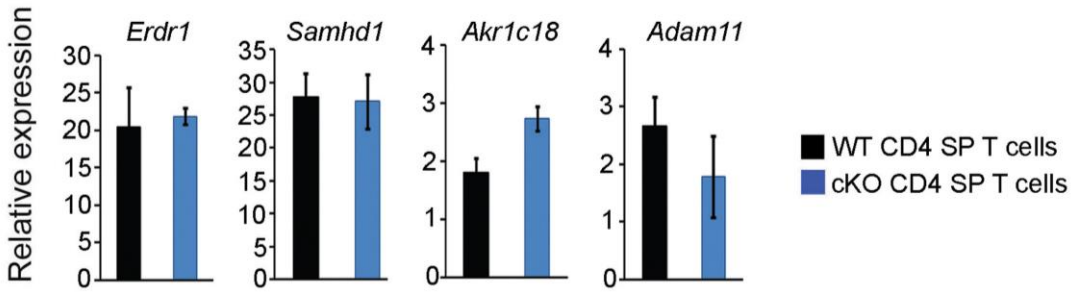

Figure 2.4 Real-time PCR analysis of genes analyzed in WT and *Jmjd3* cKO thymic CD4 SP T cells. The data are presented as means ± SD from three independent experiments.

Since PDLIM4 has been identified as a modifier of actin filament dynamics through its interaction with alpha-actinin and F-actin (Vallenius et al., 2004), we postulated that PDLIM4 might contribute to the migration defects in *Jmjd3* cKO $CD4^+$ T cells. To test this possibility, we constructed GFP-expressing retroviral vectors containing *Jmjd3* and *Pdlim4*. Splenic T cells were collected from 2D2:*Jmjd3*$^{f/f}$ (WT) and 2D2:*Jmjd3* cKO mice and activated *in vitro* before transduction with GFP-containing viruses. GFP^+ $CD4^+$ T cells were sorted, and equal numbers of GFP^+ cells were adoptively transferred into irradiated C57BL/6 recipient mice. After 48 h, single-cell suspensions were prepared from the isolated spleens and LNs of the recipient mice. MOG_{35-55} peptide-specific donor cells were analyzed by flow cytometry using 2D2 TCR specific antibodies (TCRVα3.2 and TCRVβ11). Ectopic expression of *Jmjd3* or *Pdlim4*, but not the empty vector control, restored the number of 2D2:*Jmjd3* cKO $CD4^+$ T cells in the spleens and LNs similar to 2D2:*Jmjd3*$^{f/f}$ (WT) $CD4^+$ cells **(Figure 2.3 C)**, suggesting that *Jmjd3* or *Pdlim4* may rescue any defects in T cell migration.

To further determine whether PDLIM4 could rescue the $CD4^+$ T-cell migration defect due to *Jmjd3* deficiency, we isolated bone marrow cells from either WT or *Jmjd3*-cKO mice and overexpressed control-GPF or *Pdlim4*-GFP in these bone marrow cells **(Figure 2.3 D)**. We generated chimeric mice, in which these bone marrow cells were transplanted into sublethally irradiated C57BL/6 mice. Flow cytometric analysis of splenocytes and thymocytes from these chimeric mice showed that significantly higher percentage of *Jmjd3* cKO $CD4^+$ T cells transduced with control-GFP in thymus but reduced percentage of T cells accumulated in the spleen, compared with WT $CD4^+$ T cells. However, thymic and splenic accumulation of *Jmjd3*-deficient $CD4^+$ T cells was restored upon ectopic expression of *Pdlim4* **(Figure 2.3 D)**.

In order to further demonstrate the physiological role of PDLIM4 in $CD4^+$ T-cell migration, we isolated thymic CD4 SP T cells from WT mice, generated *Pdlim4* knockout $CD4^+$ T-cells using the CRISPR-Cas9 system **(Figure 2.5 A)**, labeled the cells with carboxyfluorescein succinimidyl ester (CFSE), and then adoptively transferred them to irradiated C57BL/6 mice. After 48 h, we determined the number of T cells by FACS analysis, and found increased number of *Pdlim4*-knockout $CD4^+$ T cells in the peripheral blood of mice, but reduced number in spleen and LNs, suggesting a decreased ability of these cells to migrate into spleen and LNs **(Figure 2.3 E)**. To further determine whether *Pdlim4* knockout inhibits $CD4^+$ T cell migration, we isolated bone marrow cells from WT mice and knocked out *Pdlim4* using the CRISPR-Cas9 system to generated chimeric mice by transferring *Pdlim* KO-bone marrow cells into irradiated recipient mice. FACS analysis of cells isolated from these chimeric mice showed higher percentage of *Pdlim4* knockout

$CD4^+$ T cells accumulated in the thymus, but reduced percentage of *Pdlim4* knockout $CD4^+$ T cells in the spleen and LNs **(Figure 2.5 B)**. Taken together, these results suggest that PDLIM4, the target of Jmjd3, plays a critical role in T-cell trafficking.

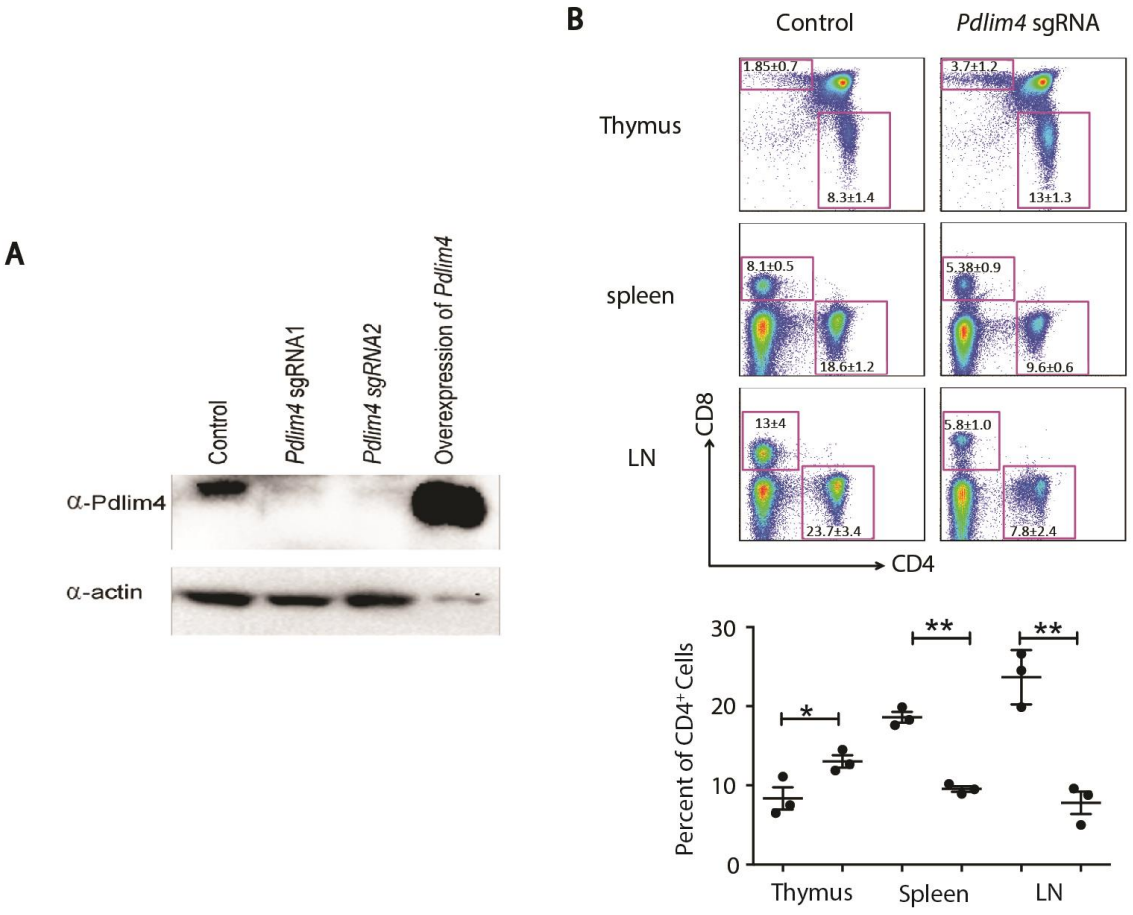

Figure 2.5 Deficiency of *Pdlim4* causes defects in T-cell migration. (A) Knockout efficiency of *Pdlim4* sgRNA1 and sgRNA2 $CD4^+$ T cells was evaluated by immunoblotting using anti-Pdlim4 antibody. α-actin was used as a loading control. **(B)** Flow cytometric analysis of $CD4^+$ and $CD8^+$ T cells isolated from thymus, spleens, and LNs of C57BL/6 chimeric mice transplanted with WT and *Pdlim4* sgRNA knockout bone marrow cells. The data are presented as means ± SD from three independent experiments. Asterisks indicate significant differences between groups (*$P < 0.05$, **$P < 0.01$, determined by Student's t test).

2.2.4 PDLIM4 regulates T cell migration through interaction with S1P1 and modulation of F-actin organization

PDLIM4 has been identified as a modifier of actin filament dynamics through its interaction with alpha-actinin and F-actin in muscle cells and nonmuscle epithelial cells (Vallenius et al., 2004). Furthermore, PDLIM4 cytoskeleton protein contains one PDZ domain, which has been reported to play a key role in anchoring receptor proteins in the membrane to cytoskeletal components (Lee and Zheng, 2010). Since S1P treatment can cause actin cytoskeleton remodeling, we next sought to determine whether S1P treatment regulates PDLIM4-mediated actin remodeling in T cells, which may be required for T cell trafficking. To this end, we isolated *Jmjd3*-deficient CD4 SP thymocytes, treated them with sphingosine 1-phosphate (S1P), and used Phalloidin for F-actin staining after fixation of T cells. As shown in **Figure 2.6 A**, in the *Jmjd3*-deficient CD4 T cells transfected with Pdlim4-GFP, we observed specific localization of PDLIM4 in lamellipodium structure of F-actin remodeling area. By contrast, we did not observe the specific localization of GFP in lamellipodium structure of F-actin remodeling area. We next determined whether ectopic expression of PDLIM4 promoted F-actin formation using WT thymic CD4 SP T cells, *Jmjd3* cKO CD4 SP T cells, *Pdlim4* KO CD4 SP T cells and *Pdlim4-expressing Jmjd3* cKO T cells, followed by Phalloidin staining and FACS analysis. We found that F-actin organization was defective in *Pdlim4* KO and *Jmjd3* cKO CD4 SP T cells based on low Phalloidin staining after S1P treatment, compared with WT and PDLIM4-expressing cells (**Figure 2.6 B**). Notably, PDLIM4-expressing cells exhibited the highest Phalloidin staining for F-actin (**Figure 2.6 B**), suggesting that PDLIM4 enhances F-actin formation. To further determine

the distribution of insoluble F-actin (pellet) and the soluble G-actin (supernatant), we treated WT and *Jmjd3* cKO CD4 SP T cells with S1P and lysed the treated cells. After removal of cellular debris by low centrifuge at 350 g for 5 min, the supernatants were further centrifuged at 150,000 g for 90 min to separate F-actin (in pellet) from soluble G-actin (in supernatant). The relative distribution of insoluble F-actin (pellet) and the soluble G-actin (supernatant) was analyzed by Western blot. We showed little or no polymerized F-actin in the *Jmjd3* cKO CD4 SP T cells, compared with WT cells (**Figure 2.6 C)**. Collectively, our results suggest that Jmjd3 or PDLIM4 deficiency markedly reduces F-actin after S1P treatment, which can be rescue by ectopic expression of PDLIM4.

S1P1 is a G-protein-coupled receptor, which binds to the bioactive signaling molecule S1P and activates intracellular signaling pathways that lead to cytoskeleton remodeling and T cell egress from the thymus (Zachariah and Cyster, 2009). We next used different immunofluorescences to label PDLIM4, S1P1 and phalloidin to stain F-actin in WT SP CD4 T cells and showed co-localization of PDLIM4 with S1P1 on lamellipodium structure in F-actin remodeling area **(Figure 2.6 D)**. Consistently, Co-IP analysis revealed that PDLIM4 was associated with S1P1 in CD4 SP thymocytes **(Figure 2.6 E)**. To determine the specific domains of PDLIM4 involved in the interaction with F-actin, we used purified recombinant GST-PDLIM4 in an *in vitro* cosedimentation assay to investigate the interaction of PDLIM4 and F-actin. The polymerized actin was incubated with GST-PDLIM4, GST-PDLIM4-N del (PDZ domain deletion) or GST PDLIM4-C del (LIM domain deletion), followed by high-speed centrifuge at 150,000 g for 90 min. The pellets and supernatants were subjected to SDS-PAGE separation after fractionation. We found that GST-PDLIM4 or GST-PDLIM4-

N del, but not GST-PDLIM4-C del, were in the pellet fraction (**Figure 2.6 F**), suggesting that the C-terminus of PDLIM4 interacts with F-actin. Since PDLIM4 interacted with S1P1 (**Figure 2.6 E**), we next determined which domain of PDLIM4 was required for interacting with S1P1. We constructed FLAG-tagged Pdlim4-N-del (PDZ domain deletion), C-del (LIM domain deletion), full-length *Pdlim4* and HA-tagged S1P1. Co-IP analysis revealed that the PDZ domain of PDLIM4 was required for interacting with S1P1 (**Figure 2.6 G**). Based on these findings, we propose a model showing that the PDLIM4 interacts with the S1P1 protein by the N-terminal PDZ domain and binds to actin cytoskeleton through its C-terminal LIM domain (**Figure 2.6 H**).

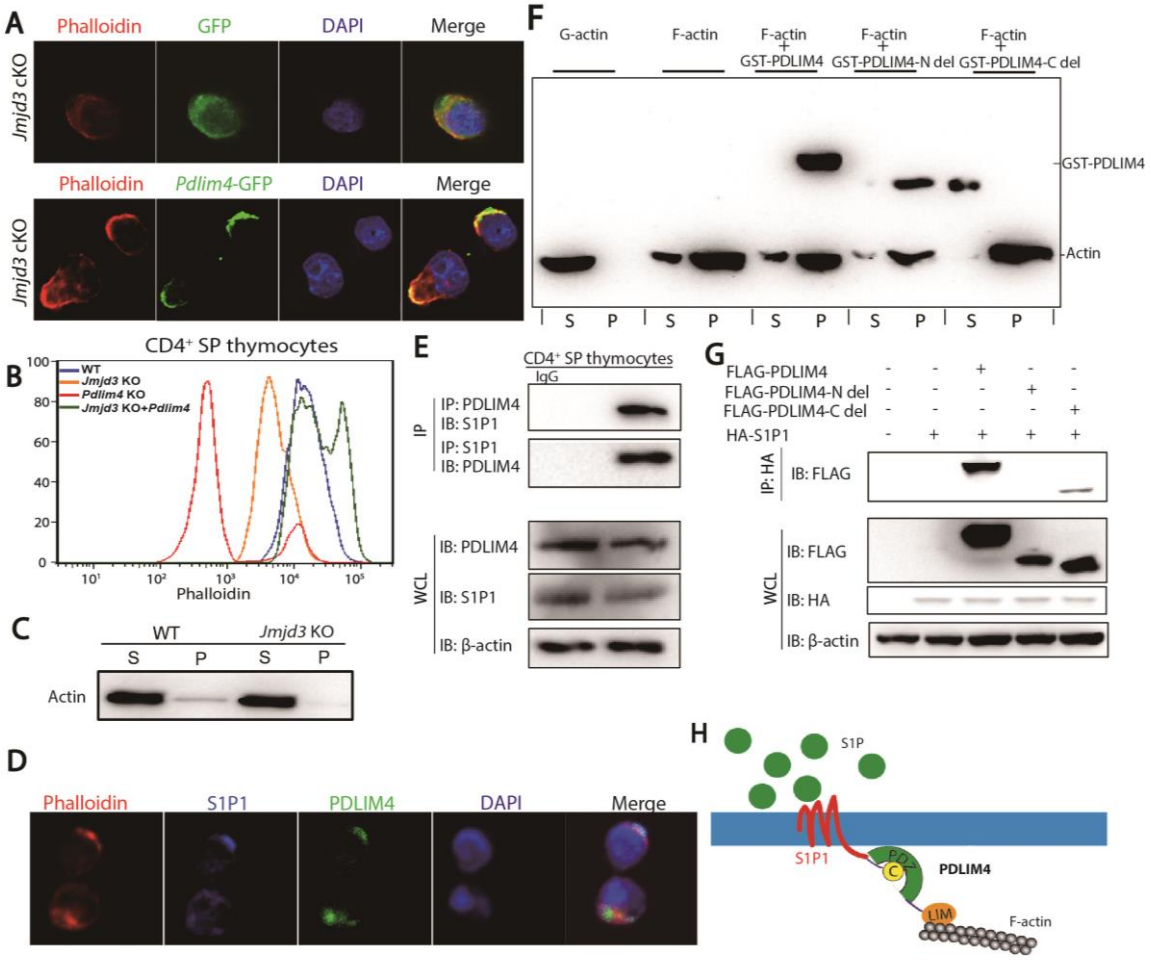

Figure 2.6 PDLIM4 regulates T-cell migration by interaction with S1P1 and modulation of F-actin reorganization. (A) Immunofluorescence microscopy of *Jmjd3* cKO CD4 T cells infected with GFP or PDLIM4-GFP. Cells were analyzed by GFP fluorescence to detect GFP or PDLIM4, and with Rhodamine-conjugated phalloidin to detect actin filaments. Merged images indicated co-localization signal. (B) FACS analysis of Phalloidin labeled F-actin in WT, *Jmjd3* cKO, *Pdlim4* KO and *Pdlim4-expressing Jmjd3* cKO CD4 SP thymocytes. (C) The F-actin (pellet) and the G-actin (supernatant) were quantified by Western blot. (D) Immunofluorescence microscopy of CD4+ SP cells stained with FITC-conjugated antibody to detect PDLIM4, Cy5-conjugated antibody to detect S1P1 and with Rhodamine-conjugated phalloidin to detect actin filaments. Merged images indicated co-localization of proteins. (E) Co-IP analysis of endogenous interaction of PDLIM4 with S1P1 in CD4 SP thymocytes. (F) Cosedimentation assay was performed using GST-PDLIM4, GST-PDLIM4 N-del, or GST-PDLIM4 C-del with F-actin, and subsequent analysis of supernatants (S) and pellets (P) by western blot analysis. (G) 293T cells were co-transfected with FLAG-*Pdlim4*-N-del, C-del, or full-length *Pdlim4* along with HA-*S1p1*. Whole cell lysates (WCLs) were immunoprecipitated with anti-HA beads and immunoblotted with anti-FLAG antibody. Three independent experiments were repeated with similar results. (H) A schematic diagram of the proposed model to show how PDLIM4 links S1P1 with F-actin. PDLIM4 interacts with the S1P1 protein by the N-terminal PDZ domain and binds F-actin by the C-terminal LIM domain.

2.2.5 Expression of *Pdlim4* is co-regulated by Jmjd3 and Klf2

During T cell differentiation Jmjd3 interacts with key differentiation regulatory transcription factors such as T-bet (Li et al., 2014; Miller et al., 2008; Miller et al., 2010). Hence, we postulated that Jmjd3 might also interact with factors involved in T-cell migration, such as Klf2 and S1P1, which are master regulators of T-cell emigration from the thymus (Carlson et al., 2006; Lee et al., 2012; Matloubian et al., 2004; Sebzda et al., 2008; Weinreich et al., 2009; Yamada et al., 2009). To test this possibility, we co-transfected 293T cells with FLAG-*Jmjd3* and HA-tagged transcription factor genes, including *Runx2*, *Klf4*, *Klf2*, *Wdr5*, *Fosl1*, *FosB*, *Wnt5a*, and *Nkx2.1* **(Figure 2.7 A)**. Co-immunoprecipitation and immunoblot analysis revealed that Jmjd3 interacted with Klf2, FosB, and Nkx2.1 *in vitro* **(Figure 2.7 A)**. A dual-luciferase assay was performed on 293T cells co-transfected with *Klf2*, *Klf4*, *Runx2*, *Nkx2.1*, *FosB*, *T-bet*, and *Rorc* with or without *Jmjd3* and -1512 bp upstream of mouse *Pdlim4* promoter-linked episomal luciferase vector **(Figure 2.7 B)**. Only Klf2 harbored transcriptional activity in regulating *Pdlim4* expression, and Jmjd3 significantly enhanced the ability of Klf2 to induce *Pdlim4* promoter-driven luciferase activity **(Figure 2.7 C)**. Jmjd3 did not enhance *Pdlim4* promoter-driven luciferase activity without Klf2, suggesting co-regulation of *Pdlim4* by Jmjd3 and Klf2. To determine whether endogenous interactions occur between Klf2 and Jmjd3, we collected thymic WT and *Jmjd3*-cKO $CD4^+$ SP T-cell lysates and co-immunoprecipitated with anti-Jmjd3 or anti-Klf2 antibodies, and then immunoblotted with anti-Klf2 or anti-Jmjd3 antibodies. We observed that Klf2 interacted with Jmjd3 in $CD4^+$ T cells **(Figure 2.7 D)**. Next, we dissected the precise *Pdlim4* promoter sequences that were responsible for Klf2 and Jmjd3 binding. We constructed a series of

Pdlim4 promoter fragment-linked episomal luciferase vectors and co-transfected 293T cells with Klf2 alone or Klf2 and Jmjd3 together **(Figure 2.7 E)**. The dual-luciferase assay indicated that sequences -100 bp upstream of the *Pdlim4* transcriptional start site (TSS) were required for Klf2 binding, and sequences -800 bp upstream of the *Pdlim4* TSS were required for Jmjd3 and Klf2 binding **(Figure 2.7 E)** and the luciferase reporter assay using CD4 SP T cells showed consistent results **(Figure 2.8 A).** To address whether the interaction between Jmjd3 and Klf2 is required for Klf2 binding to the *Pdlim4* promoter, we performed a ChIP-qPCR assay on thymic CD4 SP T cells from WT or *Jmjd3* cKO mice. We found that the binding of Klf2 to the *Pdlim4* promoter was defective in *Jmjd3*-deficient CD4 SP T cells, suggesting that Jmjd3 is required for Klf2 binding to the *Pdlim4* promoter **(Figure 2.8 B)**. This defective binding of Klf2 to the *Pdlim4* promoter could be rescued by expression of Jmjd3 in *Jmjd3* cKO CD4 SP T cells **(Figure 2.7 F)**. Taken together, our results indicate that both Jmjd3 and Klf2 are required for binding to the promoter region of *Pdlim4* and both co-regulate the expression of *Pdlim4*.

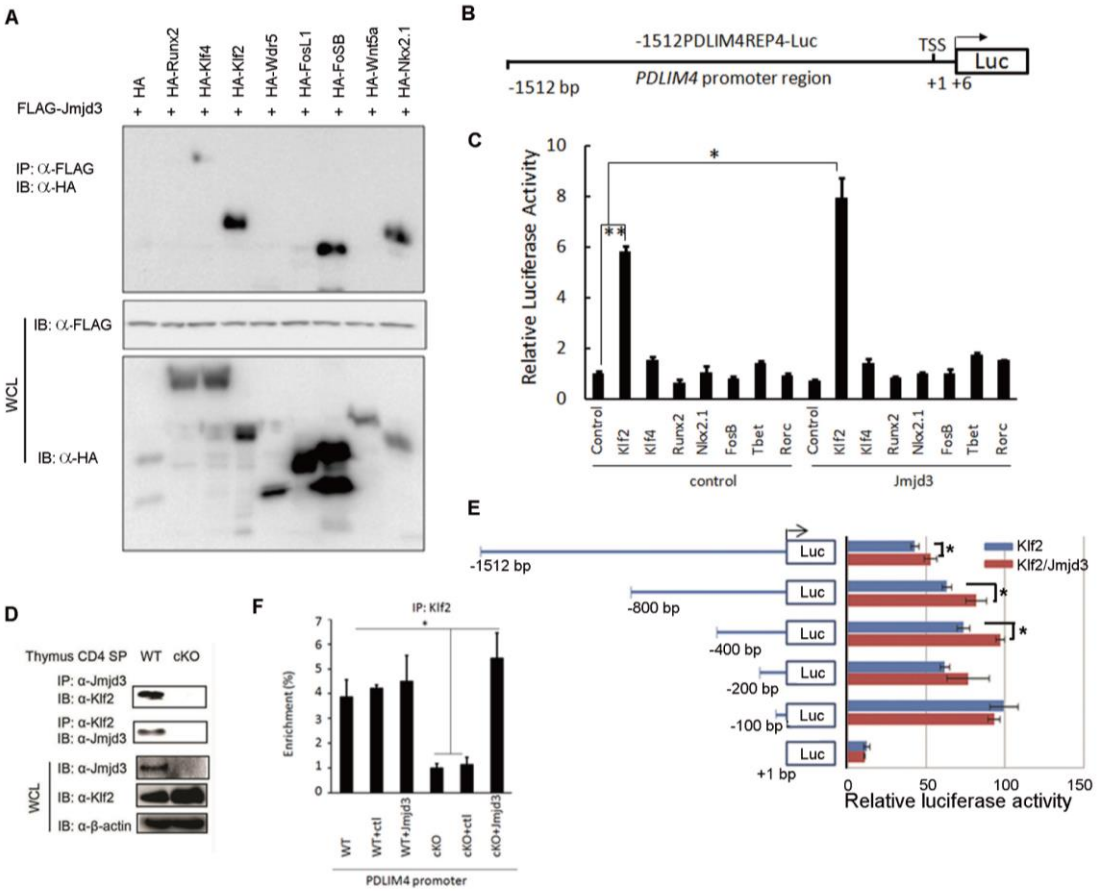

Figure 2.7 Jmjd3 regulates *Pdlim4* expression by interacting with KLF2. (A) Screening of transcription factors interacting with Jmjd3. 293T cells were co-transfected with HA-tagged *Runx2*, *Klf4*, *Klf2*, *Wdr5*, *Fosl1*, *FosB*, *Wnt5a*, *Nkx2.1*, and FLAG-*Jmjd3*. Whole cell lysates (WCLs) were immunoprecipitated with anti-FLAG antibodies and immunoblotted with anti-HA antibody. (B) Schematic presentation of the *Pdlim4* promoter-driven luciferase construct. The promoter region -1512 bp upstream was cloned into an episomal luciferase vector. (C) The transcriptional activity of proteins interacting with Jmjd3 in regulating *Pdlim4* was evaluated by dual-luciferase assay. The data are presented as means ± SD from three independent experiments. Asterisks indicate significant differences between groups (**P* < 0.05, ***P* < 0.01 determined by Student's t test). (D) Thymic CD4 SP T cells were isolated from WT and *Jmjd3* cKO mice and immunoprecipitated with anti-Jmjd3 or anti-Klf2 antibodies and protein (A+G) beads. The immunoprecipitated product was immunoblotted with anti-Klf2 or anti-Jmjd3 antibodies. (E) Mapping the Klf2 and Jmjd3 binding regions of the *Pdlim4* promoter using a dual-luciferase assay. Different regions of the *Pdlim4* promoter were cloned into the episomal luciferase vector, and then were co-transfected with *Klf2* and *Jmjd3* into 293T cells. The data are presented as means ± SD from three independent experiments. Asterisks indicate significant differences between groups (**P* < 0.05, determined by Student's t test). (F) ChIP-qPCR analysis of % enrichment of Klf2 at the *Pdlim4* promoter in WT and *Jmjd3* cKO thymic CD4 SP T cells after ectopic expression *Jmjd3* (**P* < 0.05 determined by Student's t test).

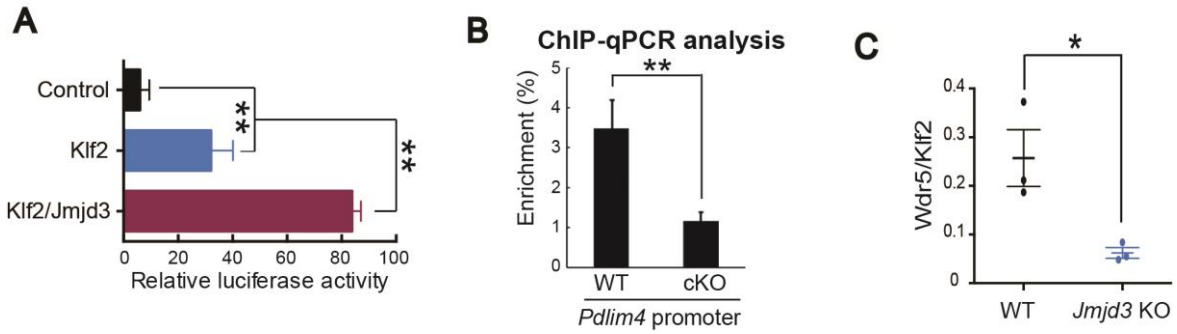

Figure 2.8 KLF2 bind to the promoter of *Pdlim4* and co-active *Pdlim4* expression by co-operating with Jmjd3. (A) 1.6K *Pdlim4* promoter were cloned into the episomal luciferase vector, and then were co-transfected with *Klf2* and *Jmjd3* into $CD4^+$ T cells. The data are presented as means ± SD from three independent experiments. (B) ChIP-qPCR analysis of the % enrichment of Klf2 binding to the *Pdlim4* promoter in WT and *Jmjd3* cKO CD4 SP T cells. (C) Klf band and Wdr5 band from Klf2 IP experiment quantified by Image J. The data are presented as means ± SD from three independent experiments. Asterisks indicate significant differences between groups (*$P < 0.05$, **$P < 0.01$, as determined by Student's t test).

2.2.6 Jmjd3 deficiency alters the methylation state of H3K27 and H3K4 on *Pdlim4* promoter

We previously reported that *Jmjd3* deletion specifically increases H3K27 di- and tri-methylation in $CD4^+$ T cells and also affected H3K4 methylation (Li et al., 2014). By dissecting the ChIP-Seq data for individual genes of interest, we found that *Pdlim4* and *S1p1*, but not *Klf2*, were highly bivalently marked in *Jmjd3* cKO CD4 SP T cells **(Figure 2.9 A)**. Both *Klf2* and *S1p1* genes contained high levels of H3K4me3, but little or low levels of H3K27me3. Conversely, the upstream promoter regions of the TSS and even gene body regions of *Pdlim4* harbored high levels of H3K27me3 in *Jmjd3* cKO CD4 SP T cells, which were higher than in WT CD4 SP T cells **(Figure 2.9 A)**. For genes such as *Ccr7, Cd62l*,

Cd69, and *Klf4*, we did not observe appreciable changes in H3K4me3 and H3K27me3 levels **(Figure 2.10)**.

To validate our ChIP-Seq data on the methylation status of *Pdlim4,* we performed ChIP-qPCR using WT CD4 SP T and *Jmjd3*-deficient CD4 SP T cells and antibodies used were against H3K4me3 and H3K27me3. Interestingly, we observed a marked decrease in H3K4me3 and a marked increase in H3K27me3 levels on the *Pdlim4* gene promoter in *Jmjd3*-deficient $CD4^+$ T cells as compared with WT cells **(Figure 2.9 B)**, suggesting that downregulation of *Pdlim4* in *Jmjd3* cKO CD4 SP T cells may be as result of changes in these epigenetic markers. To determine whether the demethylase activity of Jmjd3 is required for regulating *Pdlim4* expression, a luciferase assay was performed on 293T cells co-transfected with *Pdlim4* promoter-linked episomal luciferase vector and with *Klf2* in the presence of WT or mutant *Jmjd3* (a loss of demethylase function mutation). *Jmjd3* significantly enhanced Klf2-mediated *Pdlim4* promoter activity; whereas mutant *Jmjd3* failed to enhance Klf2-mediated *Pdlim4* promoter activity **(Figure 2.9 C)**. Altogether, these results suggest that *Pdlim4* gene expression in CD4 SP T cells is dependent on Jmjd3-dependent methylation of H3K27/H3K4 on *Pdlim4,* which may regulate T-cell trafficking.

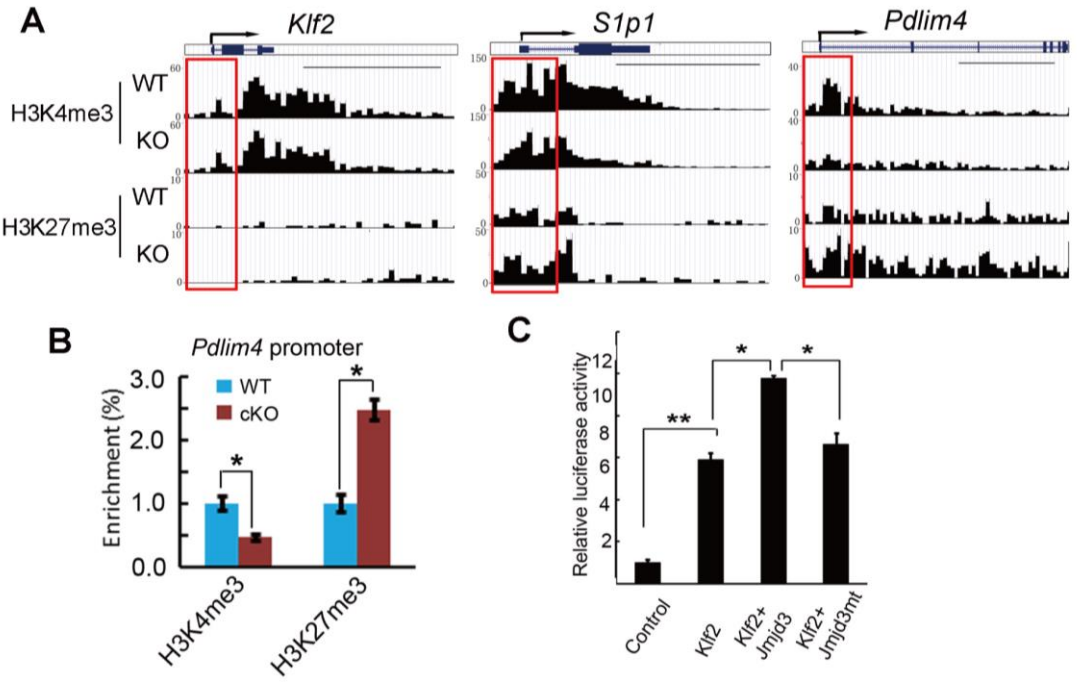

Figure 2.9 H3K27me3 and H3K4me3 levels in the *Pdlim4* promoter in WT and *Jmjd3*-deficient T cells. (A) ChIP-Seq analysis of H3K27me3 and H3K4me3 levels in the promoter and gene body regions of *Klf2*, *S1p1*, and *Pdlim4* in thymic CD4 SP T cells isolated from WT and *Jmjd3* cKO mice. A 2-kb region around the TSS is indicated in a red box. Scale bars represent 5 kb regions. (B) Validation of methylation changes on the *Pdlim4* gene in WT and *Jmjd3* cKO CD4 SP T cells by ChIP-qPCR. The data represents mean ± SD from three independent experiments (*$P < 0.05$ determined by Student's t test). (C) Luciferase assay was performed on 293T cells co-transfected with *Pdlim4* promoter-linked episomal luciferase vector and with *Klf2* in the presence of WT or mutant *Jmjd3* (a loss of demethylase function mutation). The data are presented as means ± SD from three independent experiments. Asterisks indicate significant differences between groups (*$P < 0.05$, **$P < 0.01$ determined by Student's t test).

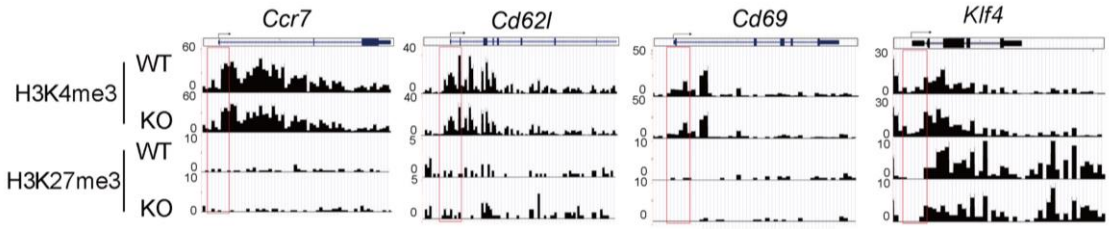

Figure 2.10 ChIP-seq analysis the H3K27me3 and H3K4me3 levels of *Ccr7*, *Cd62l*, *Cd69*, and *Klf4* in WT and *Jmjd3* cKO CD4 SP T cells. A 1-kb region around the TSS is indicated in a red box. 10 kb region is analyzed.

2.2.7 Jmjd3 stabilizes the interaction between Klf2-Wdr5 and regulates *Pdlim4* expression

Jmjd3 also co-regulates H3K4 methylation levels by interacting with the H3K4 methyltransferase complex and transcription factors (Li et al., 2014). To determine whether Klf2 also interacts with the H3K4 methyltransferase complex and Jmjd3, we performed co-immunoprecipitation and immunoblot analyses on 293T cells co-transfected with HA-*Klf2* and FLAG-tagged *Ash2l, Rbbp5, Wdr5*, and *Dpy30*. Klf2 specifically interacted with Wdr5, but not Ash2L, RbBP5, and Dpy30 **(Figure 2.11 A)**. To confirm the endogenous interaction of Klf2 with Wdr5, we isolated CD4 SP T-cell lysates, co-immunoprecipitated with anti-Klf2 antibody, and immunoblotted with anti-Jmjd3, anti-Wdr5, and anti-Klf2 antibodies respectively. Our results showed that Klf2 interacted with Wdr5, and Jmjd3 was required for stabilizing this interaction **(Figure 2.11 B and Figure 2.8 C)**. To dissect the regions responsible for this interaction, we generated HA-tagged N- and C-terminal regions of Klf2 **(Figure 2.11 C)**. 293T cells were co-transfected with HA-*Klf2*, HA-*Klf2-N*, or HA-*Klf2-C* along with either FLAG-*Wdr5* or FLAG-*Jmjd3*. We collected whole cell lysates (WCLs), immunoprecipitated with anti-FLAG beads, and immunoblotted with anti-HA antibody and co-IP experiments revealed that the N-terminal region of Klf2 interacts with FLAG-Wdr5 and the C-terminal region of Klf2 interacts with FLAG-Jmjd3 **(Figure 2.11, D** and **E)**. To address which regions of Jmjd3 are involved in the interaction with either Klf2 or Ash2L, we co-transfected 293T cells with HA-Klf2 and HA-tagged N-terminal, C-terminal, or M-middle regions of *Jmjd3*. WCLs were immunoprecipitated with anti-Klf2 antibody and immunoblotted with anti-HA antibody. We found that the N-terminal region of *Jmjd3* interacts with Klf2 **(Figure 2.11 F)**. We also performed co-immunoprecipitation and

immunoblot analysis using 293T cells, which were co-transfected with FLAG-Ash2L and HA-N-terminal, C-terminal, and M-middle regions of *Jmjd3* and found that the C-terminal region of *Jmjd3* interacts with Ash2L **(Figure 2.11 G)**. Taken together, our results demonstrate that Jmjd3 regulates *Pdlim4* expression by interacting with the transcription factor Klf2 and the H3K4 methyltransferase complex protein Ash2L **(Figure 2.11 H)**.

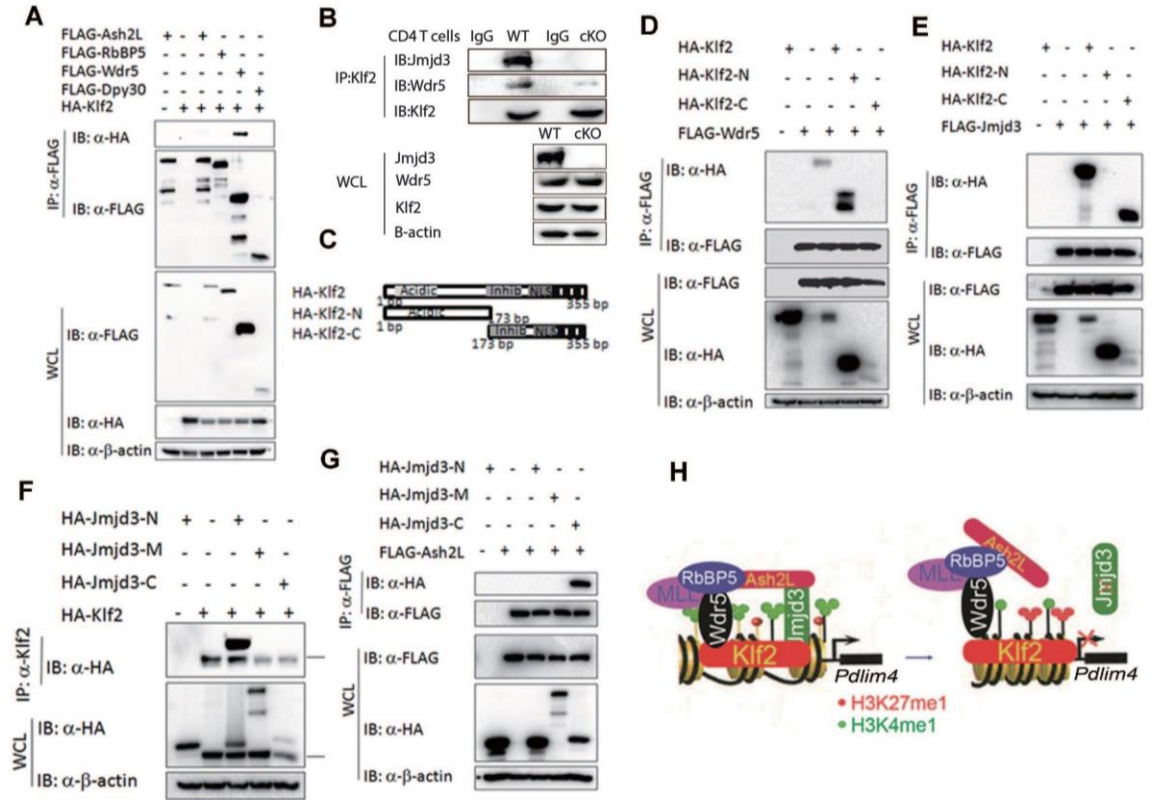

Figure 2.11 Jmjd3 regulates Pdlim4 by facilitating the interaction between Klf2-Wdr5. (A) 293T cells were co-transfected with HA-*Klf2* and FLAG-tagged *Ash2L*, *RbBP5*, *Wdr5*, or *Dpy30*. Whole cell lysates (WCLs) were immunoprecipitated with anti-FLAG beads and immunoblotted with anti-HA antibody. (B) Cell lysates from WT and *Jmjd3* cKO CD4 SP T cells were immunoprecipitated with anti-Klf2 antibody and immunoblotted with anti-Jmjd3, Wdr5, and Klf2 antibodies, respectively. (C) Schematic presentation of cloned HA-tagged N- and C-terminal regions of Klf2. (D) 293T cells were co-transfected with HA-N-terminal, C-terminal, or full-length *Klf2* along with FLAG-*Wdr5*. Whole cell lysates (WCLs) were immunoprecipitated with anti-FLAG beads and immunoblotted with anti-HA antibody. (E) 293T cells were co-transfected with HA-N-terminal, C-terminal, or full-length *Klf2* along with FLAG-*Jmjd3*. Whole cell lysates (WCLs) were immunoprecipitated with anti-FLAG beads and immunoblotted with anti-HA antibody. (F) 293T cells were co-transfected with HA-N-terminal, C-terminal, or middle region of *Jmjd3* along with HA-*Klf2*. Whole cell lysates (WCLs) were immunoprecipitated with anti-Klf2 antibody and immunoblotted with anti-HA antibody. (G) 293T cells were co-transfected with HA-N-terminal, C-terminal, or middle region of Jmjd3 along with FLAG-*Ash2L*. Whole cell lysates (WCLs) were immunoprecipitated with anti-FLAG antibody and immunoblotted with anti-HA antibody. (H) Schematic diagram of proposed mechanism of how Jmjd3 and Klf2 regulate *Pdlim4* expression. Jmjd3 interacts with the MLL4 protein Ash2L and forms a stable complex with Klf2, which is capable of binding to the *Pdlim4* promoter. This permits Jmjd3 to alter the H3K27 methylation state of *Pdlim4* and permits Ash2L to alter H3K4 methylation to control *Pdlim4* expression.

2.3 Discussion

During development, early thymic progenitor cells (TPCs) differentiate into T-cell receptor (TCR)-expressing $CD4^+CD8^+$ double-positive (DP) thymocytes in the cortex of thymus, and then mature into single-positive (SP) $CD4^+$ and $CD8^+$ T cells in the medulla (Love and Bhandoola, 2011; Petrie, 2003; Spiegel and Milstien, 2011). After negative and positive selection, CD4 SP T cells emigrate from the thymus to the periphery, e.g., peripheral blood, spleen, and LNs. The epigenetic modifier Jmjd3 has been shown to play critical role in macrophage and T-cell differentiation, but its role and mechanism in T-cell migration are not clear. In this study, we demonstrate that *Jmjd3* ablation results in diminished emigration of mature CD4 SP T cells from the thymus and decreased numbers of CD4 T cells in secondary lymphoid organs. T-cell migration from the thymus to secondary lymphoid organs is regulated by S1P1, whereas T-cell entry into resting LNs typically requires CD62L and CCR7 (Love and Bhandoola, 2011; Masopust and Soerens, 2019). It is known that Klf2 regulates expression of *S1p1*, *Cd62l* and *Ccr7* (Love and Bhandoola, 2011). S1P1 is highly expressed in mature SP T cells and mediate SP T cell migration along S1P concentration gradients from the thymus to the periphery. Deficiency in Klf2 or S1P1 leads to impaired thymic egress (Cyster and Schwab, 2012; Matloubian et al., 2004; Spiegel and Milstien, 2011). T cell migration phenotypes in in T-cell-specific *Jmjd3*-deficient mice are similar to Klf2 deficient mice (Carlson et al., 2006), leading to the accumulation of mature SP T cells in the thymus, associated with lower numbers of SP T cells in the spleen and LNs, as well as downregulation of *S1p1*, *Cd62l* and *Ccr7*. To further understand how Jmjd3 affects T-cell migration, we identified a novel Jmjd3 target gene, *Pdlim4*, which plays an important role

in T-cell trafficking. Although *Pdlim4* is the most downregulated gene, other genes including *S1p1, Cd62l* and *Ccr7, but not Klf2,* are also downregulated at the RNA level in *Jmjd3*-deficient mature SP T cells. Ectopic expression of *Pdlim4* in *Jmjd3*-deficient $CD4^+$ T cells restores their ability to migrate in both the spleen and LNs. Using chimeric mice and adoptive T-cell transfer experiments, we demonstrated that ablation of *Pdlim4* in $CD4^+$ T cells reduces splenic T-cell accumulation. Furthermore, we showed that removal of H3K27me3 by Jmjd3 is a critical event in regulating *Pdlim4 and S1p1* expression, but not in the promoter regions of *Cd62l* and *Ccr7*. Thus, our study identified a previously unrecognized role for PDLIM4 in T-cell migration.

PDLIM4 has been identified as a modifier of actin filament dynamics in muscle cells and nonmuscle epithelial cells (Boumber et al., 2007; Guryanova et al., 2011), but how PDLIM4 regulates T cell migration remains unknown. Our findings present in this study indicate that PDLIM4 could rescue the F-actin assembly and remodeling deficiency after *Pdlim4* overexpression in *Jmjd3*-deficient $CD4^+$ T-cells, thus demonstrating the critical role of PDLIM4 for F-actin organization in thymic CD4 SP T cells. Furthermore, S1P/S1P1 signaling is also known to induced cytoskeleton remodeling by increasing polymerization of actin filaments in T cells (Mudd et al., 2013), but how S1P/S1P1 signaling is linked to cytoskeleton remodeling is not clear. To understand the molecular mechanisms of how PDLIM4 regulates T cell migration, we show that PDLIM4 interacts with S1P1 through the N-terminal PDZ domain and anchors to F-actin through the C-terminal LIM domain. Thus, our mechanistic studies suggest that PDLIM4 acts as an adaptor bridging between S1P1 signaling and F-actin remodeling during T cell migration.

Previous studies have shown that due to hypermethylation, a significant inhibition of *Pdlim4* expression in prostate cancer was observed (Vanaja et al., 2006; Vanaja et al., 2009), but the epigenetic factors responsible for this hypermethylation at the *Pdlim4* promoter remains to be identified. Consistent with these observations, our ChIP-PCR and ChIP-Seq analyses show a substantial increase in H3K27me3 and a decrease in H3K4me3 in the promoter and gene body regions of *Pdlim4,* as well as *S1pr1* (but to lesser extent) in *Jmjd3*-deficient CD4 SP T cells. However, Jmjd3 alone did not enhance *Pdlim4* expression without Klf2, suggesting co-regulation of *Pdlim4* by Jmjd3 and Klf2. By contrast, we observed a marked reduction in H3K4me3 (with a small increase in H3K27me3) in the promoter and gene body regions of *S1p1*. Not only does Jmjd3 harbor H3K27 demethylase activity, it can also associate with H3K4 methyltransferase complexes and affect H3K4me3 levels at gene promoters. Indeed, we found that Jmjd3 directly interacts with Ash2L, a core component of the H3K4 methyltransferase complex (Li et al., 2014; Miller et al., 2008; Miller et al., 2010). We further showed that Klf2 interacts with Wdr5, another component of the H3K4 methyltransferase complex. However, Jmjd3 is required for stabilizing the interaction between Klf2 with Wdr5. Based on these findings, we propose that Jmjd3 regulates *Pdlim4* and known KLF2-regulated genes (*S1p1, Cd62l and Ccr7*) by interacting with Klf2, WDR5 and Ash2L in the H3K4 methyltransferase complex. Jmjd3 ablation disrupts the Klf2-Jmjd3-Ash2L complex, leading to an increase in H3K27me3 and/or a reduction in H3K4me3 in the promoter and gene body of *Pdlim4*, thus down regulating target gene expression. The changes in H3K4me3 and/or H3K27me3 in the gene body are supported by findings that Jmjd3 is involved in the protein complex engaged in transcriptional elongation (Chen et al.,

2012). Thus, our study provides the molecular insights by which Jmjd3 regulates *Pdlim4* gene expression through interaction with Klf2, Wdr5 and Ash2L as a transcription complex.

In summary, our studies provide genetic evidence that T-cell-specific deletion of *Jmjd3* results in multiple defects in T-cell migration. Gene profiling and ChIP-Seq analysis identifies a novel Jmjd3 target gene *Pdlim4.* Importantly, PDLIM4 bridges S1P1-mediated extracellular signaling and F-actin formation, which is critical for T cell migration and trafficking through its PDZ domain in the N-terminus and LIM domain in the C-terminus. Mechanistically, Jmjd3 regulates *Pdlim4* expression through interaction with Klf2, Wdr5 and Ash2L in the promoter and gene body regions of *Pdlim4.* Thus, our results have provided insights into the molecular mechanisms by which Jmjd3 and its target PDLIM4 regulate T-cell migration.

2.4 Materials and methods

Mice

Jmjd3 $^{f/f}$:CD4-Cre mice were generated as previously described (Li et al., 2014). C57BL/6 and 2D2 mice were purchased from The Jackson Laboratory. *Rag2*$^{-/-}\gamma c^{-/-}$ mice were purchased from Taconic. All the mice were re-derived by standard embryo transfer and maintained in pathogen-free animal facilities at the Houston Methodist Research Institute. These studies were reviewed and approved by Institutional Animal Care and Use Committee at the Houston Methodist Research Institute.

Immunoprecipitation and Western blot analysis

For immunoprecipitation, cells were lysed in ice-cold lysis buffer (40 mM Tris-HCl, pH7.5, 150 mM NaCl, and 1% Triton X-100) with proteinase inhibitor. Supernatants were incubated overnight with primary antibody (2μg) and immunocomplexes were allowed to bind to protein A/G beads for 90 mins at 4° C. Immunoprecipitates were washed three times with the lysis buffer. Western blotting was performed under conventional conditions after extracting the samples in SDS sample buffer. Protein extracts were separated by SDS-PAGE and electrotransferred onto PVDF membrane (Millipore). The membranes were exposed to primary antibodies, washed, incubated with secondary antibodies and proteins were visualized by using Pierce Western Blotting Substrate Plus (Thermo Fisher).

Flow cytometry

To detect the expression of surface molecules, T cells were first incubated with an anti-Fc receptor Ab (24G2) to reduce nonspecific binding of mAbs, and then labeled with the appropriate fluorescent mAbs. Appropriate fluorescein-conjugated, isotype-matched, control mAbs were used as negative controls. Cells were analyzed with BD FACS Aria II.

Real-time RT-PCR

Total RNA was extracted from cultured cells with TRIzol (Invitrogen) according to the manufacturer's instructions. Oligo (dT) primers and Superscript III reverse transcriptase (Invitrogen) were used for the generation of cDNA from mRNA. Gene expression was determined by quantitative PCR with SYBR Green MasterMix (ABI), and the reactions were

run on an ABIPRISM 7900HT Sequence Detection System (Life Science). Primers used for real-time PCR analysis are shown in **APPENDIX Table A-2**.

Microarray analysis

RNA was extracted from three sorted biological replicates of CD4 SP thymocytes from WT and *Jmjd3* cKO mice. Gene expression profiling was conducted by Genomics and Microarray Core Facility of UT Southwestern Medical Center with Illumina whole genome gene expression arrays. Gene transcripts with greater than 1.5-fold difference in expression were analyzed with Ingenuity pathway analysis software.

Phalloidin staining, Immunofluorescence, confocal image analysis

Serum-starved cells were incubated in RPMI/20 mM HEPES and 20 nM S1P was added. Whenever required, cells were first labeled with antibodies against extracellular markers such as CD4, washed, fixed in 4%PFA/PBS on ice for 2-4 h, blocked and permeabilized in PBS containing 3% FBS, and 0.5% Triton X-100 for phalloidin staining, which is specific staining for F-actin. CD4+ T cells on poly-lysine coated coverslips were processed for immunofluorescence as described (Vallenius et al., 2004). Slides were imaged by Nikon A1si confocal imaging system. The image analysis was performed by Image J software.

Bone marrow chimeras

Bone marrow cells were isolated from female C57BL6/J mice (8 to 10 weeks of age). The cells were transfected with either retrovirus vector expressing *Pdlim4* or lentivirus vector containing *Pdlim4* CRISPR/Cas9 genome editing elements. These bone marrow cells were

injected into lethally irradiated (950 rads) recipient mice (female C57BL6/J mice [8 to 10 weeks of age]).

Retrovirus production and transduction

Jmjd3 and Pdlim4 genes were cloned into retrovirus expression vector with a GFP-expressing cassette (pCLIG-IRES-GFP), respectively. Retroviral particles were produced in 293T cells transfected with retroviral vectors plus pCL-ECO retroviral packaging plasmid using Lipofectamine 2000 (Invitrogen). Sorted naïve $CD4^+$ T cells were plated and activated with anti-CD3 and anti-CD28 for 1 day, transduced with retroviral supernatants and were spun at 2500 rpm for 1.5 h at 32°C. After spin infection, the cells were cultured in T cell culture medium and harvested on day 5 for subsequent T-cell transfer experiments.

Pdlim4 knockout by CRISPR-Cas9 and T cell migration analysis

Naive thymic CD4 SP T cells collected from WT mice were transduced with lentivirus containing *Pdlim4* sgRNA plasmids. Equal number of cells (10 million) were labeled by CFSE and intravenously injected into sublethally irradiated C57BL/6 mice and 48 h later peripheral blood was collected from the recipient mice. Single-cell suspensions were prepared from the isolated spleens and LNs of the recipient mice. The CFSE-labeled CD4 SP T cells isolated from the spleens, LNs, and peripheral blood were analyzed by FACS assay.

F-actin binding assay

F-actin cosedimentation assay was performed as described previously (Vanaja et al., 2009) using the Actin Binding Protein Spin Down Assay Kit (Cytoskeleton Inc. BK001) and recombinant GST-PDLIM4 fusion protein. GST-PDLIM4 were mixed with F-actin in F-actin buffer at room temperature for 30 mins and centrifuged at 150,000g for 1.5 hours at 24°C. The supernatants were then removed and the pellets were suspended in the same buffer. Aliquots of pellets and supernatants were mixed with the loading dye and run on a SDS-PAGE gel, followed by Western blot analysis.

ChIP-Seq and Chip-PCR analyses

$CD4^+$ T cells from WT and *Jmjd3* cKO mice were purified and a total of 200 ng of DNA was used for the ChIP-Seq library construction. Illumina sequencing was performed according to previously described protocols (Barski et al., 2007; Qi et al., 2010; Wang et al., 2010). Samples in triplicate were used for all experiments. All primers are listed in **APPENDIX Table A-2**.

Statistical analyses

Results represent the mean ± SD where applicable. Student's t-test was used to all statistical analysis with the GraphPad Prism 4.0 software. For all tests, values of $p<0.05$ were considered statistically significant.

2.5 References

Agger, K., P.A. Cloos, J. Christensen, D. Pasini, S. Rose, J. Rappsilber, I. Issaeva, E. Canaani, A.E. Salcini, and K. Helin. 2007. *UTX and JMJD3 are histone H3K27 demethylases involved in HOX gene regulation and development.* Nature. 449:731-734.

Barski, A., S. Cuddapah, K. Cui, T.Y. Roh, D.E. Schones, Z. Wang, G. Wei, I. Chepelev, and K. Zhao. 2007. *High-resolution profiling of histone methylations in the human genome.* Cell. 129:823-837.

Black, J.C., C. Van Rechem, and J.R. Whetstine. 2012. *Histone lysine methylation dynamics: establishment, regulation, and biological impact.* Mol Cell. 48:491-507.

Boumber, Y.A., Y. Kondo, X. Chen, L. Shen, V. Gharibyan, K. Konishi, E. Estey, H. Kantarjian, G. Garcia-Manero, and J.P. Issa. 2007. *RIL, a LIM gene on 5q31, is silenced by methylation in cancer and sensitizes cancer cells to apoptosis.* Cancer Res. 67:1997-2005.

Cao, R., L. Wang, H. Wang, L. Xia, H. Erdjument-Bromage, P. Tempst, R.S. Jones, and Y. Zhang. 2002. *Role of histone H3 lysine 27 methylation in Polycomb-group silencing.* Science. 298:1039-1043.

Carlson, C.M., B.T. Endrizzi, J. Wu, X. Ding, M.A. Weinreich, E.R. Walsh, M.A. Wani, J.B. Lingrel, K.A. Hogquist, and S.C. Jameson. 2006. *Kruppel-like factor 2 regulates thymocyte and T-cell migration.* Nature. 442:299-302.

Chen, S., J. Ma, F. Wu, L.J. Xiong, H. Ma, W. Xu, R. Lv, X. Li, J. Villen, S.P. Gygi, X.S. Liu, and Y. Shi. 2012. *The histone H3 Lys 27 demethylase JMJD3 regulates gene expression by impacting transcriptional elongation.* Genes Dev. 26:1364-1375.

Chi, P., C.D. Allis, and G.G. Wang. 2010. *Covalent histone modifications--miswritten, misinterpreted and mis-erased in human cancers.* Nat Rev Cancer. 10:457-469.

Cloos, P.A., J. Christensen, K. Agger, and K. Helin. 2008. *Erasing the methyl mark: histone demethylases at the center of cellular differentiation and disease.* Genes Dev. 22:1115-1140.

Cyster, J.G., and S.R. Schwab. 2012. *Sphingosine-1-phosphate and lymphocyte egress from lymphoid organs.* Annu. Rev. Immunol. 30:69-94.

Garris, C.S., L. Wu, S. Acharya, A. Arac, V.A. Blaho, Y. Huang, B.S. Moon, R.C. Axtell, P.P. Ho, G.K. Steinberg, D.B. Lewis, R.A. Sobel, D.K. Han, L. Steinman, M.P. Snyder, T. Hla, and M.H. Han. 2013. *Defective sphingosine 1-phosphate receptor 1 (S1P1) phosphorylation exacerbates TH17-mediated autoimmune neuroinflammation.* Nat Immunol. 14:1166-1172.

Guryanova, O.A., J.A. Drazba, E.I. Frolova, and P.M. Chumakov. 2011. *Actin cytoskeleton remodeling by the alternatively spliced isoform of PDLIM4/RIL protein.* J. Biol. Chem. 286:26849-26859.

Hong, S., Y.W. Cho, L.R. Yu, H. Yu, T.D. Veenstra, and K. Ge. 2007. *Identification of JmjC domain-containing UTX and JMJD3 as histone H3 lysine 27 demethylases.* Proc Natl Acad Sci U S A. 104:18439-18444.

Jepsen, K., D. Solum, T. Zhou, R.J. McEvilly, H.J. Kim, C.K. Glass, O. Hermanson, and M.G. Rosenfeld. 2007. *SMRT-mediated repression of an H3K27 demethylase in progression from neural stem cell to neuron.* Nature. 450:415-419.

Jin, C., J. Li, C.D. Green, X. Yu, X. Tang, D. Han, B. Xian, D. Wang, X. Huang, X. Cao, Z. Yan, L. Hou, J. Liu, N. Shukeir, P. Khaitovich, C.D. Chen, H. Zhang, T. Jenuwein, and J.D. Han. 2011. *Histone demethylase UTX-1 regulates C. elegans life span by targeting the insulin/IGF-1 signaling pathway.* Cell Metab. 14:161-172.

Klose, R.J., and Y. Zhang. 2007. *Regulation of histone methylation by demethylimination and demethylation.* Nat Rev Mol Cell Biol. 8:307-318.

Kouzarides, T. 2007. *Chromatin modifications and their function.* Cell. 128:693-705.

Lan, F., P.E. Bayliss, J.L. Rinn, J.R. Whetstine, J.K. Wang, S. Chen, S. Iwase, R. Alpatov, I. Issaeva, E. Canaani, T.M. Roberts, H.Y. Chang, and Y. Shi. 2007. *A histone H3 lysine 27 demethylase regulates animal posterior development.* Nature. 449:689-694.

Lee, H.J., and J.J. Zheng. 2010. *PDZ domains and their binding partners: structure, specificity, and modification.* Cell Commun Signal. 8:8.

Lee, K., W. Na, J.Y. Lee, J. Na, H. Cho, H. Wu, T.Y. Yune, W.S. Kim, and B.G. Ju. 2012. *Molecular mechanism of Jmjd3-mediated interleukin-6 gene regulation in endothelial cells underlying spinal cord injury.* J Neurochem. 122:272-282.

Lee, S.H., and R. Dominguez. 2010. *Regulation of actin cytoskeleton dynamics in cells.* Mol Cells. 29:311-325.

Li, Q., J. Zou, M. Wang, X. Ding, I. Chepelev, X. Zhou, W. Zhao, G. Wei, J. Cui, K. Zhao, H.Y. Wang, and R.F. Wang. 2014. *Critical role of histone demethylase Jmjd3 in the regulation of CD4+ T-cell differentiation.* Nat Commun. 5:5780.

Love, P.E., and A. Bhandoola. 2011. *Signal integration and crosstalk during thymocyte migration and emigration.* Nat Rev Immunol. 11:469-477.

Manna, S., J.K. Kim, C. Bauge, M. Cam, Y. Zhao, J. Shetty, M.S. Vacchio, E. Castro, B. Tran, L. Tessarollo, and R. Bosselut. 2015. *Histone H3 Lysine 27 demethylases Jmjd3 and Utx are required for T-cell differentiation.* Nat Commun. 6:8152.

Margueron, R., and D. Reinberg. 2011. *The Polycomb complex PRC2 and its mark in life.* Nature. 469:343-349.

Masopust, D., and A.G. Soerens. 2019. *Tissue-Resident T Cells and Other Resident Leukocytes.* Annu. Rev. Immunol.

Matloubian, M., C.G. Lo, G. Cinamon, M.J. Lesneski, Y. Xu, V. Brinkmann, M.L. Allende, R.L. Proia, and J.G. Cyster. 2004. *Lymphocyte egress from thymus and peripheral lymphoid organs is dependent on S1P receptor 1*. Nature. 427:355-360.

Miller, S.A., A.C. Huang, M.M. Miazgowicz, M.M. Brassil, and A.S. Weinmann. 2008. *Coordinated but physically separable interaction with H3K27-demethylase and H3K4-methyltransferase activities are required for T-box protein-mediated activation of developmental gene expression.* Genes Dev. 22:2980-2993.

Miller, S.A., S.E. Mohn, and A.S. Weinmann. 2010. *Jmjd3 and UTX play a demethylase-independent role in chromatin remodeling to regulate T-box family member-dependent gene expression.* Mol Cell. 40:594-605.

Mosammaparast, N., and Y. Shi. 2010. *Reversal of histone methylation: biochemical and molecular mechanisms of histone demethylases.* Annu Rev Biochem. 79:155-179.

Mudd, J.C., P. Murphy, M. Manion, R. Debernardo, J. Hardacre, J. Ammori, G.A. Hardy, C.V. Harding, G.H. Mahabaleshwar, M.K. Jain, J.M. Jacobson, A.D. Brooks, S. Lewis, T.W. Schacker, J. Anderson, E.K. Haddad, R.A. Cubas, B. Rodriguez, S.F. Sieg, and M.M. Lederman. 2013. *Impaired T-cell responses to sphingosine-1-phosphate in HIV-1 infected lymph nodes.* Blood. 121:2914-2922.

Petrie, H.T. 2003. *Cell migration and the control of post-natal T-cell lymphopoiesis in the thymus.* Nat Rev Immunol. 3:859-866.

Qi, H.H., M. Sarkissian, G.Q. Hu, Z. Wang, A. Bhattacharjee, D.B. Gordon, M. Gonzales, F. Lan, P.P. Ongusaha, M. Huarte, N.K. Yaghi, H. Lim, B.A. Garcia, L. Brizuela, K. Zhao, T.M. Roberts, and Y. Shi. 2010. *Histone H4K20/H3K9 demethylase PHF8 regulates zebrafish brain and craniofacial development.* Nature. 466:503-507.

Samstag, Y., S.M. Eibert, M. Klemke, and G.H. Wabnitz. 2003. *Actin cytoskeletal dynamics in T lymphocyte activation and migration.* J Leukoc Biol. 73:30-48.

Satoh, T., O. Takeuchi, A. Vandenbon, K. Yasuda, Y. Tanaka, Y. Kumagai, T. Miyake, K. Matsushita, T. Okazaki, T. Saitoh, K. Honma, T. Matsuyama, K. Yui, T. Tsujimura, D.M. Standley, K. Nakanishi, K. Nakai, and S. Akira. 2010. *The Jmjd3-Irf4 axis regulates M2 macrophage polarization and host responses against helminth infection.* Nat Immunol. 11:936-944.

Sebzda, E., Z. Zou, J.S. Lee, T. Wang, and M.L. Kahn. 2008. *Transcription factor KLF2 regulates the migration of naive T cells by restricting chemokine receptor expression patterns.* Nat Immunol. 9:292-300.

Spiegel, S., and S. Milstien. 2011. *The outs and the ins of sphingosine-1-phosphate in immunity.* Nat Rev Immunol. 11:403-415.

Trujillo, J.A., R.F. Sweis, R. Bao, and J.J. Luke. 2018. *T Cell-Inflamed versus Non-T Cell-Inflamed Tumors: A Conceptual Framework for Cancer Immunotherapy Drug Development and Combination Therapy Selection.* Cancer Immunol Res. 6:990-1000.

Vallenius, T., B. Scharm, A. Vesikansa, K. Luukko, R. Schafer, and T.P. Makela. 2004. *The PDZ-LIM protein RIL modulates actin stress fiber turnover and enhances the association of alpha-actinin with F-actin.* Exp. Cell Res. 293:117-128.

van der Woude, L.L., M.A.J. Gorris, A. Halilovic, C.G. Figdor, and I.J.M. de Vries. 2017. *Migrating into the Tumor: a Roadmap for T Cells.* Trends Cancer. 3:797-808.

Vanaja, D.K., K.V. Ballman, B.W. Morlan, J.C. Cheville, R.M. Neumann, M.M. Lieber, D.J. Tindall, and C.Y. Young. 2006. *PDLIM4 repression by hypermethylation as a potential biomarker for prostate cancer.* Clin. Cancer Res. 12:1128-1136.

Vanaja, D.K., M.E. Grossmann, J.C. Cheville, M.H. Gazi, A. Gong, J.S. Zhang, K. Ajtai, T.P. Burghardt, and C.Y. Young. 2009. *PDLIM4, an actin binding protein, suppresses prostate cancer cell growth.* Cancer Invest. 27:264-272.

Wang, L., Z. Feng, X. Wang, X. Wang, and X. Zhang. 2010. *DEGseq: an R package for identifying differentially expressed genes from RNA-seq data.* Bioinformatics. 26:136-138.

Weinreich, M.A., K. Takada, C. Skon, S.L. Reiner, S.C. Jameson, and K.A. Hogquist. 2009. *KLF2 transcription-factor deficiency in T cells results in unrestrained cytokine production and upregulation of bystander chemokine receptors.* Immunity. 31:122-130.

Yamada, T., C.S. Park, M. Mamonkin, and H.D. Lacorazza. 2009. *Transcription factor ELF4 controls the proliferation and homing of CD8+ T cells via the Kruppel-like factors KLF4 and KLF2.* Nat Immunol. 10:618-626.

Zachariah, M.A., and J.G. Cyster. 2009. *Thymic egress: S1P of 1000.* F1000 Biol Rep. 1:60.

CHAPTER III

LACK OF JMJD3 PROMOTES T-CELL PERSISTENCE AND ANTICANCER FUNCTION

Our previous study has shown that Jmjd3, a histone H3K27 demethylase, plays a critical role in gene expression and T-cell differentiation. However, its role and possible mechanisms in T cell persistence and memory T cells remain poorly understood. Here we demonstrate that *Jmjd3* deficiency in $CD4^+$ T cells resulted in an increase in memory T cell population. Further studies showed that *Jmjd3* deficiency enhances T cell persistence by decreasing CD4 T cell apoptosis after stimulation. T cells Adoptive transfer immunotherapy is a potentially curative therapeutic approach for patients with advanced cancer. These results demonstrate that Jmjd3 manipulation may support the generation of superior antitumor T cell grafts for adoptive immunotherapy.

3.1 Introduction

T cells are heterogeneous population including their different differentiation stages which define their diverse functions. The epigenetic state of naïve T cells keeps them in quiescent while maintaining their ability to proliferate and differentiate after antigen stimulation(Restifo et al., 2012). During antigen priming or under influence of environmental stimulation, naïve T cells differentiate into multiple lineages of effector and memory T cells. This leads to changes in epigenetic landscape along with dynamic changes in gene expression. In addition,, histone modification and DNA methylation are characteristics of the aging process and response to cellular dysfunction in senescence. Active and repressive epigenetic modification in T cells, including histone modification and

DNA methylation, are closely link with transcription profile and gene dynamic expression alteration upon TCR stimulation. Previous studies have highlighted that the differences in epigenetic architecture among different T cell subset are responsible for their distinct functions through the differential expression of multiple key transcription factors(Araki et al., 2008; Araki et al., 2009; Crompton et al., 2016; Russ et al., 2014; Scharer et al., 2013; Wang et al., 2009). Here, we studied the role of H3K27me3/2 eraser JMJD3 in memory T cell maintenance, survival and senescence.

Adoptive T cells transfer immunotherapy is a promising therapeutic option for cancer patients. The resource of anti-tumor T cells can be expanded from tumor antigen-specific T cells in the patient's tumor or peripheral blood (Rosenberg et al., 2004; Stagg et al., 2007). Another resource is the engineered T cells with tumor-specific T cell receptors (TCRs) or chimeric antigen receptors (CARs) (Sadelain et al., 2003). Both of these two strategies face the problem of T cell exhaustion which is the reason many of patients just achieve partial responses eventually relapse (Besser et al., 2013; Dudley et al., 2008; Mackensen et al., 2006; Robbins et al., 2011; Rosenberg et al., 2011). Many reports have shown that adoptive T cells transfer therapy outcome is highly correlated with the persistence of the transferred T cells (Butler et al., 2011; Davila et al., 2014; Louis et al., 2011; Maude et al., 2014; Morgan et al., 2006; Robbins et al., 2004; Tran et al., 2014). Enhancement in the survival and persistence of T cells will be a promising strategy for improving adoptive transfer therapy. The survival and persistence of T cells related with T cells subset. Both ex vivo culture and in vivo assay demonstrate that the T cell with surface markers pattern similar to memory t cells showed superior persistence and anti-cancer effects as compared with T cells with the

effector memory T cell (Tem) markers and phenotype in both mice and human (Cieri et al., 2013; Gattinoni et al., 2005; Hinrichs et al., 2008; Louis et al., 2011; Xu et al., 2014). Therefore, manipulation of T cell differentiation may promote memory T cell generation and thus enhance anti-cancer effect and get better clinical outcome for cancer patients.

In Chapter II, we showed that the roles of Jmjd3 in quiescent T-cells trafficking from thymus to secondary lymphoid organs. In Chapter III, we study the functions of Jmjd3 in activated T cells. The persistence of CD4 T cells after *Jmjd3* ablation was enhanced due to decreased apoptosis and cellular senescence, suggesting that the H3K27 demethylase Jmjd3 is essential for $CD4^+$ T-cell persistence. These findings show Jmjd3 may be a good therapeutic target for adoptive immunotherapy for the generation of superior T cell grafts.

3.2 Results

3.2.1 *Jmjd3*-deficient $CD4^+$ T cells with increased memory population and survival

To assess the role of Jmjd3 during T-cell development and function, we analyzed $CD4^+$ naïve ($CD62L^+CD44^{lo}$), effector memory ($CD62L^{lo}CD44^{hi}$), and central memory ($CD62L^+CD44^{hi}$) cell populations in the spleens of WT and *Jmjd3* cKO mice. The percentages of naïve $CD4^+$ T cells were reduced in *Jmjd3* cKO mice compared with WT mice (51.0% vs. 74.8%, respectively) **(Figure 3.1 A)**. By contrast, the numbers of effector memory $CD4^+$ T cells in *Jmjd3* cKO mice was higher compared with WT mice (33.6% vs. 17.0%, respectively). The central memory T cell population was also elevated in *Jmjd3* cKO mice as compared with WT mice (3.78% vs. 2.73%, respectively) **(Figure 3.1 A)**. The splenocytes of four 8-week old wt mice and *Jmjd3* cKO mice were analyzed for memory T cell population by FACS

(Figure 3.1 B). These results suggest that the percentages of memory T cells are markedly increased in *Jmjd3* cKO mice.

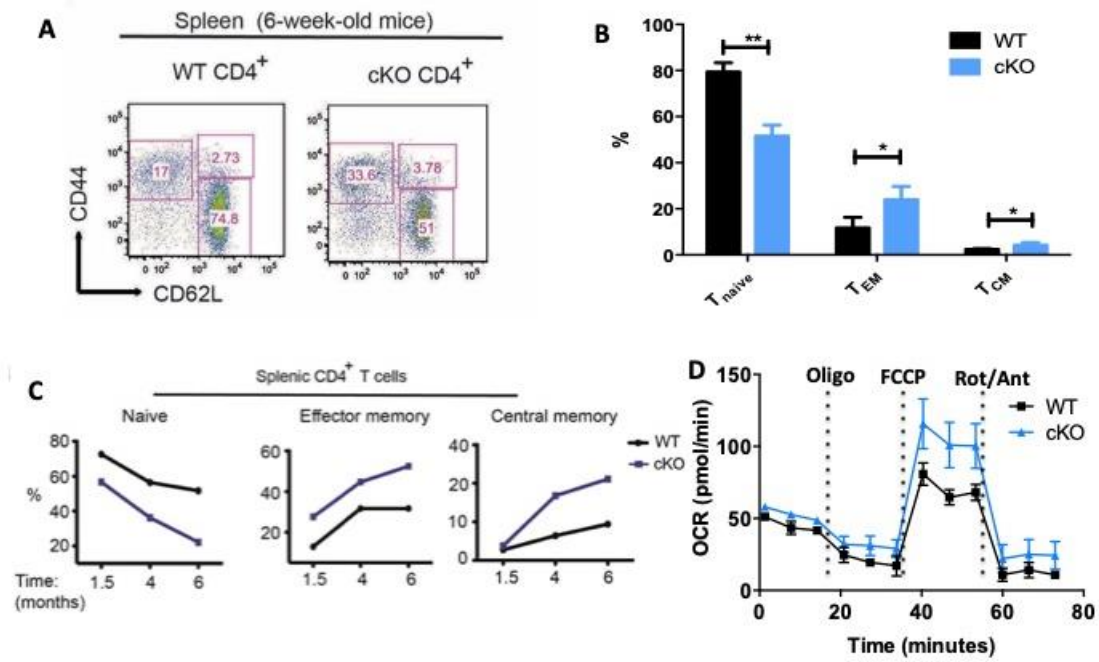

Figure 3.1 *Jmjd3* ablation increases memory CD4+ T-cell populations in naïve mice. (A) Flow cytometric analysis of naïve, effector, and central memory T cell populations in 6-week-old mice, based on CD44 and CD62L antibody positive staining gated on CD4+CD25- T cells. (B) Percentage of naïve CD4+ T cells, effector memory CD4+ T and central memory CD4+ T cells in the spleen from four 8-week WT and *Jmjd3* cKO mice. Asterisks indicate significant differences determined by Student's test (**p < 0.01, *p < 0.05 determined by Student's t test). (C) Analysis of naïve CD4+ T cells (CD4+CD25-CD62L+CD44low), effector memory CD4+ T cells (CD4+CD25-CD62L-CD44high) and central memory cells (CD4+CD25-CD62L+CD44high) in the spleens from 1.5-to-6-month-old WT and *Jmjd3* cKO mice. (D) Oxidative and glycolytic activities of one–week stimulated WT and *Jmjd3* cKO naïve CD4 T cells were detected using Mito Stress Test Kit.

To further assess the role of Jmjd3 during T-cell development and function, we analyzed $CD4^+$ naïve ($CD62L^+CD44^{lo}$), effector memory ($CD62L^{lo}CD44^{hi}$), and central memory ($CD62L^+CD44^{hi}$) cell populations in the spleens from different age WT and *Jmjd3* cKO mice. The percentages of naïve $CD4^+$ T cells was reduced (51%) in young (6 week-old) and

(20.1%) in 6 month-old Jmjd3 cKO mice, compared to 74.8% and 57.3%, respectively, in age-matched WT mice (**Figure 3.1 C**). In contrast, the effector memory $CD4^+$ T cell population was elevated (33.6%) in 6-week-old and (49.5%) 6-month-old *Jmjd3* cKO mice, compared to 17.0% and 27.2% in age-matched WT mice (**Figure 3.1 C**). Similar results were obtained for central memory T cells. These results suggest that the percentages of memory T cells are markedly increased in old *Jmjd3* cKO mice. Elevated oxidative metabolism is feature of memory T cells (van der Windt and Pearce, 2012). CD4 T cells from four 8-week WT and *Jmjd3* cKO mice were stimulated one week with anti-CD3 and anti-CD28 antibodies. We found that the O_2 consumption rate (OCR), an indicator of oxidative phosphorylation (OXPHOS), was higher in *Jmjd3* cKO group (**Figure 3.1 D**). These results support *Jmjd3* cKO CD4 T cells have higher memory T cells metabolism feature after TCR stimulation.

3.2.2 *Jmjd3*-deficiency enhances T-cell persistence

Next, we explored the molecular mechanism(s) by which *Jmjd3* ablation increases the memory T-cell population. We analyzed T-cell apoptosis and T-cell proliferation after T-cell activation. It has been reported that *Jmjd3* increases the expression of Ink4a/Arf in MEFs by demethylating H3K27 in the promoter region of the *Ink4a/Arf* locus, thus promoting p53-p21-mediated cell growth arrest, cellular senescence, and apoptosis (Agger et al., 2009; Barradas et al., 2009). Consistent with this, we have previously shown that *Jmjd3* ablation promotes MEF proliferation and reduces cell apoptosis or cellular senescence (Zhao et al., 2013). To test the possibility that *Jmjd3* ablation may lead to decreased T-cell persistence, we stimulated naïve T cells with anti-CD3 and anti-CD28 for one or two rounds of

stimulation, and then assessed the protein expression of $p19^{Arf}$, p21, and p53 between WT and *Jmjd3*-deficient $CD4^+$ T cells. Western blot analysis revealed that the expression levels of $p19^{Arf}$, p21, and p53 proteins were markedly increased in WT cells, but not in *Jmjd3* cKO $CD4^+$ T cells after the 2^{nd} round of stimulation **(Figure 3.2 A)**. Such a difference was not observed between WT and *Jmjd3* cKO $CD4^+$ T cells with only one round of TCR stimulation. Similarly, in a T-cell proliferation assay, the 2^{nd} round of stimulation of *Jmjd3*-deficient $CD4^+$ T cells resulted in increased proliferation than WT counterpart **(Figure 3.2 B)**. Furthermore, we isolated $CD4^+$ T cells based on high levels of cell surface expression of CD44 and little or no CD62L expression, and stimulated them with anti-CD3 and anti-CD28 antibodies. We found that the percentages of apoptotic *Jmjd3*-deficient $CD4^+CD25^-CD44^{high}$ T cells, but not $CD4^+CD25^-CD62L^+CD44^{low}$ T cells, were markedly reduced compared with WT cells **(Figure 3.2 C)**. These results suggest that *Jmjd3*-deficient $CD4^+$ T cells possess more proliferative activity and are less prone to apoptosis than their WT counterparts. Thus, the decreased number of *Jmjd3*-deficient $CD4^+$ T cells observed in the spleen and LNs after adoptive T cell transfer is mainly due to low trafficking from the thymus to the peripheral lymphoid organs, rather than the T-cell apoptosis or proliferation.

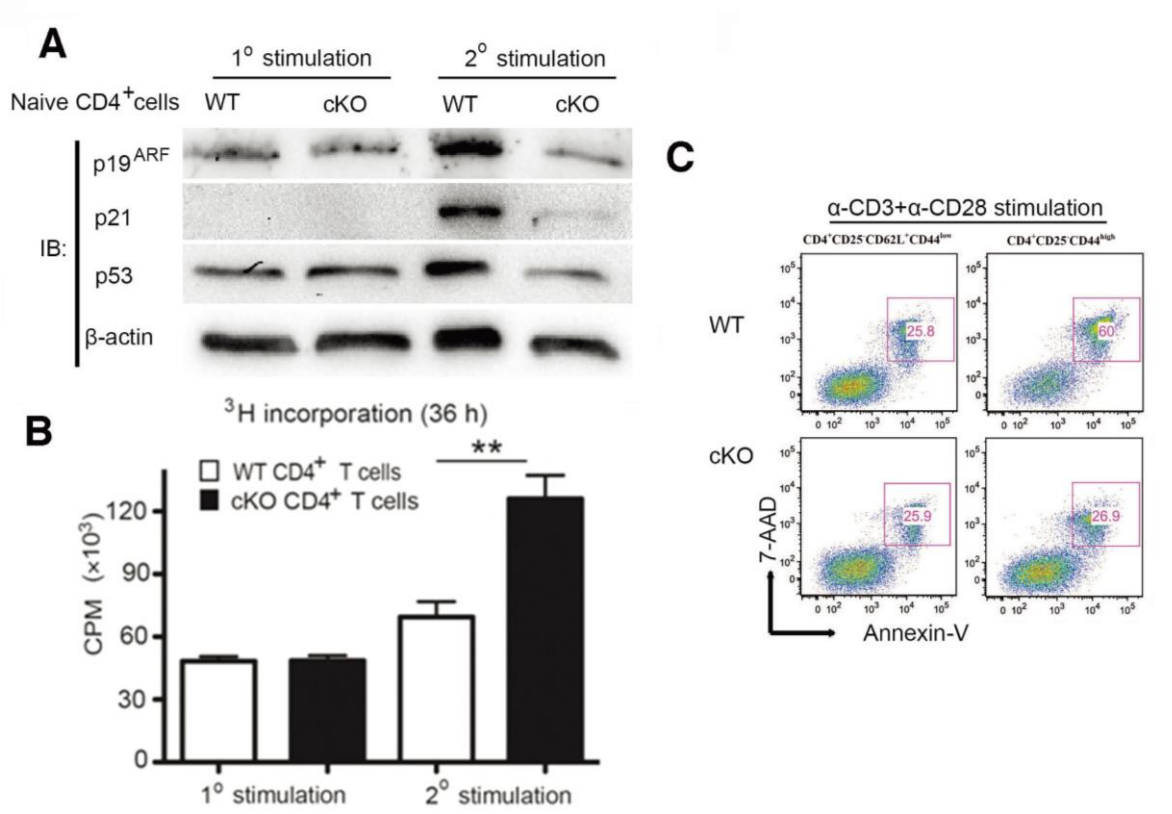

Figure 3.2 *Jmjd3*-deficiency enables T-cell persistence. (A) Western blot analysis of $p19^{Arf}$, p21, and p53 expression in naïve $CD4^+$ T cells from WT and *Jmjd3* cKO mice after one (1°) or two (2°) rounds of stimulation using anti-CD3 and anti-CD28 antibodies. β-actin was used as a loading control. (B) ^3H incorporation of WT and *Jmjd3* cKO naïve $CD4^+$ T cells after one or two rounds of anti-CD3 and anti-CD28 stimulation. The data are presented as means ± SD. (**$p < 0.01$, unpaired t test). (C) Apoptotic analysis of $CD25^-CD62L^+CD44^{low}$ or $CD25^-CD44^{high}$ $CD4^+$ T cells from WT and *Jmjd3* cKO mice after stimulation with anti-CD3 and anti-CD28 antibodies for 4 days. Cells were stained with Annexin-V and 7-AAD.

3.2.3 Growth advantage and potency of *Jmjd3*-deficient $CD4^+$ T cells in inducing EAE

Next, we next sought to determine whether the growth advantage of these antigen-experienced *Jmjd3*-deficient $CD4^+$ T cells have functional consequences for the induction of experimental autoimmune encephalomyelitis (EAE), a T-cell-mediated autoimmune disease of the central nervous system (CNS). WT and *Jmjd3* cKO mice were immunized by subcutaneous injection of the antigenic peptide for MOG (MOG_{35-55}) plus complete Freund's

adjuvant (CFA), and then injected with pertussis toxin (PTx) to induce EAE **(Figure 3.3 A)**. WT mice developed EAE disease faster and more severely than *Jmjd3* cKO mice, as evidenced by mean clinical scores **(Figure 3.3 B)**. This result may due to the lower endogenous levels of $CD4^+$ T cells in peripheral lymphoid organs in *Jmjd3* cKO mice that mediate autoimmunity.

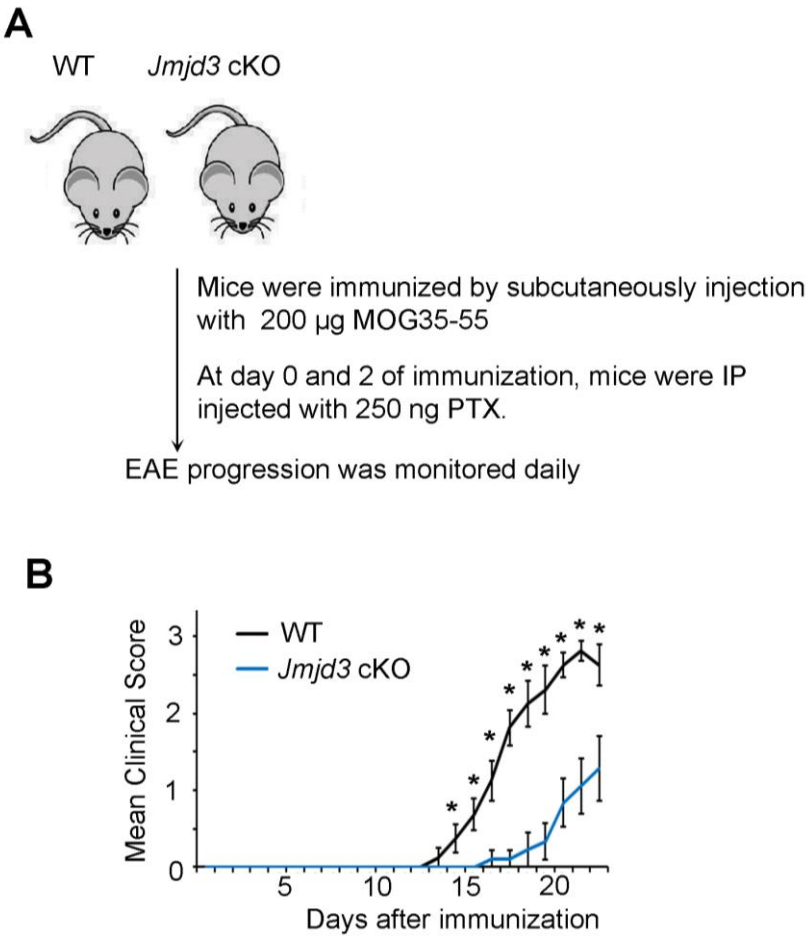

Figure 3 3 EAE model in *Jmjd3* cKO mice. (A) schematic presentation of experimental design for the induction of EAE with MOG_{35-55} peptide in wild-type and *Jmjd3*-deficiency mice. (B) The progression of EAE in *Jmjd3*-deficiency mice is delayed.

To determine whether $CD4^+$ T cells from *Jmjd3*-deficient mice could affect autoimmunity irrespective of differences in cell number, passive EAE was induced in sublethally irradiated C57BL/6 recipient mice reconstituted with equal numbers of pre-activated $CD4^+$ T cells isolated from the draining LNs (DLNs) of WT and *Jmjd3* cKO mice, which had been immunized with MOG peptide plus CFA **(Figure 3.4 A)**. Adoptive transfer of MOG_{35-55} peptide-activated *Jmjd3*-deficient T cells induced a more severe form of EAE with rapid onset than did the transfer of WT control T cells. The clinical scores for mice receiving MOG_{35-55} peptide-activated *Jmjd3*-deficient T cells were strikingly higher than those for WT control mice **(Figure 3.4 B)**. Importantly, we found a higher number of $CD4^+$ T cells that had infiltrated into the spinal cords of mice receiving MOG_{35-55} peptide-activated *Jmjd3*-deficient $CD4^+$ T cells compared with mice treated with WT control cells **(Figure 3.4 C)**. These results suggest that the increased number of *Jmjd3*-deficient memory T cells contributes to the kinetics and severity of EAE.

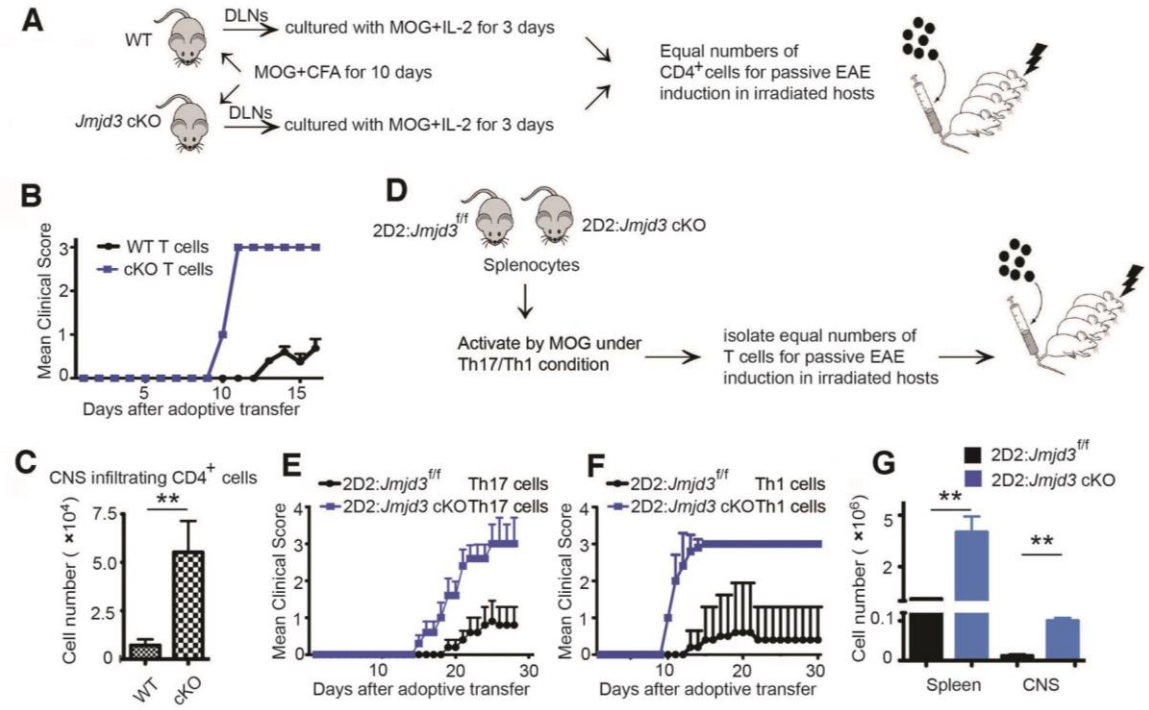

Figure 3.4 *Jmjd3* ablation induces more severe disease in an EAE model. (A) A schematic of the experimental design for the induction of passive EAE with MOG_{35-55} peptide- immunized $CD4^+$ T cells. $CD4^+$ T cells were isolated from the draining lymph nodes (DLNs) of WT and *Jmjd3* cKO, which had been immunized with MOG_{35-55} and complete Freund's adjuvant (CFA). $CD4^+$ T cells were cultured for 2 days with MOG_{35-55} and IL-2 for 3 days, and equal numbers of these $CD4^+$ T cells were intravenously injected into sublethally irradiated C57BL/6 mice. (B) Mean Clinical Score of EAE disease severity analyzed at sequential time points after adoptive transfer of WT or *Jmjd3* cKO $CD4^+$ T cells. (C) Absolute numbers of CNS infiltrating $CD4^+$ T cells from MOG_{35-55} peptide- immunized mice isolated from the spinal cords of EAE mice at day 16 after adoptive T cell transfer. (D) A schematic of the experimental design for the induction of EAE with MOG_{35-55}-peptide specific (2D2 TCR) $CD4^+$ T cells. Splenocytes were isolated from naïve 2D2:*Jmjd3*$^{f/f}$ (WT) and 2D2:*Jmjd3* cKO mice and activated with the MOG_{35-55} peptide under *in vitro* Th1 or Th17 cell conditions. These Th1/Th17-polarized 2D2:*Jmjd3*$^{f/f}$ and 2D2:*Jmjd3* cKO cells were intravenously injected into sublethally irradiated C57BL/6 mice. (E) Mean Clinical Score of EAE disease severity at sequential time points after adoptive transfer of Th17-polarized 2D2:*Jmjd3*$^{f/f}$ (WT) and 2D2:*Jmjd3* cKO cells. (F) Mean Clinical Score of EAE disease severity at sequential time points after adoptive transfer of Th1-polarized 2D2:*Jmjd3*$^{f/f}$ (WT) and 2D2:*Jmjd3* cKO cells. (G) Absolute numbers of 2D2-TCR-specific $CD4^+$ T cells from spleens and CNS-infiltrated lymphocytes of EAE mice at day 21 after adoptive Th1-cell transfer. The data in C and F are presented as means $\pm$ SD from three independent experiments. Asterisks indicate significant differences between groups (**$p < 0.01$ determined by Student's t test).

Next, we tested the ability of antigen-specific 2D2 TCR T cells to induce EAE disease. After isolating splenocytes cells from 2D2:*Jmjd3*$^{f/f}$ or 2D2:*Jmjd3* cKO mice and stimulating these

$CD4^+$ T cells with MOG_{35-55} peptide *in vitro* under Th1/Th17 culture conditions, we transferred equal numbers of 2D2:*Jmjd3*$^{f/f}$ or 2D2:*Jmjd3* cKO T cells into sublethally irradiated C57BL/6 mice **(Figure 3.4 D)**. Mice reconstituted with MOG_{35-55} peptide-stimulated 2D2:*Jmjd3* cKO Th1/Th17-polarized cells rapidly developed EAE disease compared with mice reconstituted with 2D2:*Jmjd3*$^{f/f}$ (WT) Th1/Th17-polarized cells, as evidenced by mean clinical score **(Figure 3.4, E** and **F)**. FACS analysis using antibodies against 2D2 TCR (TCRVα3.2 and TCRVβ11) revealed higher numbers of MOG_{35-55} peptide-specific T-cells in the spleens and in the CNS of C57BL/6 recipient mice receiving 2D2:*Jmjd3* cKO Th1-polarized cells compared with mice receiving 2D2:*Jmjd3*$^{f/f}$ Th1-polarized cells **(Figure 3.4 G)**. These results suggest that antigen-experienced *Jmjd3*-deficient T cells are maintained or expanded after transfer and induce EAE more rapidly and severely than WT T cells.

3.2.4 *JMJD3*-deficiency promotes CD19 CAR-T cells persistence

We demonstrated that *JMJD3* deficient dramatically enhanced the CD4 T cells persistence and survival in vitro and in vivo. Next, we investigated the in vivo effect of *JMJD3* deficient on antitumor T cells. Culturing CAR-T cells with IL-7 and IL-15 was recently found to preferentially expand the Tscm Population, and those T cells have been shown to exhibit superior antitumor responses in vivo. We analysis the in vitro and in vivo attributes of *JMJD3* knockdown CAR-T cells. CD4 T cells were transduced with an anti-CD19 CAR construct. After two-week expansion in the presence of feeder cells, the *JMJD3* knockdown CD4 T cells showed higher percentages of central memory T cells (Tcm) and T memory stem cells (Tscm). In order to assess the in vivo anti-leukemic effects of *JMJD3* deficient

CAR-T cells, we designed the experiment for in vivo assessment that is shown in the schema in **Figure 3.5 A**. Luciferase labeled control T cells, control CAR-T cells and *JMJD3* knockdown CAR-T cells were injected into NSG mice that have been transplanted with Raji. Serial imaging of the T cells showed an obvious long survival for *JMJD3* knockdown CAR-T cells (**Figure 3.5 B**). Survival of T cells population was investigated by flow cytometer. *JMJD3* knockdown CAR-T group show much more survival CD4 CAR-T cells (**Figure 3.5 C**). The survival assessment showed that all of the untreated mice died before day 20. The mice transplanted with *JMJD3* knockdown CAR-T cells showed significantly longer overall survival compared with the control CAR-T mice (**Figure 3.5 D**).

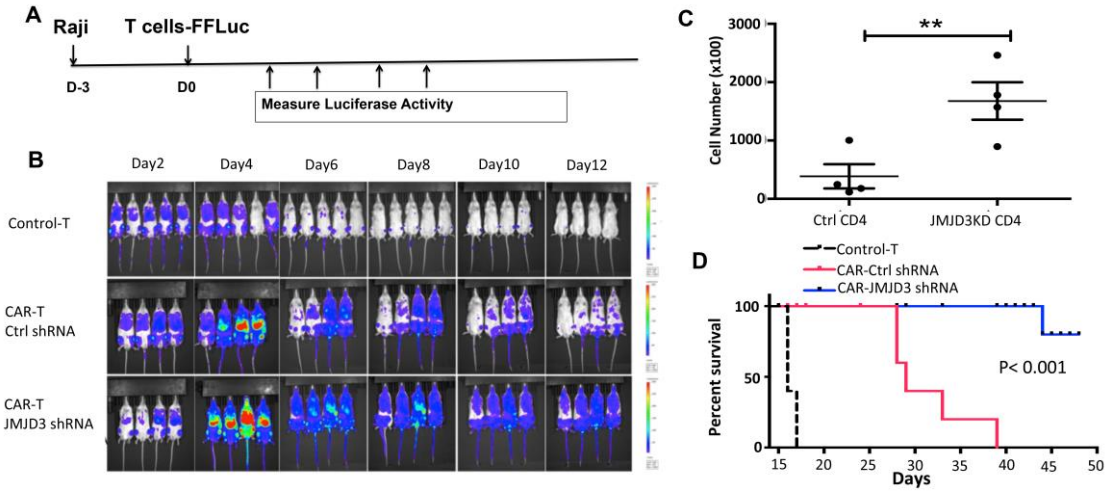

Figure 3.5 *JMJD3* knockdown improves the antitumor activity of chimeric antigen receptor-transduced T cells in a mouse leukemia model. (A) Schema of in vivo study demonstrating the anti-CD19 anti-tumor activity of transduced T cells in a disseminated human B cell malignancy xenogeneic NSG model. Raji tumor cells were injected i.v. into NSG mice on day -3. One doses (5×10^6 million cells) of either CAR T, CAR T *JMJD3*KD T cells or non-transduced T cells were injected i.v. on day 0 respectively. Whole mouse luciferase activity was measured at various time points. (B) Track CD19-CAR T cells and CD19 CAR-T *JMJD3* KO in NSG mice by in vivo bioluminescent imaging. (C) Count survival CAR positive CD4 T cell by FACS. Data represent mean + SD. (D) Kaplan-Meier survival curves of mice receiving CD19-CAR T treatment or or CD19-CAR T *JMJD3* KD or non-transduced mock T cell treatment.

3.3 Discussion

Jmjd3 has been shown to play critical roles in macrophage and T-cell differentiation, but the role and mechanisms of Jmjd3 in T cell memory maintenance remain poorly understood. In this study, we demonstrate that Jmjd3 ablation results in defects in other T cell functions, including T cell apoptosis, persistence and memory T cells maintenance.

Although Jmjd3 participates in the upregulation of Ink4a/Arf in MEFs by modifying H3K27 methylation in the promoter region of the Ink4a/Arf locus (Agger et al., 2009; Barradas et al., 2009), we did not observe any difference in p19Arf expression between WT and *Jmjd3*-

deficient CD4+ T cells after one cycle of TCR stimulation (**Figure 3.2 A**). However, we showed a marked difference in p19Arf expression between WT and *Jmjd3*-deficient CD4+ T cells after continuous TCR stimulation. Because increased expression of Ink4a/Arf further upregulates p21 and p53 and promotes cell growth arrest, cellular senescence, and apoptosis, our results show that *Jmjd3* ablation reduces cell senescence and apoptosis, and increase T cell proliferation after at least two cycles of stimulation. *Jmjd3*-deficient CD4+ T cells exhibit a remarkable ability to expand and thus accelerate disease progression in the EAE model. A typical immune response includes the expansion of activated cells and a contraction phase when most of the effector cells die and a small proportion of effector cells are converted to long-lived memory cells. Thus, our study may provide the molecular basis and mechanisms by which *Jmjd3* ablation reduces contraction phase and promote survival and maintenance of antigen-experienced memory T cell population. In the chapter 2, we show that migration of *Jmjd3*-deficiency CD4 T-cells to spleen is impaired, However, we found that there are more 2d2:*Jmjd3* cKO T cells migrated to the spleen in EAE model (**Figure 3.4 G**). One reason is the stimulated *Jmjd3*-deficient CD4+ T cells proliferated faster, therefore, there are more *Jmjd3*-deficient CD4+ T cells in the spleen after they migrated to the spleen. The other reason is the change of chemokine receptor signaling. Indeed, we found the expression a chemokine receptor CCR5, which plays a prominent role in T cell migration, is increased in *Jmjd3*-deficieny CD4 T cells (Mueller et al., 2013; Sebzda et al., 2008) (**Figure 3.6**). Overall, our findings may provide a new strategy to enhance vaccination-induced memory T cell response by inhibiting Jmjd3-mediated signaling pathway.

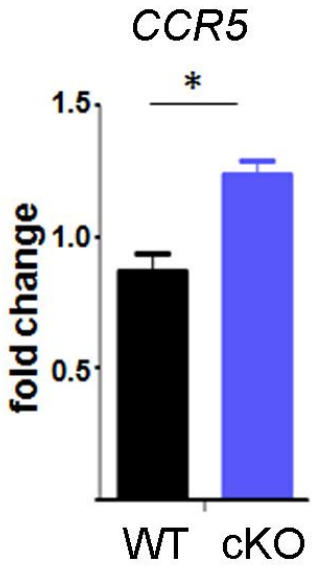

Figure 3.6 qPCR analysis the expression of CCR5 in *Jmjd3*-deficiency CD4 T cells.

In summary, our study provides genetic evidence that T-cell-specific deletion of *Jmjd3* results in multiple defects in the processes of T cell persistence and memory T cell population maintenance. These functional alterations of *Jmjd3*-deficient CD4+ T cells are demonstrated in adoptive T cell transfer experiments and in EAE disease models. Gene profiling and ChIP-Seq analysis identify Jmjd3 target genes involved in memory T-cell expansion (Ik4a/Arf). Thus, our findings provide the insights into the role of Jmjd3 in T-cell persistence and memory maintenance.

3.4 Materials and methods

Mice

Jmjd3 f/f:CD4-Cre mice were generated as previously described (Li et al., 2014b). C57BL/6, NSG and 2D2 mice were obtained from The Jackson Laboratory. All the mice were re-

derived by standard embryo transfer and maintained in pathogen-free animal facilities at the Houston Methodist Research Institute. These studies were reviewed and approved by Institutional Animal Care and Use Committee at the Houston Methodist Research Institute.

Immunoprecipitation and Western blot analysis

For immunoprecipitation, cells were lysed in ice-cold lysis buffer (40 mM Tris-HCl, pH7.5, 150 mM NaCl, and 1% Triton X-100) with proteinase inhibitor. Supernatants were incubated overnight with primary antibody (2ug) and immuncomplexes were allowed to bind to protein A/G beads for 90 mins at 4° C. Immunoprecipitates were washed three times with the lysis buffer. Western blotting was performed under conventional conditions after extracting the samples in SDS sample buffer. Protein extracts were separated by SDS-PAGE and electrotransferred onto an PVDF membrane (Millipore). The membranes were exposed to primary antibodies, washed, incubated with secondary antibodies and proteins were visualized by using Pierce Western Blotting Substrate Plus (Thermo Fisher).

Flow cytometry

To detect the expression of surface molecules, T cells were first incubated with an anti-Fc receptor Ab (24G2) to reduce nonspecific binding of mAbs, and then labeled with the appropriate fluorescent mAbs. Appropriate fluorescein-conjugated, isotype-matched, control mAbs were used as negative controls. Cells were analyzed with BD FACS Aria II.

Real-time RT-PCR

Total RNA was extracted from cultured cells with TRIzol (Invitrogen) according to the manufacturer's instructions. Oligo (dT) primers and Superscript III reverse transcriptase (Invitrogen) were used for the generation of cDNA from mRNA. Gene expression was determined by quantitative PCR with SYBR Green MasterMix (ABI), and the reactions were run on an ABIPRISM 7900HT Sequence Detection System (Life Science). Primers used for real-time PCR analysis are shown in Table S2.

Statistical analyses

Results represent the mean ± SD where applicable. Student's t-test was used to all statistical analysis with the GraphPad Prism 4.0 software. For all tests, values of $p<0.05$ were considered statistically significant.

Cell purification and population assess *in vitro*

Mouse splenocytes were first isolated using a negative selection kit (Stem Cell) and stained for CD4, CD25, CD44, and CD62L. Naïve $CD4^+$ ($CD4^+$ $CD25^-$ $CD44^{low}$ $CD62L^+$) cells were sorted by BD FACSAria II to >95% purity. For *in vitro* activation, isolated $CD4^+$ T cells were stimulated by coated 0.5 μg/mL anti-CD3 and 1 μg/mL anti-CD28 in the presence of 3000 rads-irradiated T-cell-depleted splenocytes as APCs. RPMI medium was supplemented with 10% FCS, L-glutamine (2 mM), 2-Mercaptoethanol (55 μM), penicillin (50 U/mL), streptomycin (50 mg/mL), sodium pyruvate (1 mM), and HEPES (25 mM).

3.5 References

Agger, K., P.A. Cloos, L. Rudkjaer, K. Williams, G. Andersen, J. Christensen, and K. Helin. 2009. *The H3K27me3 demethylase JMJD3 contributes to the activation of the INK4A-ARF locus in response to oncogene- and stress-induced senescence.* Genes Dev. 23:1171-1176.

Araki, Y., M. Fann, R. Wersto, and N.P. Weng. 2008. *Histone acetylation facilitates rapid and robust memory CD8 T cell response through differential expression of effector molecules (eomesodermin and its targets: perforin and granzyme B).* J Immunol. 180:8102-8108.

Araki, Y., Z. Wang, C. Zang, W.H. Wood, 3rd, D. Schones, K. Cui, T.Y. Roh, B. Lhotsky, R.P. Wersto, W. Peng, K.G. Becker, K. Zhao, and N.P. Weng. 2009. *Genome-wide analysis of histone methylation reveals chromatin state-based regulation of gene transcription and function of memory CD8+ T cells.* Immunity. 30:912-925.

Barradas, M., E. Anderton, J.C. Acosta, S. Li, A. Banito, M. Rodriguez-Niedenfuhr, G. Maertens, M. Banck, M.M. Zhou, M.J. Walsh, G. Peters, and J. Gil. 2009. *Histone demethylase JMJD3 contributes to epigenetic control of INK4a/ARF by oncogenic RAS.* Genes Dev. 23:1177-1182.

Besser, M.J., R. Shapira-Frommer, O. Itzhaki, A.J. Treves, D.B. Zippel, D. Levy, A. Kubi, N. Shoshani, D. Zikich, Y. Ohayon, D. Ohayon, B. Shalmon, G. Markel, R. Yerushalmi, S. Apter, A. Ben-Nun, E. Ben-Ami, A. Shimoni, A. Nagler, and J. Schachter. 2013. *Adoptive transfer of tumor-infiltrating lymphocytes in patients with metastatic melanoma: intent-to-treat analysis and efficacy after failure to prior immunotherapies.* Clin Cancer Res. 19:4792-4800.

Burchfield, J.S., Q. Li, H.Y. Wang, and R.F. Wang. 2015. *JMJD3 as an epigenetic regulator in development and disease.* Int J Biochem Cell Biol.

Burgold, T., N. Voituron, M. Caganova, P.P. Tripathi, C. Menuet, B.K. Tusi, F. Spreafico, M. Bevengut, C. Gestreau, S. Buontempo, A. Simeone, L. Kruidenier, G. Natoli, S. Casola, G. Hilaire, and G. Testa. 2012. *The H3K27 demethylase JMJD3 is required for maintenance of the embryonic respiratory neuronal network, neonatal breathing, and survival.* Cell reports. 2:1244-1258.

Butler, M.O., P. Friedlander, M.I. Milstein, M.M. Mooney, G. Metzler, A.P. Murray, M. Tanaka, A. Berezovskaya, O. Imataki, L. Drury, L. Brennan, M. Flavin, D. Neuberg, K. Stevenson, D. Lawrence, F.S. Hodi, E.F. Velazquez, M.T. Jaklitsch, S.E. Russell, M. Mihm, L.M. Nadler, and N. Hirano. 2011. *Establishment of antitumor memory in humans using in vitro-educated CD8+ T cells.* Sci Transl Med. 3:80ra34.

Carlson, C.M., B.T. Endrizzi, J. Wu, X. Ding, M.A. Weinreich, E.R. Walsh, M.A. Wani, J.B. Lingrel, K.A. Hogquist, and S.C. Jameson. 2006. *Kruppel-like factor 2 regulates thymocyte and T-cell migration.* Nature. 442:299-302.

Chen, S., J. Ma, F. Wu, L.J. Xiong, H. Ma, W. Xu, R. Lv, X. Li, J. Villen, S.P. Gygi, X.S. Liu, and Y. Shi. 2012. *The histone H3 Lys 27 demethylase JMJD3 regulates gene expression by impacting transcriptional elongation.* Genes & development. 26:1364-1375.

Cieri, N., B. Camisa, F. Cocchiarella, M. Forcato, G. Oliveira, E. Provasi, A. Bondanza, C. Bordignon, J. Peccatori, F. Ciceri, M.T. Lupo-Stanghellini, F. Mavilio, A. Mondino, S. Bicciato, A. Recchia, and C. Bonini. 2013. *IL-7 and IL-15 instruct the generation of human memory stem T cells from naive precursors.* Blood. 121:573-584.

Crompton, J.G., M. Narayanan, S. Cuddapah, R. Roychoudhuri, Y. Ji, W. Yang, S.J. Patel, M. Sukumar, D.C. Palmer, W. Peng, E. Wang, F.M. Marincola, C.A. Klebanoff, K. Zhao, J.S. Tsang, L. Gattinoni, and N.P. Restifo. 2016. *Lineage relationship of CD8(+) T cell subsets is revealed by progressive changes in the epigenetic landscape.* Cell Mol Immunol. 13:502-513.

Cyster, J.G., and S.R. Schwab. 2012. *Sphingosine-1-phosphate and lymphocyte egress from lymphoid organs.* Annu Rev Immunol. 30:69-94.

Davila, M.L., I. Riviere, X. Wang, S. Bartido, J. Park, K. Curran, S.S. Chung, J. Stefanski, O. Borquez-Ojeda, M. Olszewska, J. Qu, T. Wasielewska, Q. He, M. Fink, H. Shinglot, M. Youssif, M. Satter, Y. Wang, J. Hosey, H. Quintanilla, E. Halton, Y. Bernal, D.C. Bouhassira, M.E. Arcila, M. Gonen, G.J. Roboz, P. Maslak, D. Douer, M.G. Frattini, S. Giralt, M. Sadelain, and R. Brentjens. 2014. *Efficacy and toxicity management of 19-28z CAR T cell therapy in B cell acute lymphoblastic leukemia.* Sci Transl Med. 6:224ra225.

Dudley, M.E., J.C. Yang, R. Sherry, M.S. Hughes, R. Royal, U. Kammula, P.F. Robbins, J. Huang, D.E. Citrin, S.F. Leitman, J. Wunderlich, N.P. Restifo, A. Thomasian, S.G. Downey, F.O. Smith, J. Klapper, K. Morton, C. Laurencot, D.E. White, and S.A. Rosenberg. 2008. *Adoptive cell therapy for patients with metastatic melanoma: evaluation of intensive myeloablative chemoradiation preparative regimens.* J Clin Oncol. 26:5233-5239.

Gattinoni, L., C.A. Klebanoff, D.C. Palmer, C. Wrzesinski, K. Kerstann, Z. Yu, S.E. Finkelstein, M.R. Theoret, S.A. Rosenberg, and N.P. Restifo. 2005. *Acquisition of full effector function in vitro paradoxically impairs the in vivo antitumor efficacy of adoptively transferred CD8+ T cells.* J Clin Invest. 115:1616-1626.

Guryanova, O.A., J.A. Drazba, E.I. Frolova, and P.M. Chumakov. 2011. *Actin cytoskeleton remodeling by the alternatively spliced isoform of PDLIM4/RIL protein.* J Biol Chem. 286:26849-26859.

Hinrichs, C.S., R. Spolski, C.M. Paulos, L. Gattinoni, K.W. Kerstann, D.C. Palmer, C.A. Klebanoff, S.A. Rosenberg, W.J. Leonard, and N.P. Restifo. 2008. *IL-2 and IL-21 confer opposing differentiation programs to CD8+ T cells for adoptive immunotherapy.* Blood. 111:5326-5333.

Lee, J.Y., C.N. Skon, Y.J. Lee, S. Oh, J.J. Taylor, D. Malhotra, M.K. Jenkins, M.G. Rosenfeld, K.A. Hogquist, and S.C. Jameson. 2015. *The transcription factor KLF2 restrains CD4(+) T follicular helper cell differentiation.* Immunity. 42:252-264.

Li, Q., H.Y. Wang, I. Chepelev, Q. Zhu, G. Wei, K. Zhao, and R.F. Wang. 2014a. *Stage-dependent and locus-specific role of histone demethylase Jumonji D3 (JMJD3) in the embryonic stages of lung development.* PLoS Genet. 10:e1004524.

Li, Q., J. Zou, M. Wang, X. Ding, I. Chepelev, X. Zhou, W. Zhao, G. Wei, J. Cui, K. Zhao, H.Y. Wang, and R.F. Wang. 2014b. *Critical role of histone demethylase Jmjd3 in the regulation of CD4+ T-cell differentiation.* Nat Commun. 5:5780.

Louis, C.U., B. Savoldo, G. Dotti, M. Pule, E. Yvon, G.D. Myers, C. Rossig, H.V. Russell, O. Diouf, E. Liu, H. Liu, M.F. Wu, A.P. Gee, Z. Mei, C.M. Rooney, H.E. Heslop, and M.K. Brenner. 2011. *Antitumor activity and long-term fate of chimeric antigen receptor-positive T cells in patients with neuroblastoma.* Blood. 118:6050-6056.

Mackensen, A., N. Meidenbauer, S. Vogl, M. Laumer, J. Berger, and R. Andreesen. 2006. *Phase I study of adoptive T-cell therapy using antigen-specific CD8+ T cells for the treatment of patients with metastatic melanoma.* J Clin Oncol. 24:5060-5069.

Manna, S., J.K. Kim, C. Bauge, M. Cam, Y. Zhao, J. Shetty, M.S. Vacchio, E. Castro, B. Tran, L. Tessarollo, and R. Bosselut. 2015. *Histone H3 Lysine 27 demethylases Jmjd3 and Utx are required for T-cell differentiation.* Nat Commun. 6:8152.

Matloubian, M., C.G. Lo, G. Cinamon, M.J. Lesneski, Y. Xu, V. Brinkmann, M.L. Allende, R.L. Proia, and J.G. Cyster. 2004. *Lymphocyte egress from thymus and peripheral lymphoid organs is dependent on S1P receptor 1.* Nature. 427:355-360.

Maude, S.L., N. Frey, P.A. Shaw, R. Aplenc, D.M. Barrett, N.J. Bunin, A. Chew, V.E. Gonzalez, Z. Zheng, S.F. Lacey, Y.D. Mahnke, J.J. Melenhorst, S.R. Rheingold, A. Shen, D.T. Teachey, B.L. Levine, C.H. June, D.L. Porter, and S.A. Grupp. 2014. *Chimeric antigen receptor T cells for sustained remissions in leukemia.* N Engl J Med. 371:1507-1517.

Miller, S.A., A.C. Huang, M.M. Miazgowicz, M.M. Brassil, and A.S. Weinmann. 2008. *Coordinated but physically separable interaction with H3K27-demethylase and H3K4-methyltransferase activities are required for T-box protein-mediated activation of developmental gene expression.* Genes Dev. 22:2980-2993.

Miller, S.A., S.E. Mohn, and A.S. Weinmann. 2010. *Jmjd3 and UTX play a demethylase-independent role in chromatin remodeling to regulate T-box family member-dependent gene expression.* Mol Cell. 40:594-605.

Morgan, R.A., M.E. Dudley, J.R. Wunderlich, M.S. Hughes, J.C. Yang, R.M. Sherry, R.E. Royal, S.L. Topalian, U.S. Kammula, N.P. Restifo, Z. Zheng, A. Nahvi, C.R. de Vries, L.J. Rogers-Freezer, S.A. Mavroukakis, and S.A. Rosenberg. 2006. *Cancer regression in patients after transfer of genetically engineered lymphocytes.* Science. 314:126-129.

Mueller, S.N., T. Gebhardt, F.R. Carbone, and W.R. Heath. 2013. *Memory T cell subsets, migration patterns, and tissue residence.* Annu Rev Immunol. 31:137-161.

Ohtani, K., C. Zhao, G. Dobreva, Y. Manavski, B. Kluge, T. Braun, M.A. Rieger, A.M. Zeiher, and S. Dimmeler. 2013. *Jmjd3 controls mesodermal and cardiovascular differentiation of embryonic stem cells.* Circ Res. 113:856-862.

Restifo, N.P., M.E. Dudley, and S.A. Rosenberg. 2012. *Adoptive immunotherapy for cancer: harnessing the T cell response.* Nat Rev Immunol. 12:269-281.

Robbins, P.F., M.E. Dudley, J. Wunderlich, M. El-Gamil, Y.F. Li, J. Zhou, J. Huang, D.J. Powell, Jr., and S.A. Rosenberg. 2004. *Cutting edge: persistence of transferred lymphocyte clonotypes correlates with cancer regression in patients receiving cell transfer therapy.* J Immunol. 173:7125-7130.

Robbins, P.F., R.A. Morgan, S.A. Feldman, J.C. Yang, R.M. Sherry, M.E. Dudley, J.R. Wunderlich, A.V. Nahvi, L.J. Helman, C.L. Mackall, U.S. Kammula, M.S. Hughes, N.P. Restifo, M. Raffeld, C.C. Lee, C.L. Levy, Y.F. Li, M. El-Gamil, S.L. Schwarz, C. Laurencot, and S.A. Rosenberg. 2011. *Tumor regression in patients with metastatic synovial cell sarcoma and melanoma using genetically engineered lymphocytes reactive with NY-ESO-1*. J Clin Oncol. 29:917-924.

Rosenberg, S.A., J.C. Yang, and N.P. Restifo. 2004. *Cancer immunotherapy: moving beyond current vaccines.* Nat Med. 10:909-915.

Rosenberg, S.A., J.C. Yang, R.M. Sherry, U.S. Kammula, M.S. Hughes, G.Q. Phan, D.E. Citrin, N.P. Restifo, P.F. Robbins, J.R. Wunderlich, K.E. Morton, C.M. Laurencot, S.M. Steinberg, D.E. White, and M.E. Dudley. 2011. *Durable complete responses in heavily pretreated patients with metastatic melanoma using T-cell transfer immunotherapy.* Clin Cancer Res. 17:4550-4557.

Russ, B.E., M. Olshanksy, H.S. Smallwood, J. Li, A.E. Denton, J.E. Prier, A.T. Stock, H.A. Croom, J.G. Cullen, M.L. Nguyen, S. Rowe, M.R. Olson, D.B. Finkelstein, A. Kelso, P.G. Thomas, T.P. Speed, S. Rao, and S.J. Turner. 2014. *Distinct epigenetic signatures delineate transcriptional programs during virus-specific CD8(+) T cell differentiation.* Immunity. 41:853-865.

Sadelain, M., I. Riviere, and R. Brentjens. 2003. *Targeting tumours with genetically enhanced T lymphocytes.* Nat Rev Cancer. 3:35-45.

Satoh, T., O. Takeuchi, A. Vandenbon, K. Yasuda, Y. Tanaka, Y. Kumagai, T. Miyake, K. Matsushita, T. Okazaki, T. Saitoh, K. Honma, T. Matsuyama, K. Yui, T. Tsujimura, D.M. Standley, K. Nakanishi, K. Nakai, and S. Akira. 2010. *The Jmjd3-Irf4 axis regulates M2 macrophage polarization and host responses against helminth infection.* Nat Immunol. 11:936-944.

Scharer, C.D., B.G. Barwick, B.A. Youngblood, R. Ahmed, and J.M. Boss. 2013. *Global DNA methylation remodeling accompanies CD8 T cell effector function.* J Immunol. 191:3419-3429.

Sebzda, E., Z. Zou, J.S. Lee, T. Wang, and M.L. Kahn. 2008. *Transcription factor KLF2 regulates the migration of naive T cells by restricting chemokine receptor expression patterns.* Nat Immunol. 9:292-300.

Spiegel, S., and S. Milstien. 2011. *The outs and the ins of sphingosine-1-phosphate in immunity.* Nat Rev Immunol. 11:403-415.

Stagg, J., R.W. Johnstone, and M.J. Smyth. 2007. *From cancer immunosurveillance to cancer immunotherapy.* Immunol Rev. 220:82-101.

Tran, E., S. Turcotte, A. Gros, P.F. Robbins, Y.C. Lu, M.E. Dudley, J.R. Wunderlich, R.P. Somerville, K. Hogan, C.S. Hinrichs, M.R. Parkhurst, J.C. Yang, and S.A. Rosenberg. 2014. *Cancer immunotherapy based on mutation-specific CD4+ T cells in a patient with epithelial cancer.* Science. 344:641-645.

Vanaja, D.K., K.V. Ballman, B.W. Morlan, J.C. Cheville, R.M. Neumann, M.M. Lieber, D.J. Tindall, and C.Y. Young. 2006. *PDLIM4 repression by hypermethylation as a potential biomarker for prostate cancer.* Clin Cancer Res. 12:1128-1136.

Vanaja, D.K., M.E. Grossmann, J.C. Cheville, M.H. Gazi, A. Gong, J.S. Zhang, K. Ajtai, T.P. Burghardt, and C.Y. Young. 2009. *PDLIM4, an actin binding protein, suppresses prostate cancer cell growth.* Cancer Invest. 27:264-272.

Wang, Z., C. Zang, K. Cui, D.E. Schones, A. Barski, W. Peng, and K. Zhao. 2009. *Genome-wide mapping of HATs and HDACs reveals distinct functions in active and inactive genes.* Cell. 138:1019-1031.

Weinreich, M.A., K. Takada, C. Skon, S.L. Reiner, S.C. Jameson, and K.A. Hogquist. 2009. *KLF2 transcription-factor deficiency in T cells results in unrestrained cytokine production and upregulation of bystander chemokine receptors.* Immunity. 31:122-130.

Xu, Y., M. Zhang, C.A. Ramos, A. Durett, E. Liu, O. Dakhova, H. Liu, C.J. Creighton, A.P. Gee, H.E. Heslop, C.M. Rooney, B. Savoldo, and G. Dotti. 2014. *Closely related T-memory stem cells correlate with in vivo expansion of CAR.CD19-T cells and are preserved by IL-7 and IL-15.* Blood. 123:3750-3759.

Yamada, T., C.S. Park, M. Mamonkin, and H.D. Lacorazza. 2009. *Transcription factor ELF4 controls the proliferation and homing of CD8+ T cells via the Kruppel-like factors KLF4 and KLF2.* Nat Immunol. 10:618-626.

Zhao, W., Q. Li, S. Ayers, Y. Gu, Z. Shi, Q. Zhu, Y. Chen, H.Y. Wang, and R.F. Wang. 2013. *Jmjd3 inhibits reprogramming by upregulating expression of INK4a/Arf and targeting PHF20 for ubiquitination.* Cell. 152:1037-1050.

CHAPTER IV

CONCLUSION

4.1 Jmjd3 involves in T cell trafficking

T-cell development in the thymus is a multistep process. Inside the thymus, early thymic progenitor cells (TPCs) differentiate into T-cell receptor (TCR)-expressing $CD4^+CD8^+$ double-positive (DP) thymocytes in the cortex, and then mature into single-positive (SP) $CD4^+$ and $CD8^+$ T cells in the medulla (Love and Bhandoola, 2011; Petrie, 2003; Spiegel and Milstien, 2011). After negative and positive selection, CD4 SP T cells emigrate from the thymus to the periphery, e.g., peripheral blood, spleen, and LNs. The epigenetic modifier Jmjd3 has been shown to play critical role in macrophage and T-cell differentiation, but its (Jmjd3) role and mechanism in T-cell migration remain poorly understood. In this study, we demonstrate that *Jmjd3* ablation results in diminished emigration of mature SP T cells from the thymus and elevated numbers of T cells were observed in secondary lymphoid organs. To further substantiate this phenotype, we performed adoptive transfer of TCR-specific $CD4^+$ T cells. All results suggest that *Jmjd3*-deficient $CD4^+$ T cells show reduced migration to peripheral lymphoid organs as compared with WT control cells.

4.2 Jmjd3 regulates T cell trafficking by targeting PDLIM4 expression

Next, I sought to identify Jmjd3 target genes that affect CD4 SP T cell trafficking. Gene profiling and qPCR analysis identified a number of genes that were either upregulated or downregulated in *Jmjd3*-deficient CD4 SP T cells. In agreement with the recent report on *Jmjd3/Utx* dKO CD4 SP T cells, we found that the gene expression of cell migration

molecules, *Ccr7* and *Cd62l*, was downregulated in *Jmjd3*-deficient CD4 SP T cells. However, in both studies, this was independent of the H3K27me3 levels, suggesting that Jmjd3 may also affect target gene expression in a demethylase- independent manner during T-cell migration. Among the genes we measured, *Pdlim4* was markedly downregulated in *Jmjd3*-deficient CD4 SP T cells compared to WT cells. Although a function for this gene specifically in T cells has not been described, it is known to be involved in the organization of actin cytoskeleton, cell motility, and cell apoptosis (Boumber et al., 2007; Guryanova et al., 2011). We show that ectopic expression of *Pdlim4* in *Jmjd3*-deficient $CD4^+$ T cells restores their ability to migrate in both the spleen and LNs. Furthermore, using chimeric mice and/or adoptive T-cell experiments, we demonstrate that knockout of *Pdlim4* in $CD4^+$ T cells reduces splenic T-cell accumulation. Thus, our study identifies a previously unrecognized role for Pdlim4 in T-cell migration. Our results suggest that the removal of H3K27me3 is a critical event in activating *Pdlim4* expression and that ectopic expression of *Pdlim4* restores T-cell accumulation in LNs of *Jmjd3*-deficient $CD4^+$ T cells to WT levels.

4.3 PDLIM4 as an adaptor connect S1P1 and F-actin to drive T cell migration

T-cell migration from the thymus is regulated by Klf2 and its target $S1p_1$. Klf2 and S1P1 are highly expressed in mature SP T cells and mediate SP T-cell migration along S1P concentration gradients from the thymus to the periphery (Cyster and Schwab, 2012; Matloubian et al., 2004; Spiegel and Milstien, 2011). Similarly, we show that $CD4^+$ T-cell-specific deletion of *Jmjd3* in mice leads to the accumulation of mature SP T cells in the thymus, which is associated with lower numbers of SP T cells in the spleen and LNs, suggesting a failure of thymocyte emigration to the periphery. Our study is supported by a

recent publication demonstrating a similar phenotype in CD4-specific *Jmjd3* KO and CD4-specific *Jmjd3/Utx* dKO T cells (Manna et al., 2015). However, in that study, authors mainly investigated the role of Jmjd3 and Utx in dKO mice. Critical role and precise mechanisms of Jmjd3 and its target genes in the regulation of T cell trafficking have not been fully elucidated.

In this study, we show that the migration of *Jmjd3*-deficient $CD4^+$ T-cells was significantly impaired, suggesting that the H3K27 demethylase Jmjd3 is essential for $CD4^+$ T-cell migration. Our study further dissected the molecular mechanisms of how Jmjd3 affects T-cell migration, and identified a novel Jmjd3 target gene, *Pdlim4* which translates to PDLIM4 protein. PDLIM4 is a cytoskeleton binding protein that has one PDZ domain and one LIM domain. PDZ domain plays a key role in anchoring receptor proteins in the membrane to cytoskeletal components (Lee and Zheng, 2010) and LIM domain has a role in cytoskeletal organization (Kadrmas and Beckerle, 2004). We found PDLIM4 interact with S1P1 and colocalizes with PDLIM4 after S1P treatment. Consistently, Co-IP analysis indicated that PDLIM4 was associated with S1P1 in CD4 T cells. We used phalloidin staining to analyze the correlation between F-actin organization and PDLIM4 in thymic CD4 SP T cells. The result show PDLIM4 can rescue the F-actin assembly and remodeling deficiency after *Pdlim4* overexpression. Next, Co-IP assay and cosedimentation assay found PDLIM4 interacts with the S1P1 protein by N terminal PDZ domain and bind F-actin by C terminal LIM domain. Then, we propose a model the PDLIM4 as an adaptor connecting S1P1 and F-actin to drive T cell migration (**Figure 4.1** right panel).

4.4 Jmjd3 activates PDLIM4 expression by cooperating with Klf2 and the H3K4 methyltransferase complex

Previous studies have shown that *Pdlim4* expression is highly inhibited by hypermethylation in prostate cancer (Vanaja et al., 2006; Vanaja et al., 2009), but the epigenetic factors responsible for this hypermethylation at the *Pdlim4* promoter remain to be identified. Consistent with these observations, our ChIP-PCR and ChIP-Seq analyses show a substantial increase in H3K27me3 and a decrease in H3K4me3 in the promoter and gene body regions of *Pdlim4* in *Jmjd3*-deficient CD4 SP T cells. However, Jmjd3 can't directly bind to special site of chromatin. Thus, further studies are needed to identify these key transcription factors, which act in concert with Jmjd3 to regulate target genes expression. We found Jmjd3 did not enhance *Pdlim4* expression without Klf2, suggesting co-regulation of *Pdlim4* by Jmjd3 and Klf2. By contrast, we observed a marked reduction in H3K4me3 (with a small increase in H3K27me3) in the promoter and gene body regions of $S1p_1$. Not only does Jmjd3 harbor H3K27 demethylase activity, Jmjd3 can also associate with H3K4 methyltransferase complexes; and thus, affect gene H3K4me3 levels. Indeed, we found that Jmjd3 directly interacts with Ash2L, a core component of the H3K4 methyltransferase complex (Li et al., 2014; Miller et al., 2008; Miller et al., 2010). We also found that Klf2 interacts with other H3K4 methyltransferase components. Specifically, Klf2 interacted with Wdr5, and Jmjd3 was required for stabilizing this interaction. This role for Jmjd3 in stabilizing transcription factors has been previously shown in T-cell differentiation (Li et al., 2014). Specifically, Jmjd3 enhances the interaction between the transcription factors T-bet and RbBP5 in Th1-cell differentiation and between the transcription factors SMAD3 and Ash2L in Treg-cell

differentiation. Based on these findings, we propose that Jmjd3 regulates Klf2 target genes *S1p1* and *Pdlim4* by interacting with both Klf2 and Ash2L in the H3K4 methyltransferase complex. Jmjd3 ablation disrupts the Klf2-Jmjd3-Ash2L complex, leading to an increase in H3K27me3 and/or a reduction in H3K4me3 in the promoter and gene body of *Pdlim4* and *S1p1*, thus down regulating gene expression. The changes in H3K4me3 and/or H3K27me3 in the gene body are supported by a finding that Jmjd3 is involved in the protein complex engaged in transcriptional elongation (Chen et al., 2012).

In sum, Jmjd3 regulates *Pdlim4* by interacting with both Klf2 and Ash2L in the H3K4 methyltransferase complex. Jmjd3 ablation disrupts the Klf2-Jmjd3-Ash2L complex, leading to an increase in H3K27me3 and/or a reduction in H3K4me3 in the promoter and gene body of *Pdlim4*, *S1p1* and other target genes, thus reducing target genes expression. Importantly, PDLIM4 bridges S1P1-mediated extracellular signaling and F-actin formation, which is critical for T cell migration and trafficking through its PDZ domain in the N-terminus and LIM domain in the C-terminus (**Figure 4.1**). Mechanistically, Jmjd3 regulates *Pdlim4* expression through interaction with Klf2, Wdr5 and Ash2L in the promoter and gene body regions of *Pdlim4*. Thus, our results have provided insights into the molecular mechanisms by which Jmjd3 and its target PDLIM4 regulate T-cell migration.

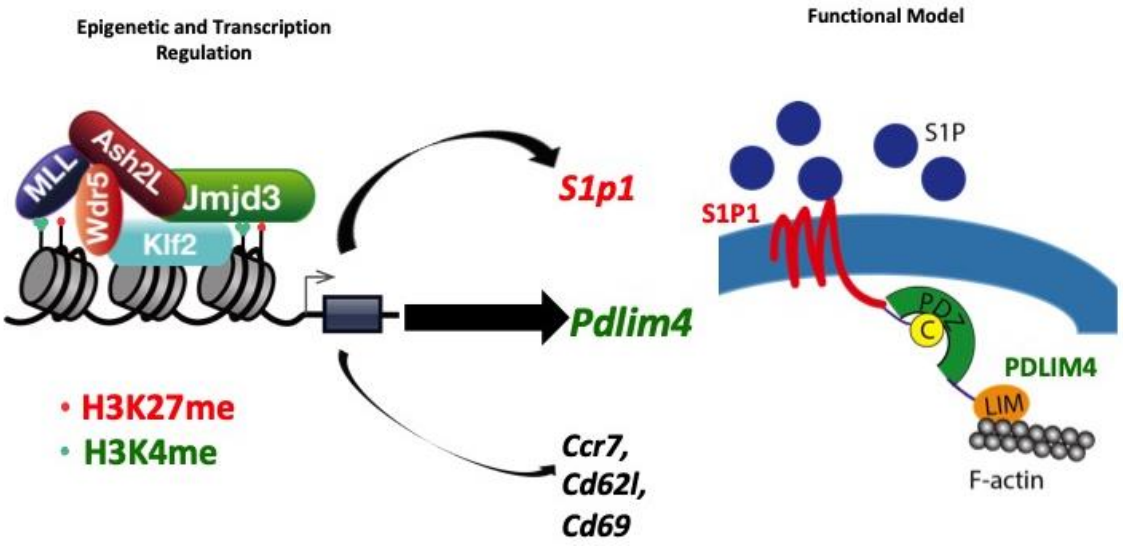

Figure 4.1 Schematic diagram of proposed model of how Jmjd3 regulate T cell trafficking by targeting *S1p1* and *Pdlim4*.

4.5 *Jmjd3* deficiency enables T-cell persistence by altering Ink4a/Arf - p53 pathway

A typical immune response includes the expansion of activated effector T cells and a contraction phase, in which most of the effector T cells die and a small proportion of effector T cells are converted into long-lived memory T cells (MacLeod et al., 2010). The phenotype of these long-lived memory T cells is acquired upon migration into secondary lymphoid and peripheral organs (Kassiotis and Stockinger, 2004). During these processes, T-cell persistence could promote the survival and functional competence of activated/memory T cells, and changes in gene expression affecting these T-cell function may be regulated by epigenetic mechanisms. Jmjd3 was reported involving in cellular aging and senescence in MEFs through the upregulation of Ink4a/Arf in MEFs by modifying H3K27 methylation in the promoter region of the *Ink4a/Arf* locus, which encodes $p19^{Arf}$ (Agger et al., 2009;

Barradas et al., 2009). Expression of $p19^{Arf}$ leads to thymocyte cell death upstream of the transcriptional factor p53 pathway (Miyazaki et al., 2008). Moreover, increased expression of Ink4a/Arf further upregulates p21 and p53, promoting cell growth arrest, cellular senescence, and apoptosis (Mitra et al., 1999; Wei et al., 2001; Zindy et al., 1998). We did not observe any differences in $p19^{Arf}$, p21, and p53 protein expression between WT and *Jmjd3*-deficient naïve $CD4^+$ T cells after one round of TCR stimulation. However, we found an increase in $p19^{Arf}$, p21, and p53 protein expression in WT cells after a second round of TCR stimulation, but not in *Jmjd3*-deficient $CD4^+$ T cells. Hence, our results suggest that the lack of an increase in $p19^{Arf}$, p21, and p53 protein expression in *Jmjd3*-deficient $CD4^+$ T cells after a second round of antigen stimulation may prevent activated T cell death, cell growth arrest, and cellular senescence. Indeed, we found that after anti-CD3 and anti-CD28 stimulation *Jmjd3*-deficient $CD4^+$ T cells isolated, based on $CD44^+$ and $CD62L^-$ expression, lacked an increase in apoptosis, as evidenced by 7-AAD and Annexin-V staining. Although neither Jmjd3 nor Utx was essential for T-cell proliferation within the thymus (Manna et al., 2015), *Jmjd3*-deficient splenic $CD4^+$ T cells exhibit a remarkable ability to proliferate after a second round of stimulation, suggesting that Jmjd3 may regulate memory T-cell expansion upon re-encounter with the same antigen in the periphery. Using an EAE model, a previous study demonstrated that memory $CD4^+$ T cells induce more severe EAE than effector T cells or naïve T cells that is caused by a preferential differentiation of memory T cells into the Th1/Th17 phenotype, increased cell proliferation, and a differential expression of chemokine receptors (Elyaman et al., 2008). Accordingly, we found higher numbers of antigen-specific *Jmjd3*-deficient $CD4^+$ T cells and in antigen-specific *Jmjd3*-deficient Th1/Th17-polarized cells in the spleens and in the CNS, respectively, of recipient mice after passive EAE-

induction and adoptive T cell transfer. This suggests that after *Jmjd3*-deficient $CD4^+$ T-cells migrate to the spleen, the cells may proliferate at a faster rate that their WT counterparts. Our results clearly suggest that antigen-experienced *Jmjd3*-deficient $CD4^+$ T cells are maintained or expanded after transfer and induce EAE more rapidly and severely than WT $CD4^+$ T cells. Our study may provide the molecular basis and mechanisms by which *Jmjd3* ablation regulates T cell migration, reduces the T cell contraction phase, and promotes survival and maintainence of antigen-experienced memory T cells.

In summary, our study provides genetic evidence that T-cell-specific deletion of *Jmjd3* results in multiple defects in T-cell persistence. These functional alterations of *Jmjd3*-deficient $CD4^+$ T cells are demonstrated by adoptive T-cell transfer experiments and in EAE disease models. *Jmjd3*-deficient $CD4^+$ T showed decreased $p19^{Arf}$, p21, and p53 protein expression and apoptosis after TCR stimulation. Thus, our findings provide insights into the molecular mechanisms by which Jmjd3 regulates activated T-cell persistence.

4.6 *Jmjd3*-deficiency promotes engineered T cells survival and generate superior T cell grafts for adoptive immunotherapy

Adoptive T cells transfer immunotherapy is a promising therapeutic option for cancer patient. The resource of anti-tumor T cells can be expanded from tumor antigen-specific T cells in the patient's tumor or peripheral blood (Rosenberg et al., 2004; Stagg et al., 2007). Another resource is the engineered of T cells with tumor-specific T cell receptors (TCRs) or chimeric antigen receptors (CARs) (Sadelain et al., 2003). Both of these two strategies face problem is T cell exhaustion which is the reason many of patients just achieve partial responses eventually relapse (Besser et al., 2013; Dudley et al., 2008; Mackensen et al.,

2006; Robbins et al., 2011; Rosenberg et al., 2011). Many reports shown adoptive T cells transfer therapy outcome is highly correlated with the persistence of the transferred T cells(Butler et al., 2011; Davila et al., 2014; Louis et al., 2011; Maude et al., 2014; Morgan et al., 2006; Robbins et al., 2004; Tran et al., 2014). Enhance the survival and persistence of T cells will be a promised strategy to benefit the patient with adoptive transfer therapy. In chapter 3, our study shows *JMJD3* deficient enhance engineered human CAR-T cell survival in adoptive transfer model. The survival assay displayed *JMJD3* knockdown CAR-T cells showed better treatment outcome. These results how JMJD3 played similar function in human CD4 T cells. we proposed that the H3K27 demethylase JMJD3 is essential for activated human CD4+ T-cell persistence. These findings show JMJD3 can be a good target to apply to adoptive immunotherapy for the generation of better T cell grafts.

4.7 Future prospects

We elucidated a clear mechanism in which Jmjd3 targets *Pdlim4* by cooperating with Klf2 to regulate T cell trafficking. Additionally, we found that *Jmjd3* deficiency will enhance T cell persistence and increase memory T cell populations in mouse and human engineered T cells. However, there remain as yet many undiscovered roles of Jmjd3 in T cells and the immune response. In naive T cells, the expression of Jmjd3 was dramatically induced by TCR stimulation. The expression of *Jmjd3* mRNA was dramatically induced by TCR stimulation with peak expression at 2 hours post stimulation will peak at 2 hours and remained elevated for 48 hours, after which it returned to baseline (Liu et al., 2015). What is the reason for the rapid upregulation of Jmjd3 after stimulation? Why does the upregulation of Jmjd3 return to baseline after 48 hours? Additionally, the mechanism of how

Jmjd3 protein are degraded during rapid up-regulation and recovery has not been determined, which may help us to understand Jmjd3's epigenetic role in rapid immune responses. What is the downstream target of Jmjd3 during rapid immune responses? Further investigations are needed to characterize the role of Jmjd3 in the T cell immune response, which may be dependent or independent of its histone demethylase activity.

In T cell persistence, we found that *Jmjd3* ablation will increase the memory T cell population. However, the details of Jmjd3's role in memory T cell formation and differentiation need future investigation. Based on metabolism assay data, *Jmjd3* deficiency enhances the oxygen consumption rate, which mirrors the metabolic profile of memory T cells. This raises the question of what signals are responsible for this metabolism alteration in *Jmjd3* deficiency. Furthermore, the targets of Jmjd3 that are responsible for metabolism alterations, and whether or not these alterations drive memory T cell generation merit additional investigation. In addition, T cell apoptosis and senescence show significant alteration after changes in Jmjd3 expression. INK4a and p53 may contribute to this phenotype, but whether or not other target genes of Jmjd3 are involved in T cell persistence needs further study. Finally, an important question will be whether decreases in apoptosis in *Jmjd3* deficient CD4 T cells contributes to the increase in the memory T cell population.

For therapeutic purpose, published results and our study show that targeting JMJD3 for the development of therapeutics to treat a number of diseases may be feasible and efficacious. As a cancer therapy target, manipulation of JMJD3 expression may actually produce a deleterious response as JMJD3 has been reported to play both positive and negative roles in cancer development depending on the specific cancer and other circumstances. Accordingly,

inhibition of JMJD3 may provide benefit in some cancer patients but produce a deleterious response in others. Additionally, JMJD3 is involved in a plethora of cellular processes in different cell types. Globally, JMJD3 inhibition or activation may cause serious off-target side effects. Therefore, using a different strategy to achieve cell-specific overexpression or knockdown/knockout may help control for any non-specific effects.

4.8 References

Agger, K., P.A. Cloos, L. Rudkjaer, K. Williams, G. Andersen, J. Christensen, and K. Helin. 2009. *The H3K27me3 demethylase JMJD3 contributes to the activation of the INK4A-ARF locus in response to oncogene- and stress-induced senescence.* Genes Dev. 23:1171-1176.

Barradas, M., E. Anderton, J.C. Acosta, S. Li, A. Banito, M. Rodriguez-Niedenfuhr, G. Maertens, M. Banck, M.M. Zhou, M.J. Walsh, G. Peters, and J. Gil. 2009. *Histone demethylase JMJD3 contributes to epigenetic control of INK4a/ARF by oncogenic RAS.* Genes Dev. 23:1177-1182.

Besser, M.J., R. Shapira-Frommer, O. Itzhaki, A.J. Treves, D.B. Zippel, D. Levy, A. Kubi, N. Shoshani, D. Zikich, Y. Ohayon, D. Ohayon, B. Shalmon, G. Markel, R. Yerushalmi, S. Apter, A. Ben-Nun, E. Ben-Ami, A. Shimoni, A. Nagler, and J. Schachter. 2013. *Adoptive transfer of tumor-infiltrating lymphocytes in patients with metastatic melanoma: intent-to-treat analysis and efficacy after failure to prior immunotherapies.* Clin Cancer Res. 19:4792-4800.

Boumber, Y.A., Y. Kondo, X. Chen, L. Shen, V. Gharibyan, K. Konishi, E. Estey, H. Kantarjian, G. Garcia-Manero, and J.P. Issa. 2007. *RIL, a LIM gene on 5q31, is silenced by methylation in cancer and sensitizes cancer cells to apoptosis.* Cancer Res. 67:1997-2005.

Butler, M.O., P. Friedlander, M.I. Milstein, M.M. Mooney, G. Metzler, A.P. Murray, M. Tanaka, A. Berezovskaya, O. Imataki, L. Drury, L. Brennan, M. Flavin, D. Neuberg, K. Stevenson, D. Lawrence, F.S. Hodi, E.F. Velazquez, M.T. Jaklitsch, S.E. Russell, M. Mihm, L.M. Nadler, and N. Hirano. 2011. *Establishment of antitumor memory in humans using in vitro-educated CD8+ T cells.* Sci Transl Med. 3:80ra34.

Chen, S., J. Ma, F. Wu, L.J. Xiong, H. Ma, W. Xu, R. Lv, X. Li, J. Villen, S.P. Gygi, X.S. Liu, and Y. Shi. 2012. *The histone H3 Lys 27 demethylase JMJD3 regulates gene expression by impacting transcriptional elongation.* Genes & development. 26:1364-1375.

Cyster, J.G., and S.R. Schwab. 2012. *Sphingosine-1-phosphate and lymphocyte egress from lymphoid organs.* Annu Rev Immunol. 30:69-94.

Davila, M.L., I. Riviere, X. Wang, S. Bartido, J. Park, K. Curran, S.S. Chung, J. Stefanski, O. Borquez-Ojeda, M. Olszewska, J. Qu, T. Wasielewska, Q. He, M. Fink, H. Shinglot, M. Youssif, M. Satter, Y. Wang, J. Hosey, H. Quintanilla, E. Halton, Y. Bernal, D.C. Bouhassira, M.E. Arcila, M. Gonen, G.J. Roboz, P. Maslak, D. Douer, M.G. Frattini, S. Giralt, M. Sadelain, and R. Brentjens. 2014. *Efficacy and toxicity management of 19-28z CAR T cell therapy in B cell acute lymphoblastic leukemia.* Sci Transl Med. 6:224ra225.

Dudley, M.E., J.C. Yang, R. Sherry, M.S. Hughes, R. Royal, U. Kammula, P.F. Robbins, J. Huang, D.E. Citrin, S.F. Leitman, J. Wunderlich, N.P. Restifo, A. Thomasian, S.G. Downey, F.O. Smith, J. Klapper, K. Morton, C. Laurencot, D.E. White, and S.A. Rosenberg. 2008. *Adoptive cell therapy for patients with metastatic melanoma: evaluation of intensive myeloablative chemoradiation preparative regimens.* J Clin Oncol. 26:5233-5239.

Elyaman, W., P. Kivisakk, J. Reddy, T. Chitnis, K. Raddassi, J. Imitola, E. Bradshaw, V.K. Kuchroo, H. Yagita, M.H. Sayegh, and S.J. Khoury. 2008. *Distinct functions of autoreactive memory and effector CD4+ T cells in experimental autoimmune encephalomyelitis.* Am J Pathol. 173:411-422.

Guryanova, O.A., J.A. Drazba, E.I. Frolova, and P.M. Chumakov. 2011. *Actin cytoskeleton remodeling by the alternatively spliced isoform of PDLIM4/RIL protein.* J Biol Chem. 286:26849-26859.

Kadrmas, J.L., and M.C. Beckerle. 2004. *The LIM domain: from the cytoskeleton to the nucleus.* Nat Rev Mol Cell Biol. 5:920-931.

Kassiotis, G., and B. Stockinger. 2004. *Anatomical heterogeneity of memory CD4+ T cells due to reversible adaptation to the microenvironment.* J Immunol. 173:7292-7298.

Lee, H.J., and J.J. Zheng. 2010. *PDZ domains and their binding partners: structure, specificity, and modification.* Cell Commun Signal. 8:8.

Li, Q., J. Zou, M. Wang, X. Ding, I. Chepelev, X. Zhou, W. Zhao, G. Wei, J. Cui, K. Zhao, H.Y. Wang, and R.F. Wang. 2014. *Critical role of histone demethylase Jmjd3 in the regulation of CD4+ T-cell differentiation.* Nat Commun. 5:5780.

Liu, Z., W. Cao, L. Xu, X. Chen, Y. Zhan, Q. Yang, S. Liu, P. Chen, Y. Jiang, X. Sun, Y. Tao, Y. Hu, C. Li, Q. Wang, Y. Wang, C.D. Chen, Y. Shi, and X. Zhang. 2015. *The histone H3 lysine-27 demethylase Jmjd3 plays a critical role in specific regulation of Th17 cell differentiation.* J Mol Cell Biol. 7:505-516.

Louis, C.U., B. Savoldo, G. Dotti, M. Pule, E. Yvon, G.D. Myers, C. Rossig, H.V. Russell, O. Diouf, E. Liu, H. Liu, M.F. Wu, A.P. Gee, Z. Mei, C.M. Rooney, H.E. Heslop, and M.K. Brenner. 2011. *Antitumor activity and long-term fate of chimeric antigen receptor-positive T cells in patients with neuroblastoma.* Blood. 118:6050-6056.

Mackensen, A., N. Meidenbauer, S. Vogl, M. Laumer, J. Berger, and R. Andreesen. 2006. *Phase I study of adoptive T-cell therapy using antigen-specific CD8+ T cells for the treatment of patients with metastatic melanoma.* J Clin Oncol. 24:5060-5069.

MacLeod, M.K., J.W. Kappler, and P. Marrack. 2010. *Memory CD4 T cells: generation, reactivation and re-assignment.* Immunology. 130:10-15.

Manna, S., J.K. Kim, C. Bauge, M. Cam, Y. Zhao, J. Shetty, M.S. Vacchio, E. Castro, B. Tran, L. Tessarollo, and R. Bosselut. 2015. *Histone H3 Lysine 27 demethylases Jmjd3 and Utx are required for T-cell differentiation.* Nat Commun. 6:8152.

Matloubian, M., C.G. Lo, G. Cinamon, M.J. Lesneski, Y. Xu, V. Brinkmann, M.L. Allende, R.L. Proia, and J.G. Cyster. 2004. *Lymphocyte egress from thymus and peripheral lymphoid organs is dependent on S1P receptor 1.* Nature. 427:355-360.

Maude, S.L., N. Frey, P.A. Shaw, R. Aplenc, D.M. Barrett, N.J. Bunin, A. Chew, V.E. Gonzalez, Z. Zheng, S.F. Lacey, Y.D. Mahnke, J.J. Melenhorst, S.R. Rheingold, A. Shen, D.T. Teachey, B.L. Levine, C.H. June, D.L. Porter, and S.A. Grupp. 2014. *Chimeric antigen receptor T cells for sustained remissions in leukemia.* N Engl J Med. 371:1507-1517.

Miller, S.A., A.C. Huang, M.M. Miazgowicz, M.M. Brassil, and A.S. Weinmann. 2008. *Coordinated but physically separable interaction with H3K27-demethylase and H3K4-methyltransferase activities are required for T-box protein-mediated activation of developmental gene expression.* Genes Dev. 22:2980-2993.

Miller, S.A., S.E. Mohn, and A.S. Weinmann. 2010. *Jmjd3 and UTX play a demethylase-independent role in chromatin remodeling to regulate T-box family member-dependent gene expression.* Mol Cell. 40:594-605.

Mitra, J., C.Y. Dai, K. Somasundaram, W.S. El-Deiry, K. Satyamoorthy, M. Herlyn, and G.H. Enders. 1999. *Induction of p21 WAF1/CIP1 and Inhibition of Cdk2 Mediated by the Tumor Suppressor p16 INK4a.* Molecular and cellular biology. 19:3916-3928.

Miyazaki, M., K. Miyazaki, M. Itoi, Y. Katoh, Y. Guo, R. Kanno, Y. Katoh-Fukui, H. Honda, T. Amagai, M. van Lohuizen, H. Kawamoto, and M. Kanno. 2008. *Thymocyte proliferation induced by pre-T cell receptor signaling is maintained through polycomb gene product Bmi-1-mediated Cdkn2a repression.* Immunity. 28:231-245.

Morgan, R.A., M.E. Dudley, J.R. Wunderlich, M.S. Hughes, J.C. Yang, R.M. Sherry, R.E. Royal, S.L. Topalian, U.S. Kammula, N.P. Restifo, Z. Zheng, A. Nahvi, C.R. de Vries, L.J. Rogers-Freezer, S.A. Mavroukakis, and S.A. Rosenberg. 2006. *Cancer regression in patients after transfer of genetically engineered lymphocytes.* Science. 314:126-129.

Robbins, P.F., M.E. Dudley, J. Wunderlich, M. El-Gamil, Y.F. Li, J. Zhou, J. Huang, D.J. Powell, Jr., and S.A. Rosenberg. 2004. *Cutting edge: persistence of transferred lymphocyte clonotypes correlates with cancer regression in patients receiving cell transfer therapy.* J Immunol. 173:7125-7130.

Robbins, P.F., R.A. Morgan, S.A. Feldman, J.C. Yang, R.M. Sherry, M.E. Dudley, J.R. Wunderlich, A.V. Nahvi, L.J. Helman, C.L. Mackall, U.S. Kammula, M.S. Hughes, N.P. Restifo, M. Raffeld, C.C. Lee, C.L. Levy, Y.F. Li, M. El-Gamil, S.L. Schwarz, C. Laurencot, and S.A. Rosenberg. 2011. *Tumor regression in patients with metastatic synovial cell sarcoma and melanoma using genetically engineered lymphocytes reactive with NY-ESO-1*. J Clin Oncol. 29:917-924.

Rosenberg, S.A., J.C. Yang, and N.P. Restifo. 2004. *Cancer immunotherapy: moving beyond current vaccines.* Nat Med. 10:909-915.

Rosenberg, S.A., J.C. Yang, R.M. Sherry, U.S. Kammula, M.S. Hughes, G.Q. Phan, D.E. Citrin, N.P. Restifo, P.F. Robbins, J.R. Wunderlich, K.E. Morton, C.M. Laurencot, S.M. Steinberg, D.E. White, and M.E. Dudley. 2011. *Durable complete responses in heavily pretreated patients with metastatic melanoma using T-cell transfer immunotherapy.* Clin Cancer Res. 17:4550-4557.

Sadelain, M., I. Riviere, and R. Brentjens. 2003. *Targeting tumours with genetically enhanced T lymphocytes.* Nat Rev Cancer. 3:35-45.

Spiegel, S., and S. Milstien. 2011. *The outs and the ins of sphingosine-1-phosphate in immunity.* Nat Rev Immunol. 11:403-415.

Stagg, J., R.W. Johnstone, and M.J. Smyth. 2007. *From cancer immunosurveillance to cancer immunotherapy.* Immunol Rev. 220:82-101.

Tran, E., S. Turcotte, A. Gros, P.F. Robbins, Y.C. Lu, M.E. Dudley, J.R. Wunderlich, R.P. Somerville, K. Hogan, C.S. Hinrichs, M.R. Parkhurst, J.C. Yang, and S.A. Rosenberg. 2014. *Cancer immunotherapy based on mutation-specific CD4+ T cells in a patient with epithelial cancer.* Science. 344:641-645.

Vanaja, D.K., K.V. Ballman, B.W. Morlan, J.C. Cheville, R.M. Neumann, M.M. Lieber, D.J. Tindall, and C.Y. Young. 2006. *PDLIM4 repression by hypermethylation as a potential biomarker for prostate cancer.* Clin Cancer Res. 12:1128-1136.

Vanaja, D.K., M.E. Grossmann, J.C. Cheville, M.H. Gazi, A. Gong, J.S. Zhang, K. Ajtai, T.P. Burghardt, and C.Y. Young. 2009. *PDLIM4, an actin binding protein, suppresses prostate cancer cell growth.* Cancer Invest. 27:264-272.

Wei, W., R.M. Hemmer, and J.M. Sedivy. 2001. *Role of p14(ARF) in replicative and induced senescence of human fibroblasts.* Mol Cell Biol. 21:6748-6757.

Zindy, F., C.M. Eischen, D.H. Randle, T. Kamijo, J.L. Cleveland, C.J. Sherr, and M.F. Roussel. 1998. *Myc signaling via the ARF tumor suppressor regulates p53-dependent apoptosis and immortalization.* Genes Dev. 12:2424-2433.

APPENDIX

Table A-1 Microarray analysis of WT and *Jmjd3* cKO CD4 SP T cells (Genes with a difference >2.0 folds are listed).

geneSymbol	refseq_ID	avg_WT	avg_KO	logRatio_KO/WT	pValue	adj_pValue
Pdlim4	NM_019417.2	9.688	7.32	-2.368	0	0.04
Igfbp4	NM_010517.2	12.346	10.559	-1.787	0	0.171
Amigo2	NM_178114.3	11.44	9.798	-1.642	0	0.024
Igfbp4	NM_010517.3	12.793	11.2	-1.593	0	0.049
Myo6	NM_001039546.1	9.748	8.171	-1.577	0	0.043
Lgals1	NM_008495.1	10.455	9.036	-1.419	0.002	0.254
Ccnd2	NM_009829.3	12.39	11.116	-1.274	0	0.04
Erdr1	NM_133362.1	11.206	9.98	-1.226	0	0.153
Samhd1	NM_018851.2	11.708	10.488	-1.219	0.001	0.236
Akr1c18	NM_134066.2	8.96	7.759	-1.201	0	0.04
Erdr1	NM_133362.2	10.22	9.031	-1.189	0.001	0.186
Prlr	NM_011169.4	8.737	7.58	-1.158	0	0.153
E2f2	NM_177733.2	9.757	8.607	-1.149	0.005	0.338
Zfp608	NM_175751.3	8.487	7.357	-1.129	0	0.165
Uhrf1	NM_010931.2	9.638	8.516	-1.121	0	0.087
E2f2	NM_177733.2	9.812	8.757	-1.055	0	0.078
Lgals3	NM_010705.2	9.219	8.225	-0.995	0.002	0.254
Pla2g4f	NM_001024145.1	9.056	8.145	-0.911	0	0.147
Cd44	NM_001039150.1	9.45	8.589	-0.861	0	0.123
E430002D04Rik	NM_172909.1	8.044	7.203	-0.841	0.001	0.244
Csprs	NM_033616.3	7.913	7.085	-0.829	0.003	0.293
Ckb	NM_021273.3	13.314	12.5	-0.814	0.001	0.202
E2f1	NM_007891.3	8.405	7.6	-0.805	0.001	0.243
LOC666403	XR_034389.1	13.332	12.538	-0.794	0	0.153
Top2a	NM_011623.1	8.159	7.365	-0.794	0.002	0.25
Lmna	NM_019390.1	10.092	9.299	-0.792	0.001	0.199
Nudt6	NM_153561.2	8.225	7.449	-0.776	0	0.075

Table A-1 Continued.

geneSymbol	refseq_ID	avg_WT	avg_KO	logRatio_KO/WT	pValue	adj_pValue
Nrn1	NM_153529.1	7.838	7.087	-0.751	0.003	0.287
LOC270152	XM_194453.3	8.444	7.694	-0.75	0.001	0.172
Cdca7	NM_025866.3	10.241	9.518	-0.723	0.001	0.25
Lmna	NM_019390.1	9.638	8.928	-0.71	0	0.153
Arhgap20	NM_175535.3	9.682	8.991	-0.691	0	0.155
Ddit4	NM_029083.1	10.941	10.254	-0.687	0	0.127
Gramd4	NM_172611.2	8.127	7.444	-0.682	0.004	0.297
LOC100041103	XM_001476013.1	10.965	10.286	-0.679	0.002	0.268
Rora	NM_013646.1	8.961	8.285	-0.676	0.009	0.387
Myl4	NM_010858.4	8.647	7.972	-0.675	0.001	0.192
Lmna	NM_001002011.1	9.24	8.571	-0.669	0.001	0.193
Mki67	XM_001000692.2	7.707	7.051	-0.656	0	0.098
Inppl1	NM_010567.1	8.179	7.529	-0.65	0.002	0.258
Mmp9	NM_013599.2	7.891	7.251	-0.64	0.001	0.226
Mcm10	NM_027290.1	7.7	7.061	-0.638	0.003	0.294
Tyms	NM_021288.3	8.756	8.12	-0.636	0	0.098
F13a1	NM_028784.2	8.96	8.327	-0.633	0.001	0.181
Zfp467	NM_001085416.1	8.978	8.347	-0.631	0.006	0.355
Il18r1	NM_008365.1	9.054	8.43	-0.624	0.009	0.386
Tesc	NM_021344.2	10.001	9.382	-0.62	0.006	0.345
LOC100046855	XM_001476916.1	9.82	9.203	-0.618	0.023	0.499
Rassf3	NM_138956.3	9.378	8.777	-0.602	0	0.087
Dtx1	NM_008052.3	9.037	8.436	-0.601	0.006	0.343
Cd7	NM_009854.1	8.102	7.501	-0.6	0	0.042
E130016E03Rik	NM_001039556.2	7.769	7.169	-0.6	0.007	0.361
Lig1	NM_010715.2	8.752	8.157	-0.595	0.003	0.284
Lmna	NM_019390.1	9.082	8.49	-0.591	0.02	0.485
Cish	NM_009895.3	10.801	10.221	-0.58	0.001	0.173
Mmp14	NM_008608.2	8.058	7.488	-0.571	0	0.081
1110017D15Rik	NM_028624.1	7.698	7.147	-0.551	0.001	0.24
Sidt1	NM_198034.2	9.759	9.211	-0.548	0	0.171

Table A-1 Continued.

geneSymbol	refseq_ID	avg_WT	avg_KO	logRatio_KO/WT	pValue	adj_pValue
Clspn	NM_175554.3	7.953	7.413	-0.54	0.002	0.254
Hist1h2ah	NM_175659.1	11.343	10.802	-0.54	0.011	0.407
Hist1h2ah	NM_175659.1	11.573	11.042	-0.531	0.001	0.199
LOC100046608	XM_001476583.1	11.146	10.617	-0.529	0.003	0.293
Gpr83	NM_010287.2	11.011	10.485	-0.526	0.012	0.429
Bcl2	NM_009741.2	10.493	9.97	-0.523	0.002	0.259
Tcf19	NM_025674.1	9.035	8.514	-0.521	0.001	0.24
Glrx	NM_053108.2	10.441	9.92	-0.521	0.002	0.254
Tomm22	NM_172609.3	10.677	10.162	-0.515	0.01	0.397
Birc5	NM_009689.1	7.671	7.157	-0.514	0	0.098
Lad1	NM_133664.2	8.464	7.949	-0.514	0.035	0.554
Cacnb3	NM_007581.2	8.372	7.864	-0.508	0	0.04
Capn2	NM_009794.1	9.194	8.687	-0.507	0.001	0.237
Hist1h2ak	NM_178183.1	11.527	11.021	-0.507	0.002	0.257
Trat1	NM_198297.3	11.36	10.855	-0.505	0.003	0.293
Hist1h2ao	NM_178185.1	13.464	12.96	-0.504	0	0.098
Asb2	NM_023049.1	9.542	9.039	-0.504	0.001	0.194
Cd44	NM_001039150.1	8.116	7.614	-0.502	0.001	0.193
H2-T10	NM_010395.5	11.473	10.971	-0.502	0.009	0.394
Chaf1a	NM_013733.3	7.782	7.282	-0.5	0.001	0.242
Gpc1	NM_016696.3	10.253	9.759	-0.495	0	0.157
Hist1h2ai	NM_178182.1	12.442	11.952	-0.491	0.003	0.281
Tyms-ps	NR_000040.1	8.207	7.716	-0.491	0.01	0.399
Trat1	NM_198297.3	10.175	9.689	-0.486	0.002	0.259
Mapk11	NM_011161.4	10.603	10.118	-0.485	0.001	0.173
Tnfrsf9	NM_011612.2	8.705	8.221	-0.485	0.007	0.362
Inppl1	NM_010567.1	8.016	7.532	-0.484	0.002	0.268
Mcm6	NM_008567.1	9.711	9.229	-0.483	0.002	0.254
Rec8	NM_020002.2	7.599	7.118	-0.481	0.007	0.366
Tnfrsf9	NM_011612.2	8.357	7.877	-0.48	0.01	0.397
Birc5	NM_009689.2	7.824	7.344	-0.48	0.013	0.438

Table A-1 Continued.

geneSymbol	refseq_ID	avg_WT	avg_KO	logRatio_KO/WT	pValue	adj_pValue
Tgfbr3	NM_011578.2	10.435	9.957	-0.477	0.002	0.251
2510009E07Rik	NM_001001881.1	9.611	9.134	-0.477	0.003	0.293
Mansc1	NM_026345.2	8.618	8.143	-0.476	0.002	0.258
Hist1h2ad	NM_178188.3	11.562	11.085	-0.476	0.006	0.345
Acpl2	NM_153420.2	10.051	9.576	-0.475	0.001	0.193
Btbd14a	NM_001037098.1	7.969	7.496	-0.473	0	0.153
Rasgrp4	NM_145149.3	7.982	7.511	-0.471	0.004	0.316
Mcm5	NM_008566.2	11.155	10.686	-0.469	0.001	0.184
Lmna	NM_019390.1	8.267	7.798	-0.469	0.003	0.281
H2-T10	NM_010395.2	12.507	12.038	-0.469	0.006	0.359
Hist1h2ag	NM_178186.2	8.505	8.038	-0.467	0.008	0.381
Appl2	NM_145220.2	9.31	8.843	-0.466	0.001	0.193
Hist1h2af	NM_175661.1	11.991	11.525	-0.466	0.004	0.308
Tnfrsf25	NM_033042.3	9.732	9.269	-0.463	0.001	0.193
LOC381738	XM_355721.1	7.646	7.184	-0.462	0.001	0.196
Prc1	NM_145150.1	8.091	7.633	-0.457	0.003	0.293
Gpr97	NM_173036.2	9.349	8.893	-0.456	0.013	0.432
Hist1h2ad	NM_178188.3	13.139	12.685	-0.454	0.002	0.261
Clspn	NM_175554.3	7.77	7.319	-0.452	0.008	0.379
2810001G20Rik	XM_001476904.1	10.355	9.904	-0.451	0.005	0.336
Glo1	NM_025374.2	11.615	11.167	-0.448	0	0.125
3830406C13Rik	NM_178141.2	8.3	7.853	-0.447	0.002	0.254
Gpr97	NM_173036.2	9.252	8.805	-0.447	0.004	0.297
Capn2	NM_009794.2	9.48	9.034	-0.446	0.01	0.407
Foxo1	NM_019739.2	11.182	10.738	-0.444	0.001	0.178
Atf4	NM_009716.2	11.314	10.871	-0.443	0.001	0.217
Capn2	NM_009794.2	9.399	8.956	-0.443	0.002	0.254
LOC381000	XM_354911.1	8.287	7.847	-0.44	0.004	0.3
Mllt4	NM_010806.1	9.062	8.625	-0.437	0	0.153
2810417H13Rik	NM_026515.2	7.589	7.154	-0.436	0.001	0.173
Abhd7	NM_001001804.1	7.831	7.395	-0.436	0.001	0.236

Table A-1 Continued.

geneSymbol	refseq_ID	avg_WT	avg_KO	logRatio_KO/WT	pValue	adj_pValue
Sp6	NM_031183.1	8.365	7.93	-0.435	0.002	0.258
Nmral1	NM_026393.1	8.224	7.789	-0.434	0.006	0.342
Itm2a	NM_008409.2	13.948	13.517	-0.431	0.001	0.225
Mcm3	NM_008563.2	8.601	8.169	-0.431	0.004	0.299
F2rl3	NM_007975.3	8.042	7.612	-0.43	0.007	0.364
Hist1h2an	NM_178184.1	11.536	11.107	-0.429	0.01	0.397
Klhdc2	NM_027117.1	12.175	11.748	-0.427	0	0.042
Litaf	NM_019980.1	10.504	10.077	-0.427	0	0.098
Pdgfb	NM_011057.2	7.812	7.385	-0.427	0.002	0.271
Hmgn3	NM_175074.1	9.931	9.505	-0.426	0.006	0.342
Amica1	NM_001005421.3	7.941	7.517	-0.424	0	0.153
Acot7	NM_133348.1	11.155	10.731	-0.423	0.005	0.328
1190002F15Rik	NR_037965.1	7.787	7.369	-0.419	0.002	0.25
Acot7	NM_133348.1	9.347	8.929	-0.418	0.001	0.246
Acvrl1	NM_009612.2	7.699	7.281	-0.418	0.002	0.254
Adam15	NM_009614.2	8.662	8.245	-0.418	0.008	0.381
S100a13	NM_009113.3	9.787	9.37	-0.417	0.007	0.366
Aqp9	NM_022026.2	8.54	8.122	-0.417	0.008	0.372
Birc5	NM_009689.2	7.484	7.068	-0.416	0.001	0.236
Sec61b	NM_024171.1	8.909	8.493	-0.415	0.017	0.464
Anxa2	NM_007585.3	10.235	9.822	-0.413	0	0.166
LOC100046608	XM_001476583.1	10.096	9.682	-0.413	0.002	0.259
Tubb2b	NM_023716.1	10.292	9.888	-0.403	0.003	0.281
Mapre2	NM_153058.3	8.586	8.183	-0.403	0.091	0.674
Sp6	NM_031183.1	8.599	8.198	-0.401	0.008	0.379
Mcm6	NM_008567.1	9.597	9.196	-0.401	0.014	0.444
Cdca8	NM_026560.3	8.13	7.732	-0.398	0.008	0.373
Fibcd1	NM_178887.3	8.553	8.157	-0.396	0.002	0.268
Fas	NM_007987.1	9.824	9.428	-0.396	0.009	0.388
Lyz	NM_013590.2	9.196	8.801	-0.395	0	0.172
Dclk2	NM_027539.3	8.654	8.259	-0.395	0.001	0.208

Table A-1 Continued.

geneSymbol	refseq_ID	avg_WT	avg_KO	logRatio_KO/WT	pValue	adj_pValue
Axl	NM_009465.3	9.311	8.917	-0.394	0.005	0.337
Ager	NM_007425.2	9.012	8.618	-0.394	0.012	0.421
Tbc1d1	NM_019636.2	9.034	8.641	-0.393	0.004	0.318
Gfer	NM_023040.3	10.57	10.179	-0.391	0.004	0.297
BC017643	NM_144832.1	9.255	8.868	-0.387	0.003	0.281
Rasal1	NM_013832.3	8.313	7.926	-0.387	0.006	0.346
Gpnmb	NM_053110.3	8.868	8.485	-0.384	0.007	0.364
Ptgir	NM_008967.1	8.396	8.014	-0.382	0.001	0.226
LOC100040525	XR_031953.1	9.848	9.466	-0.382	0.009	0.387
Cdc45l	NM_009862.1	7.705	7.326	-0.379	0.002	0.26
Klra3	NM_010648.2	7.339	6.961	-0.378	0.001	0.183
Aim1	NM_172393.1	10.493	10.117	-0.377	0.013	0.437
Aldh2	NM_009656.3	11.111	10.734	-0.376	0.001	0.217
Pole	NM_011132.1	7.639	7.264	-0.375	0.003	0.281
A430093F15Rik	XR_035341.1	11.359	10.985	-0.375	0.008	0.379
1500031L02Rik	NM_025892.1	10.392	10.017	-0.375	0.01	0.397
Jmjd3	NM_001017426.1	9.951	9.577	-0.374	0.088	0.669
Pcbp4	NM_021567.2	10.317	9.945	-0.372	0.01	0.399
H2-Eb1	NM_010382.2	8.43	8.059	-0.371	0.015	0.452
Samhd1	NM_018851.2	7.81	7.44	-0.37	0.025	0.511
Sec61b	NM_024171.2	9.883	9.514	-0.369	0.01	0.397
Klhdc1	NM_178253.4	9.091	8.723	-0.368	0.002	0.268
1110038D17Rik	NM_175133.1	10.893	10.525	-0.368	0.004	0.313
Ifi30	NM_023065.3	9.097	8.731	-0.366	0.002	0.254
scl0004175.1_57	BC026739.1	7.723	7.357	-0.366	0.004	0.302
Mllt4	NM_010806.1	8.261	7.899	-0.363	0	0.128
Map3k8	NM_007746.2	8.095	7.733	-0.362	0.005	0.341
Hectd2	NM_172637.1	9.335	8.976	-0.359	0.005	0.332
Hap1	NM_010404.2	8.329	7.97	-0.359	0.012	0.421
Tipin	NM_025372.1	9.836	9.478	-0.358	0.027	0.518
Ppp3cc	NM_008915.2	9.687	9.334	-0.354	0.026	0.515

Table A-1 Continued.

geneSymbol	refseq_ID	avg_WT	avg_KO	logRatio_KO/WT	pValue	adj_pValue
St3gal1	NM_009177.4	9.172	8.821	-0.351	0.004	0.296
Irf6	NM_016851.2	8.677	8.326	-0.351	0.016	0.455
Gng2	NM_001038637.1	8.849	8.498	-0.351	0.072	0.644
Oasl2	NM_011854.1	9.063	8.713	-0.35	0	0.128
Bcl2	NM_177410.2	10.874	10.524	-0.35	0.03	0.531
E2f2	NM_183301.1	7.938	7.589	-0.349	0.003	0.293
Ncaph	NM_144818.1	8.145	7.795	-0.349	0.005	0.341
Fignl1	NM_021891.2	7.396	7.047	-0.349	0.011	0.41
Itgb7	NM_013566.1	11.779	11.43	-0.348	0	0.139
Anxa6	NM_013472.2	12.938	12.59	-0.347	0.004	0.308
Nt5e	NM_011851.2	8.357	8.013	-0.344	0.021	0.492
Saps3	NM_029456.1	10.929	10.586	-0.343	0.007	0.366
Tk1	NM_009387.1	7.345	7.001	-0.343	0.035	0.554
LOC100047579	XM_001478437.1	9.291	8.95	-0.342	0	0.158
Acot7	NM_133348.1	9.161	8.82	-0.341	0	0.098
Rrm1	NM_009103.2	8.693	8.351	-0.341	0.003	0.293
LOC100046608	XM_001476583.1	9.11	8.768	-0.341	0.033	0.546
2900062L11Rik	NR_003642.1	9.483	9.144	-0.34	0.019	0.478
Fdps	NM_134469.3	10.151	9.813	-0.339	0.014	0.447
Whsc1	XM_898312.2	8.011	7.673	-0.337	0.003	0.281
Il6ra	NM_010559.2	8.713	8.376	-0.337	0.017	0.462
Klrd1	NM_010654.2	7.532	7.196	-0.336	0.003	0.281
Qpct	NM_027455.1	7.996	7.661	-0.335	0.001	0.244
Cchcr1	NM_146248.1	8.545	8.211	-0.335	0.011	0.409
Acot7	NM_133348.1	8.707	8.372	-0.335	0.044	0.585
Garnl4	NM_001015046.2	7.831	7.497	-0.334	0.003	0.293
Hist1h2ai	NM_178182.1	13.209	12.874	-0.334	0.005	0.328
H1f0	NM_008197.3	7.471	7.137	-0.334	0.018	0.47
Ccrn4l	NM_009834.1	9.469	9.136	-0.333	0	0.049
Cdca3	NM_013538.4	8.018	7.686	-0.332	0.003	0.293
Rad54l	NM_009015.2	7.454	7.122	-0.332	0.018	0.477

Table A-1 Continued.

geneSymbol	refseq_ID	avg_WT	avg_KO	logRatio_KO/WT	pValue	adj_pValue
AI467606	NM_178901.3	11.395	11.064	-0.331	0.001	0.211
Mcm6	NM_008567.1	9.897	9.567	-0.331	0.032	0.541
Tnfrsf18	NM_009400.2	11.519	11.189	-0.33	0.006	0.343
S100a8	NM_013650.2	7.207	6.878	-0.329	0.001	0.173
Trappc1	NM_001024206.1	10.118	9.789	-0.329	0.001	0.202
Xcl1	NM_008510.1	7.547	7.218	-0.329	0.007	0.364
Fcgrt	NM_010189.1	7.965	7.637	-0.328	0.003	0.281
Cox7a2l	XM_123188.1	12.506	12.178	-0.328	0.005	0.326
2510009E07Rik	NM_001001881.1	8.041	7.714	-0.328	0.007	0.368
Ccr8	NM_007720.2	10.097	9.769	-0.328	0.041	0.576
Tiam1	NM_009384.2	10.361	10.034	-0.327	0.006	0.341
Maged2	NM_030700.1	8.976	8.649	-0.326	0.011	0.41
Kif1b	NM_008441.2	9.132	8.806	-0.326	0.023	0.499
Psat1	NM_177420.1	10.128	9.804	-0.324	0.064	0.626
LOC100045677	XR_031705.1	8.623	8.301	-0.323	0.002	0.253
LOC625360	NM_001037925.1	8.832	8.509	-0.323	0.005	0.334
Ifitm3	NM_025378.2	8.605	8.283	-0.322	0.002	0.252
D16Bwg1494e	XM_358773.6	8.374	8.053	-0.321	0.022	0.495
Lxn	NM_016753.4	9.881	9.561	-0.32	0.003	0.293
Mrpl33	NM_025796.2	12.452	12.132	-0.32	0.01	0.406
Lcmt1	NM_025304.3	10.891	10.571	-0.32	0.033	0.547
LOC100046608	XM_001476583.1	8.695	8.375	-0.32	0.033	0.546
Vim	NM_011701.3	11.994	11.676	-0.318	0.005	0.328
Il6ra	NM_010559.2	10.315	9.997	-0.318	0.045	0.587
Ptms	NM_026988.1	8.186	7.87	-0.316	0.013	0.434
Rab4a	NM_009003.2	8.112	7.796	-0.316	0.014	0.44
LOC381770	XM_355767.1	8.149	7.835	-0.315	0.002	0.254
Hmgn3	NM_026122.3	9.676	9.362	-0.315	0.005	0.332
Akr1c12	NM_013777.2	9.132	8.817	-0.314	0.006	0.341
0610007P14Rik	NM_021446.1	9.532	9.219	-0.313	0.001	0.249
Arhgef6	NM_152801.1	11.984	11.673	-0.311	0.014	0.447

Table A-1 Continued.

geneSymbol	refseq_ID	avg_WT	avg_KO	logRatio_KO/WT	pValue	adj_pValue
Gins2	NM_178856.1	7.638	7.327	-0.311	0.03	0.533
LOC100040592	XM_001475189.1	11.33	11.02	-0.31	0.005	0.326
Psme2	NM_011190.3	9.499	9.189	-0.31	0.01	0.397
Bcor	NM_029510.1	10.18	9.871	-0.309	0.006	0.358
Zmat3	NM_009517.2	9.129	8.819	-0.309	0.065	0.628
Gsto1	NM_010362.2	9.823	9.516	-0.307	0.002	0.265
Hist2h2ac	NM_175662.1	13.389	13.082	-0.307	0.007	0.365
Fas	NM_007987.1	10.63	10.324	-0.306	0.004	0.302
Dnahc8	NM_013811.3	9.621	9.316	-0.306	0.017	0.46
Trappc1	NM_001024206.1	10.48	10.175	-0.306	0.025	0.509
EG433229	XM_899874.3	11.386	11.081	-0.305	0.006	0.355
Atn1	NM_007881.4	9.061	8.757	-0.304	0.002	0.268
Zdhhc15	NM_175358.2	8.316	8.012	-0.304	0.003	0.289
Cd74	NM_010545.3	9.633	9.33	-0.303	0.024	0.506
ENSMUSG00000043795	XM_001480835.1	13.167	12.865	-0.302	0.007	0.368
2010001J22Rik	NM_001013022.1	8.198	7.896	-0.302	0.012	0.421
Sqstm1	NM_011018.2	10.888	11.189	0.301	0.004	0.314
Ddx6	NM_007841.3	9.671	9.971	0.301	0.12	0.711
BC094916	NM_001024721.1	9.071	9.373	0.302	0.013	0.434
Pecam1	NM_001032378.1	8.679	8.981	0.302	0.034	0.548
LOC433955	XR_033167.1	11.844	12.148	0.303	0.004	0.308
Slc25a25	NM_146118.2	8.966	9.268	0.303	0.03	0.531
scl0002975.1_346	AK088505.1	10.127	10.43	0.303	0.089	0.671
Btbd11	NM_001017525.1	9.793	10.097	0.304	0.002	0.27
Pdcd4	NM_011050.3	11.185	11.489	0.304	0.024	0.505
D12Ertd551e	NM_028731.2	8.523	8.827	0.304	0.043	0.582
Hcn3	NM_008227.1	7.447	7.753	0.306	0.016	0.455
H6pd	NM_173371.3	9.417	9.724	0.307	0.001	0.228
LOC100043821	XM_001481017.1	9.966	10.274	0.307	0.012	0.419
Csde1	NM_144901.2	8.42	8.727	0.307	0.022	0.495
EG434404	XM_486222.5	10.709	11.016	0.307	0.134	0.726

Table A-1 Continued.

geneSymbol	refseq_ID	avg_WT	avg_KO	logRatio_KO/WT	pValue	adj_pValue
Wdr51b	NM_027740.5	7.834	8.142	0.308	0.002	0.259
Peli1	NM_023324.2	10.049	10.358	0.309	0.001	0.244
LOC624083	XR_035632.1	10.818	11.127	0.309	0.046	0.589
2210010C17Rik	NM_027308.2	8.143	8.454	0.311	0.001	0.244
0610007P22Rik	NM_026676.2	7.962	8.273	0.311	0.005	0.328
BC022224	NM_177564.4	7.546	7.856	0.311	0.02	0.487
LOC667370	XM_001480084.1	8.999	9.311	0.312	0.033	0.545
2010308M01Rik	XM_131083.2	9.31	9.622	0.312	0.062	0.623
Pitpnm2	NM_011256.1	11.158	11.471	0.313	0.012	0.417
Eef2	NM_007907.1	11.443	11.756	0.313	0.055	0.608
B230342M21Rik	NM_133898.3	10.428	10.742	0.314	0.003	0.293
Rpl29	NM_009082.2	11.692	12.006	0.314	0.003	0.293
Arrdc4	NM_001042592.2	7.92	8.235	0.315	0	0.123
Zfp295	NM_001081684.1	8.459	8.775	0.316	0.003	0.281
Smpdl3a	NM_020561.2	9.325	9.643	0.317	0.011	0.409
Per1	NM_011065.2	11.644	11.962	0.318	0	0.153
Cbx7	NM_144811.3	9.705	10.023	0.318	0.01	0.397
Gnptg	NM_172529.3	10.705	11.023	0.318	0.015	0.45
C030048B08Rik	NM_172991.2	9.069	9.388	0.319	0.029	0.528
EG382843	XM_905000.3	10.782	11.103	0.32	0.001	0.199
Galnt9	NM_198306.1	7.653	7.973	0.32	0.002	0.254
Gimap5	NM_175035.5	8.99	9.31	0.32	0.017	0.46
Gpr137b-ps	NR_003568.1	7.056	7.378	0.323	0	0.157
Xdh	NM_011723.2	7.568	7.891	0.323	0	0.078
Psd2	NM_028707.3	7.34	7.663	0.323	0.003	0.293
Gimap5	NM_175035.5	8.556	8.879	0.323	0.021	0.49
Jun	NM_010591.1	8.236	8.56	0.324	0.001	0.244
Rgs11	XM_128488.3	8.769	9.093	0.324	0.003	0.293
Inadl	NM_172696.2	7.916	8.24	0.324	0.078	0.656
Eef2	NM_007907.1	12.049	12.374	0.325	0.04	0.571
Sfxn4	NM_053198.2	7.761	8.089	0.328	0.022	0.493

Table A-1 Continued.

geneSymbol	refseq_ID	avg_WT	avg_KO	logRatio_KO/WT	pValue	adj_pValue
Gprasp1	NM_001005385.1	10.693	11.021	0.328	0.025	0.511
Ifit3	NM_010501.2	8.849	9.177	0.329	0.003	0.293
Srfbp1	NM_026040.2	8.475	8.804	0.329	0.023	0.5
Rn18s	NR_003278.1	11.008	11.339	0.331	0.019	0.478
Oat	NM_016978.1	10.693	11.026	0.332	0.001	0.193
Plp1	NM_011123.2	7.647	7.981	0.334	0.047	0.591
Smyd3	NM_027188.3	7.854	8.19	0.336	0	0.128
Plk3	NM_013807.1	9.732	10.069	0.336	0.011	0.407
Egr1	NM_007913.5	13.522	13.861	0.339	0.005	0.326
Sdcbp2	NM_145535.1	8.611	8.95	0.339	0.007	0.369
LOC100046232	XM_001475817.1	8.518	8.858	0.34	0.02	0.487
D12Ertd551e	NM_028731.5	8.683	9.023	0.34	0.028	0.522
LOC100045780	XM_001475019.1	9.516	9.857	0.341	0.007	0.366
4631423B10Rik	NM_175422.2	9.934	10.276	0.342	0.001	0.228
Atg16l2	XM_001476186.1	9.509	9.851	0.342	0.006	0.349
Ppic	NM_008908.3	7.792	8.135	0.343	0.007	0.362
Ggnbp1	NM_027544.1	8.759	9.102	0.343	0.01	0.397
Specc1	NM_001029936.2	7.911	8.254	0.344	0.004	0.32
Aebp2	NM_009637.1	8.633	8.978	0.344	0.016	0.455
Pknox1	NM_016670.2	8.586	8.931	0.344	0.02	0.486
Ephx1	NM_010145.2	11.553	11.898	0.345	0	0.078
LOC100048331	XR_034509.1	7.517	7.863	0.345	0.011	0.408
Tardbp	NM_001008545.1	9.972	10.318	0.346	0.005	0.328
Iqgap2	NM_027711.1	10.394	10.74	0.346	0.015	0.452
LOC100045617	XM_001474613.1	11.826	12.173	0.347	0.002	0.258
Tob2	NM_020507.3	10.68	11.026	0.347	0.012	0.425
Pknox1	NM_016670.2	8.974	9.321	0.347	0.026	0.513
Ifit3	NM_010501.1	11.325	11.673	0.348	0.005	0.332
Hsd3b2	NM_153193.2	11.119	11.467	0.348	0.015	0.452
Numa1	NM_133947.2	9.026	9.375	0.349	0.035	0.554
Rn18s	NR_003278.1	12.645	12.994	0.349	0.046	0.589

Table A-1 Continued.

geneSymbol	refseq_ID	avg_WT	avg_KO	logRatio_KO/WT	pValue	adj_pValue
EG434197	NM_001013811.2	11.372	11.722	0.35	0.012	0.421
LOC384710	XR_003896.1	11.3	11.651	0.351	0.118	0.707
Gramd1a	NM_027898.3	8.823	9.177	0.354	0.018	0.475
Nfkbib	NM_010908.3	8.5	8.855	0.355	0.011	0.41
AI450540	NM_145505.2	10.416	10.771	0.356	0.001	0.173
LOC667337	XM_990977.1	9.123	9.479	0.356	0.005	0.33
Wdr89	XM_001479426.1	10.385	10.742	0.357	0.094	0.677
Ccdc126	NM_175098.2	8.751	9.112	0.361	0.002	0.251
Pkp4	NM_175464.2	9.639	10	0.361	0.003	0.281
Dap	NM_146057.1	8.729	9.09	0.361	0.022	0.493
Ppargc1b	NM_133249.2	9.024	9.386	0.362	0.003	0.281
Folr4	NM_022888.1	8.384	8.747	0.363	0	0.098
E130012A19Rik	NM_175332.3	7.869	8.232	0.363	0.069	0.64
4930431B09Rik	XR_002338.2	9.304	9.668	0.364	0	0.098
Fbxl12	NM_013911.2	8.352	8.716	0.364	0.004	0.307
Tcf25	NM_001037878.1	9.679	10.043	0.364	0.015	0.452
LOC623121	XM_001480713.1	10.335	10.7	0.365	0.003	0.281
Ube2n	NM_080560.3	8.594	8.959	0.365	0.009	0.387
H2-Q8	NM_023124.2	9.677	10.042	0.365	0.015	0.452
Klf6	NM_011803.2	11.694	12.06	0.366	0.032	0.541
Lincr	NM_153408.2	7.55	7.917	0.367	0.003	0.281
Klf6	NM_011803.2	8.189	8.556	0.367	0.016	0.455
LOC630146	XM_973806.1	7.731	8.098	0.367	0.019	0.482
Tlr1	NM_030682.1	8.361	8.735	0.374	0.006	0.355
Rabac1	NM_010261.2	10.892	11.266	0.374	0.01	0.397
Rapgef6	NM_175258.3	8.842	9.216	0.374	0.016	0.455
Ifngr1	NM_010511.2	9.765	10.144	0.379	0.024	0.505
EG668300	XM_001000750.1	9.736	10.117	0.38	0.053	0.606
Gprasp1	NM_026081.5	8.882	9.265	0.382	0.026	0.514
Adh1	NM_007409.2	7.967	8.351	0.384	0.016	0.455
Asah3l	NM_139306.1	7.849	8.234	0.385	0.006	0.346

Table A-1 Continued.

geneSymbol	refseq_ID	avg_WT	avg_KO	logRatio_KO/WT	pValue	adj_pValue
Adi1	NM_134052.2	10.729	11.117	0.388	0.006	0.353
Errfi1	NM_133753.1	8.917	9.306	0.389	0.002	0.259
Ccdc117	NM_134033.1	9.134	9.525	0.391	0.007	0.362
1810054D07Rik	NM_027238.2	8.155	8.548	0.393	0.005	0.337
LOC674427	XR_030796.1	8.457	8.85	0.393	0.011	0.407
Accs	NM_183220.2	9.242	9.637	0.394	0.009	0.393
Actb	NM_007393.3	8.265	8.66	0.395	0.136	0.73
H2-Q6	NM_207648.1	9.216	9.612	0.396	0.032	0.541
Mycbp2	NM_207215.2	11.013	11.409	0.397	0.003	0.293
EG384179	XM_912278.3	8.256	8.653	0.397	0.049	0.597
LOC675899	XM_985882.1	11.245	11.645	0.4	0.031	0.536
Ttc3	NM_009441.2	8.364	8.766	0.402	0.012	0.426
Ogfrl1	XM_973033.1	7.87	8.273	0.403	0.014	0.444
Cldn10	NM_023878.2	8.244	8.649	0.405	0.001	0.223
Wdr51b	NM_027740.3	9.212	9.619	0.406	0	0.093
LOC385615	XM_358790.1	10.099	10.505	0.407	0.002	0.259
A230050P20Rik	NM_175687.1	10.425	10.832	0.407	0.012	0.415
D330028D13Rik	NM_172727.2	8.307	8.715	0.408	0.002	0.254
Adh1	NM_007409.2	7.755	8.163	0.408	0.003	0.293
Icam1	NM_010493.2	9.248	9.656	0.408	0.03	0.534
Ldhd	NM_027570.3	7.44	7.849	0.409	0.001	0.223
9430079M16Rik	NM_175414.2	7.677	8.086	0.409	0.003	0.281
LOC100040505	XM_001475564.1	8.977	9.389	0.411	0	0.098
Arsb	NM_009712.3	8.87	9.283	0.413	0	0.153
C030048B08Rik	NM_172991.2	10.389	10.806	0.416	0.007	0.366
Trub1	NM_028115.2	9.256	9.672	0.416	0.007	0.361
Rab6b	NM_173781.3	9.212	9.63	0.418	0.001	0.244
Gm484	NM_001033356.2	7.866	8.285	0.419	0.007	0.366
LOC623121	XM_001480713.1	12.083	12.505	0.422	0.016	0.455
Xist	NR_001463.2	11.926	12.35	0.424	0.006	0.346
Rundc3b	NM_198620.1	8.51	8.939	0.43	0	0.089

Table A-1 Continued.

geneSymbol	refseq_ID	avg_WT	avg_KO	logRatio_KO/WT	pValue	adj_pValue
Xist	NR_001463.2	11.783	12.215	0.432	0.016	0.457
Trub1	NM_028115.2	9.194	9.628	0.434	0.003	0.293
Ctsw	NM_009985.3	12.385	12.82	0.435	0.004	0.303
Ppic	NM_008908.1	9.332	9.778	0.445	0.003	0.293
Itgae	NM_008399.1	7.897	8.343	0.446	0.001	0.244
Ltb	NM_008518.1	11.509	11.965	0.456	0.001	0.236
Gpsm1	NM_153410.4	9.322	9.777	0.456	0.006	0.343
Fanci	NM_145946.2	7.794	8.252	0.458	0.005	0.328
Magi1	NM_001029850.2	7.013	7.472	0.46	0.014	0.442
Tmem108	NM_178638.2	9.636	10.097	0.461	0.006	0.359
Iqgap2	NM_027711.1	9.415	9.88	0.465	0	0.153
Gbp3	NM_018734.3	8.508	8.973	0.465	0.004	0.302
Il8ra	NM_178241.4	7.187	7.653	0.466	0	0.157
Egr2	NM_010118.1	10.3	10.767	0.467	0.001	0.184
Tgif1	NM_009372.2	7.708	8.176	0.468	0.002	0.254
EG665378	NM_001081746.1	8.774	9.256	0.483	0.005	0.326
Usp11	NM_145628.3	7.42	7.904	0.484	0.001	0.249
Dusp2	NM_010090.2	12.918	13.406	0.488	0	0.147
Rp23-357i14.1	NM_001085518.1	8.835	9.325	0.49	0.003	0.281
Snf1lk	NM_010831.2	8.287	8.78	0.494	0	0.153
Klf9	NM_010638.4	9.353	9.847	0.494	0.002	0.257
Irs2	NM_001081212.1	9.099	9.597	0.499	0.005	0.337
Cldn10	NM_021386.3	9.035	9.537	0.502	0	0.153
Eif4a2	NM_013506.1	10.507	11.013	0.506	0.009	0.384
Actb	NM_007393.1	8.292	8.802	0.511	0.126	0.718
Itgae	NM_008399.1	7.869	8.394	0.525	0.005	0.328
Pstpip2	NM_013831.4	8.417	8.952	0.535	0.014	0.441
Abcb1b	NM_011075.1	8.042	8.589	0.547	0.004	0.308
Gbp3	NM_018734.2	8.207	8.771	0.564	0	0.04
Ldhd	NM_027570.3	7.228	7.798	0.571	0	0.153
Ank	NM_020332.3	7.842	8.427	0.586	0.001	0.238

Table A-1 Continued.

geneSymbol	refseq_ID	avg_WT	avg_KO	logRatio_KO/WT	pValue	adj_pValue
Folr4	NM_176807.3	8.462	9.053	0.592	0	0.168
Camk2b	NM_007595.3	7.891	8.486	0.594	0	0.171
A630023P12Rik	NM_173766.2	8.824	9.43	0.606	0.026	0.515
Stx1a	NM_016801.3	10.363	10.971	0.608	0	0.153
LOC100046770	XM_001476780.1	8.55	9.169	0.619	0	0.098
Ccl4	NM_013652.2	8.584	9.203	0.619	0.022	0.496
Folr4	NM_176807.3	8.578	9.205	0.627	0.001	0.24
Tgif1	NM_009372.2	8.75	9.38	0.63	0.001	0.223
Actb	NM_007393.3	11.825	12.455	0.63	0.144	0.734
Art4	NM_026639.2	8.98	9.616	0.636	0	0.128
Art2b	NM_019915.2	7.874	8.529	0.655	0	0.098
Lpxn	NM_134152.3	10.975	11.636	0.661	0.001	0.184
Dusp2	NM_010090.2	11.848	12.511	0.663	0	0.128
Igf1r	NM_010513.2	8.117	8.786	0.669	0.001	0.244
H2-Ob	NM_010389.3	8.558	9.228	0.67	0.003	0.281
Ebi2	NM_183031.1	10.663	11.341	0.678	0	0.049
Arrdc3	NM_178917.2	8.788	9.469	0.68	0.014	0.444
Magi1	NM_010367.2	7.046	7.749	0.703	0.004	0.315
2610035D17Rik	XM_902349.2	9.242	9.956	0.714	0	0.078
Gfi1	NM_010278.1	9.533	10.264	0.731	0	0.127
Foxq1	NM_008239.3	7.228	7.981	0.753	0	0.04
Adam11	NM_009613.1	8.105	8.93	0.825	0	0.04
Eng	NM_007932.1	7.963	8.816	0.853	0.001	0.232
Rgs1	NM_015811.1	9.251	10.167	0.916	0.002	0.269
Rgs1	NM_015811.1	10.054	10.997	0.943	0	0.128
Rgs1	NM_015811.1	9.268	10.247	0.979	0	0.156
Slc15a2	NM_021301.1	8.733	10.155	1.423	0.002	0.254
Slc15a2	XM_147213.1	9.697	11.197	1.501	0	0.04
Gbp1	NM_010259.2	6.973	9.273	2.3	0	0.04

Table A-2. A list of primers used in this study

Primers	Sequence
Real-time Primers	
m*Pdlim4*-1F	5'-CACCATCTCGCGGGTTCAT-3'
m*Pdlim4*-1R	5'-GCAGCCTTTAATGCGGTTCT-3'
m*S1P1*-1F	5'-ATGGTGTCCACTAGCATCCC-3'
m*S1P1*-1R	5'-CGATGTTCAACTTGCCTGTGTAG-3'
m*Klf2*-1F	5'-CTAAAGGCGCATCTGCGTA-3'
m*Klf2*-1R	5'-TAGTGGCGGGTAAGCTCGT-3'
m*Amigo2*-1F	5'-CTGTGTCTGTTGGTGATCGCA-3'
m*Amigo2*-1R	5'-CGGGCACCTTAGATAGGTTTTTG-3'
m*CCR7*-1F	5'-GCTCCAGGCACGCAACTTT-3'
m*CCR7*-1R	5'-GACTACCACCACGGCAATGA-3'
m*Slc15a2*-1F	5'-GGCACGGACTAGATACTTCTCG-3'
m*Slc15a2*-1R	5'-AACGGCTGTTCACATCCTTTT-3'
m*CD62L*-1F	5'-TGGCAAGGCGGTTAAAAA-3'
m*CD62L*-1R	5'-AAAACTGCAGCAGACTGTGG-3'
m*Igfbp4*-1F	5'-AGAAGCCCCTGCGTACATTG-3'
m*Igfbp4*-1R	5'-TGTCCCCACGATCTTCATCTT-3'
m*Gbp1*-1F	5'- ACAACTCAGCTAACTTTGTGGG-3'
m*Gbp1*-1R	5'- TGATACACAGGCGAGGCATATTA-3'
m*Lgals1*-1F	5'-AACCTGGGGAATGTCTCAAAGT-3'
m*Lgals1*-1R	5'-GGTGATGCACACCTCTGTGA-3'
m*Erdr1*-1F	5'-GGTCAAGATGTATGTGCCACC-3'
m*Erdr1*-1R	5'-GCTTCTACGTGTGTGCTTTCG-3'
m*Samhd1*-1F	5'- CAGCTCATTCGGGTGTACTGT-3'
m*Samhd1*-1R	5'- GTGGCTTGGTGAAGTCCCT-3'
m*Akr1c18*-1F	5'- TCGTCCAGAGTTGGTCAGAC-3'
m*Akr1c18*-1R	5'- GCCTGGCCTATCTCTTCTTCAT-3
m*Adam11*-1F	5'- ATCGTAGAGCCTAAGGAGATAGC -3'
m*Adam11*-1R	5'- TTGGGGAGAGCAGACTGGG -3'
m*Actin*-1F	5'-CCTCTGGTCGTACCACAG-3'
m*Actin*-1R	5'-GCCACAGGATTCCATACCC-3'
m*Gapdh*-1F	5'- CTGCACCACCAACTGCTTAG-3'
m*Gapdh*-1R	5'-GTCGCTGTTGAAGTCAGAGG-3'
m*CCR5*-1F	5'-AGGCCATGCAGGCAACAG-3'
m*CCR5*-1R	5'-TCTCTCCAACAAAGGCATAGATGA-3'
ChIP-qPCR Primers	
m*Pdlim4*-2F	5'-TCCTCCGTGTCCGGCTCCAG-3'
m*Pdlim4*-2R	5'-GCGGAAGCCCCAGGGTGAAG-3'
m*S1P1*-2F	5'- GAGAGGGGAACCCCCGGTCC-3'
m*S1P1*-2R	5'- CCTCCACCCCCTCCACTCCG-3'
sgRNA Primers	
m*Pdlim4*-sgRNA-1F	5'-CACCG ACCCA CTCGG TGACCCTGCG-3'
m*Pdlim4*-sgRNA-1R	5'-AAACCGCAGGGTCACCGAGTGGGTC-3'
m*Pdlim4*-sgRNA-2F	5'-CACCG GCCGCGCAGGGTCACCGAGT-3'
m*Pdlim4*-sgRNA-2R	5'-AAACACTCGGTGACCCTGCGCGGCC-3'
Cloning Primers	
m*Pdlim4*-3F	5'-TCTGCTAGCCAGCCCCCAGAGACCATGCAGG-3'
m*Pdlim4*-3R	5'-GGTGCTAGCGGGCCGGAGCTGCAGCCAGAGC-3'
m*Pdlim4*-4F	5'-GGGGCTAGCTGGTTGCCAGCCCCCAGAGAC-3'
m*Pdlim4*-5F	5'-AGAGCTAGCCAAGACAAGGCCCAAGAAGC-3'
m*Pdlim4*-6F	5'-ACGGCTAGCTGGTTTGGGAACAAGGCACG-3'
m*Pdlim4*-7F	5'-CCT GCTAGCGGCAGAACTCAGACATCCAAG-3'
m*Pdlim4*-8F	5'-GGTGCTAGCAGCCCCCAAAGTGGGAGGGT-3'